LABELLING OF PROTEINACEOUS BINDERS IN ART

Su Yin Ooi

Tese apresentada à Universidade de Évora
para obtenção do Grau de Doutor em Bioquímica

ORIENTADOR (A/ES): *Ana Teresa Caldeira*
João Paulo Prates Ramalho
António Manuel Deométrio Rodrigues Lourenço Pereira

ÉVORA, JULHO 2019

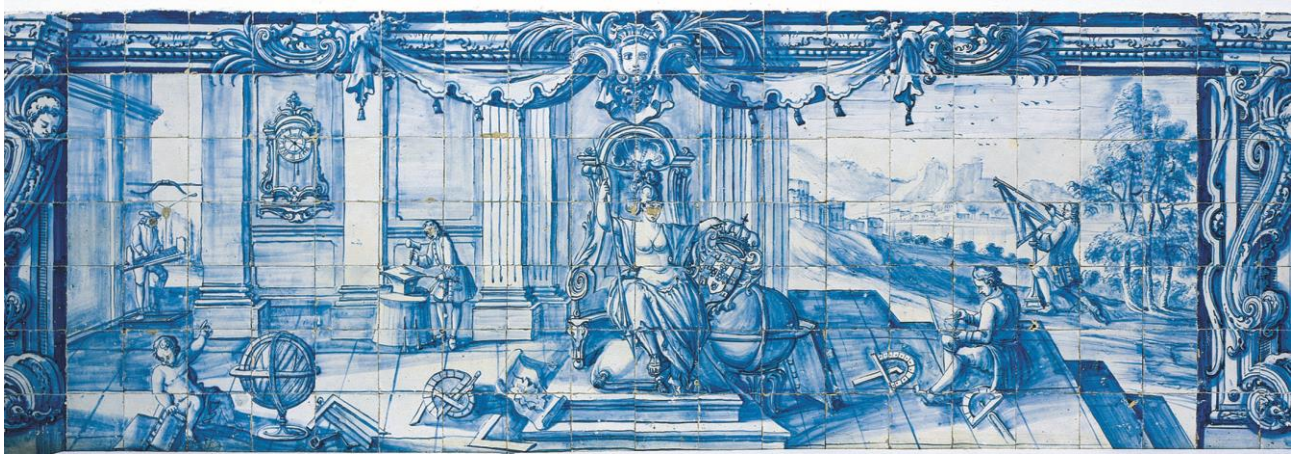

INSTITUTO DE INVESTIGAÇÃO E FORMAÇÃO AVANÇADA

President of the jury

Name	António José Estevão Grande Candeias
Email	candeias@uevora.pt
Department	Chemistry department
Professional category	Associate Professor with Aggregation

Vowels

Name	Maria do Rosário Caeiro Martins **(Member)**
Email	mrm@uevora.pt
Department	Chemistry department
Professional category	Assistant professor
Name	Alfredo Jorge Palace Carvalho **(Member)**
Email	ajpalace@uevora.pt
Department	Chemistry department
Professional category	Assistant professor
Name	Rui Miguel Azevedo Bordalo **(Member)**
Email	rbordalo@ucp.pt
Department	Catholic University of Porto
Professional category	Investigator
Name	Luís Miguel Santos Loura **(Member)**
Email	lloura@ff.uc.pt
Department	Coimbra University
Professional category	Associate Professor
Name	Paula Cristina de Sério Branco **(Member)**
Email	psb@dq.fct.unl.pt
Department	New University of Lisbon - Faculty of Science and Technology
Professional category	Assistant Professor w / aggregation
Name	João Paulo Cristovão Almeida Prates Ramalho **(Advisor)**
Email	jpcar@uevora.pt
Department	Chemistry department
Professional category	Associate Professor

Dedicated to my beloved family

Para a minha familia

ABSTRACT

Easel paintings are important Cultural Heritage assets with significant historic and cultural value. They usually possess a multi-tiered structure, composed of different layers, some of which may present protein binders. Proteins have been commonly used as paintings medium, adhesives and coating layers in easel paintings. Hence, their recognition is a crucial step for easel painting's conservation and restoration processes. The present work presents a novel fluorescent labelling methodology, using a coumarin derivative chromophore, C392STP (sodium (*E/Z*)-4-(4-(2-(6,7-dimethoxycoumarin-3-yl)vinyl)benzoyl)-2,3,5,6-tetrafluorobenzenesulfonate) as a fluorophore probe to bond proteinaceous binders used in paintings. The method was developed and optimized using commercial proteins and proteins extracted from hen's egg yolk and white, bovine milk, and rabbit skin. In order to mimic the real conditions, paint models of easel paintings have been prepared by mixing proteins such as ovalbumin, casein and rabbit glue with different pigments (lead white, chrome yellow and black bone) and the fluorescent labelling method was miniaturized and tested. The results revealed that proteins in concentration as low as 6.0 µg/ml could be detected.

Finally, for validation methodology, real micro samples of easel paintings were analyzed. The extracted proteins were submitted to the fluorescent labelling method developed and clearly identified in electrophoretic profiles. The results evidence the applicability of this methodology as an effective and useful analytical tool for the identification of protein binders obtained from easel paintings and, possibly in other art work.

Additionally, theoretical quantum chemical calculations based on the Density Functional Theory (DFT) and Time Dependent Density Functional Theory (TD-DFT) have been performed in the C392STP coumarin and in a related coumarin derivative ((*E/Z*)-4-(2-(6,7- dimethoxycoumarin-3-yl)vinyl)-N-propylbenzamide), that mimics the coumarin bonded to lysine. The calculations confirm the experimental trends in absorption wavelengths and are in good agreement with the experimental absorption spectra, providing a comprehensive characterization of the main spectral features of the studied compounds.

KEYWORDS

fluorescent labelling method, coumarins, protein binders, easel paintings.

RESUMO

Identificação de ligantes proteicos em arte

As pinturas de cavalete são um componente importante do Património Cultural, com um significativo valor histórico e cultural. Geralmente possuem uma estrutura composta por diferentes camadas, algumas das quais podem apresentar ligantes proteicos. As proteínas surgem geralmente em pinturas de cavalete como meio de suporte da pintura, adesivos e camadas de revestimento. A sua identificação é, portanto, um passo crucial para os processos de conservação e restauração da pintura de cavalete. O presente trabalho apresenta uma nova metodologia de marcação fluorescente, utilizando um cromóforo derivado da cumarina, C392STP ((*E/Z*)-4-(2-(6,7- dimetoxicoumarin-3-yl)vinil)-N-propilbenzamida) como sonda fluorescente para marcar os ligantes proteicos usados em pinturas. O método foi desenvolvido e otimizado utilizando proteínas comerciais e proteínas extraídas da gema e clara de ovo de galinha, de leite de bovino e de pele de coelho. Para simular as condições reais, foram preparados modelos de pintura de pinturas de cavalete, misturando-se proteínas como ovalbumina, caseína e cola de coelho, com diferentes pigmentos (branco de chumbo, amarelo de crómio e negro de osso) e o método de marcação fluorescente foi miniaturizado e testado. Com base nos resultados obtidos, o método revelou-se capaz de detetar proteínas a concentração tão baixa quanto 6,0 µg / ml.

Finalmente, para validação do método, foram analisadas micro amostras reais de pinturas de cavalete. As proteínas extraídas foram submetidas ao método de marcação fluorescente desenvolvido, tendo sido claramente identificadas em perfis eletroforéticos. Os resultados evidenciam a aplicabilidade desta metodologia como uma ferramenta analítica eficaz e útil para a identificação de ligantes proteicos extraídos de pinturas de cavalete e, possivelmente, de outras obras de arte.

Adicionalmente, foram realizados cálculos quânticos baseados na Teoria Funcional da Densidade (DFT) e na Teoria do Funcional da Densidade Dependente do Tempo (TD-DFT) da cumarina C392STP de um derivado desta cumarina, ((*E/Z*)-N-propyl-4-(2-(6,7-dimethoxy-2-

oxo-2H-chromen-3-yl)vinyl)benzamide)), que modela a cumarina ligada a lisina. Os cálculos confirmam as tendências experimentais observadas nos comprimentos de onda de absorção e estão de acordo com os espectros de absorção experimentais, fornecendo uma caracterização abrangente das principais características espectrais dos compostos estudados.

PALAVRAS-CHAVE

método de marcação fluorescente, cumarinas, ligantes proteicos, pinturas de cavalete

ACKNOWLEDGEMENT

There have been many people who have helped me during the research. I am grateful to the Erasmus Mundus Programme for the financial support for a duration of 27 months through the gLINK project. I would like to thank them especially my supervisors, Professor Ana Teresa Caldeira for helping me a lot during the research especially in the application on paint models and easel paintings. Specially thanks to Professor João Paulo Prates Ramalho, who has allocated a lot of times with me to do the theoretical quantum chemical calculations. Much appreciation from me to Professor António Manuel Deométrio Rodrigues Lourenço Pereira who taught me a lot on the lab work in fluorescent labelling. With your guidance, the research has been progressing more smoothly. I would also like to thank Glink project for the financial support. A big thank you especially to Miss Cátia Salvador who have helped me in operating some procedures in the laboratory also all the colleagues in the laboratory who provided helps when I needed and special thanks to my dearest friend, Miss Reaksa, who has helped me in reading the thesis. Finally, special thanks to my family members, my parents: Cheng Huat and Ah Lik, siblings: Su Min, Su Li, Yin Pin who support me throughout the journey unconditionally.

TABLE OF CONTENTS

LIST OF TABLES

LIST OF FIGURES

LIST OF ABBREVIATIONS

C392STP	Coumarin 392 4-sulfotetrafluorophenyl coumarin ester
DFT	Density functional theory
TD-DFT	Time dependent density functional theory
PAGE	Plyacrylamide gel electrophoresis
BNP	Biblioteca nacional de portugal
XRF	X-ray fluorescence
SEM-EDX	Scanning electron microscope with energy dispersive X-ray spectroscopy
GC-MS	Gas chromatography-mass spectrometry
LC-MS	Liquid chromatography-mass spectrometry
ELISA	Enzyme-linked immunosorbent assay
SERS	Surface enhanced raman scattering
UV	ultraviolet
MM	Molecular mechanics
IR	infrared
HOMO	Highest occupied molecular orbital
LUMO	Lowest unoccupied molecular orbital
g	gram
mmol	milimoles
equiv	equivalent
nm	Nano-meter
kcal	kilocalorie
THF	tetrahydrofuran
BSA	Bovine serum albumin
R.T.	Room temperature
ml	millilitre

rpm	Rotation per minute
HCl	Hydrochloric acid
µg	Microgram
µl	microliter
MW	Molecular weight
kDa	kilodalton
mg	miligram
µm	Micrometer
PM	Paint model
h	hour

Chapter 1 INTRODUCTION

Easel paintings are extremely important Cultural Heritage assets with significant historic and cultural value. It emerged in the Middle Ages and since then have become one of the most important art expressions. Possessing multilayered structures composed of different layers, these artworks contain a diversity of organic materials, namely proteic compounds commonly produced from egg, milk or animal skin and bones. Proteins in paintings can be found in painting binders, adhesives, and additives in coating layers. The wide range of organic and inorganic materials mixtures in the painting's matrices makes the detection of the different protein materials a difficult task and contribute to the complexity of the materials identification [1]. The degradation of the materials in the paintings due to aging and improper storage conditions also complicate the protein materials detection [2, 3]. Furthermore, improper restoration practices like repainting, coatings application and over cleaning that can cause alteration of the original painting materials can interfere with the protein identification too [2, 4, 5]. Besides that, strategies commonly used to detect proteins, such as chromatographic, spectroscopic and proteomic techniques are useful but costly because the instruments involved are expensive, while immunological methodologies involve expensive commercially manufactured antibodies. It is then of paramount importance to develop analytical, low invasive, approaches in protein identification in order to design appropriate restoration and conservation methods or even to acquire deeper insights into a particular artist's technique.

1.1 Scope and objectives

The main objective of this PhD research was to develop a new fluorescent labelling method to identify different proteinaceous materials usually used in art. In order to perform the fluorescent labelling, a coumarin chromophore has been used. Initially, computational studies on the coumarin chromophore and of a related compound intended to mimic the chromophore-amino acid complex were done to explore its spectral features. Following the theoretical quantum chemical calculations, experimental works using C392STP [6] to fluorescent label the protein binders followed by electrophoretic separation and identification with protein patterns by PAGE (Polyacrylamide gel electrophoresis), that allows its detection and identification, were performed. Firstly, we have tested and optimized the protocols to bond C392STP to commercial proteins such as BSA (A2153), ovalbumin (A5378), casein (C3400), collagen (C9879) and fish gelatin (G7765). The optimized method was then used on proteins extracted from hens' egg yolk and white, bovine milk and rabbit skin using the previously optimized protocol [7]. To improve the fluorescent labelling methodology, by taking into account the complexity of the painting matrices, namely the presence of pigments and the aging processes, we have studied the method on laboratory made paint models. The proteinaceous content was extracted from the paint models and the extracted protein was used to bind with C392STP. Finally, the method was applied on real easel paintings samples.

Figure 1.1 shows the PhD research roadmap of the work developed on this thesis. From the studies of C392STP using theoretical methods to the construction of the protocols for fluorescent labelling using C392STP and continuing to applications, this roadmap can provide the reader with a brief overview of this research route.

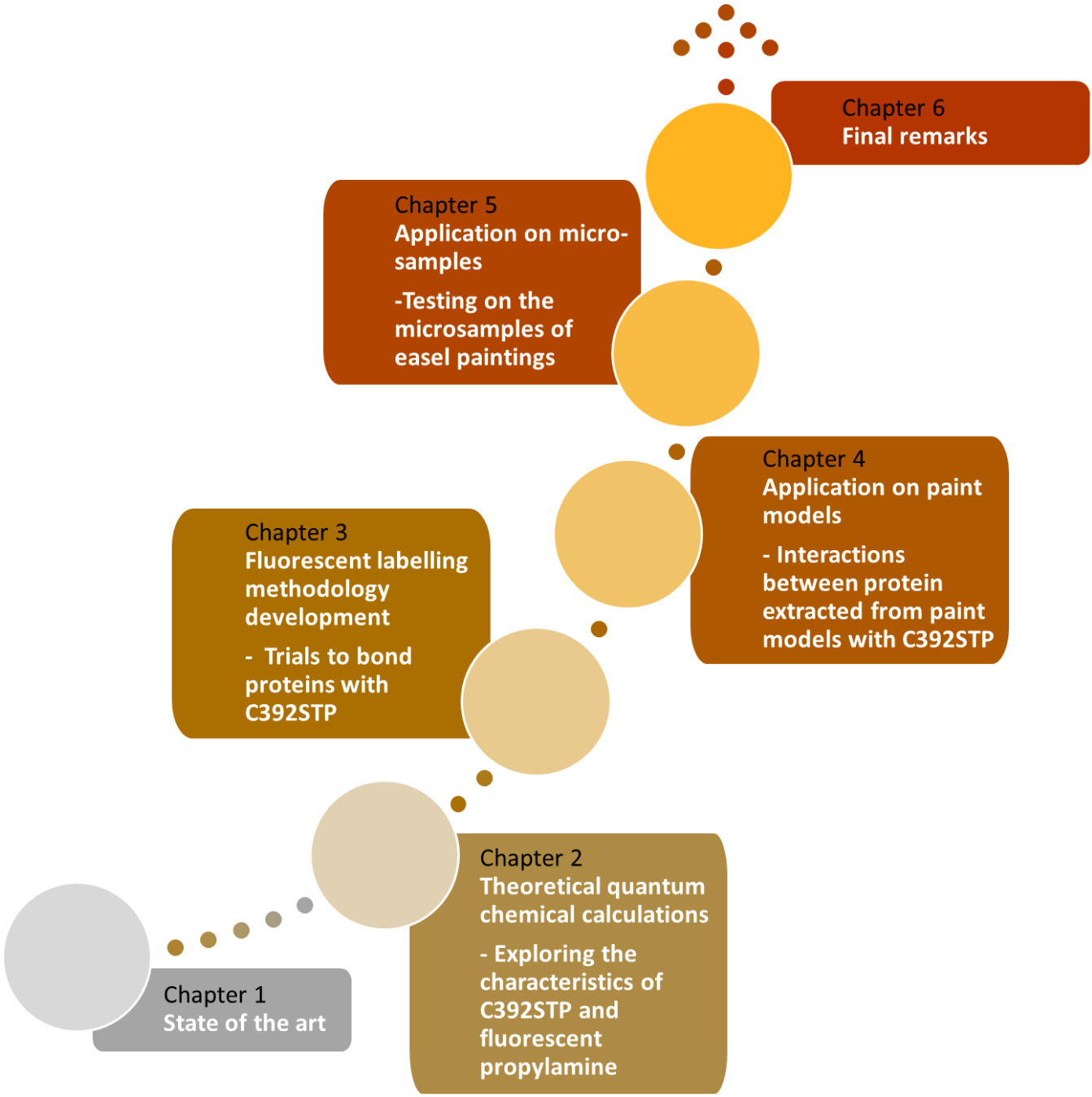

Figure 1.1 PhD research roadmap.

1.2 Easel painting

Generally, easel means a frame with legs which is made from wood. It is used to hold either a picture, a painting or a drawing [8, 9]. Easel painting refers to a midsize painting that an artist has painted on an easel. Easel paintings are composed of a few layers as shown in Figure 1.2. Usually, the materials used for the supports are either wood, canvas or metal.

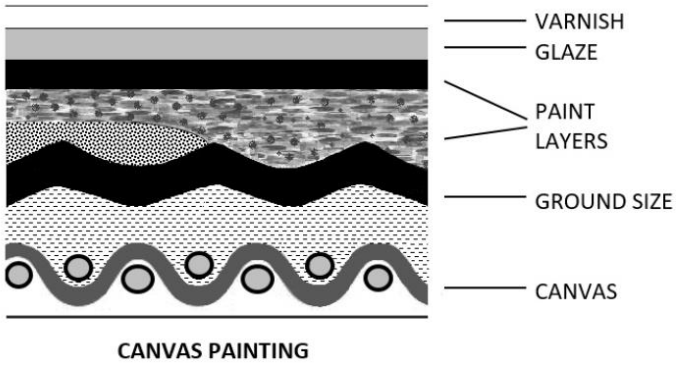

Figure 1.2 Structure of an easel painting [10].

The first layer applied on the support is the ground layer/preparation layer which can either be gesso (animal glue and calcium sulfate or animal glue with calcium carbonate), oil (drying oil and white lead pigment) or bole (red clay, normally applied on gesso layer). After producing a smooth surface, chromatic layers/paint layers (a mixture of organic binders and pigments) are applied. Several binders used include egg tempera (egg yolk and pigment), drying oil (linseed/walnut/poppyseed), distemper (animal glue or casein paint) and ecaustic (wax). Lastly, a surface coating (semitransparent glazes and transparent varnish) is applied for the aesthetic presentation as well as for protective purposes [8–12]. Easel paintings emerged in the Middle Ages and since then have been one of the most important art expressions, constituting today's relevant Cultural Heritage assets with important historical and cultural values. Paintings as earlier as 15th century are exhibited in the museums.

In the history of art, artists used a variety of materials to paint. The materials and techniques used may vary among the artists, studios or guilds [11]. Since the period of Renaissance, artists chose natural binding media which can produce the desired effects [12]. Another interesting point to consider is the techniques to draw the underdrawing which also differed among the artists and workshops [13]. The compositions of the easel paintings produced in different countries might be different, depending on the availability of the materials and the difference in the practice of the artists. For an example, the painting “Lady of the Rose” in the National Museum of Machado de Castro, Coimbra, dating from the first half of the 15th century, exhibits as main characteristics the use of vibrant colors, the lack of perspective, and larger scale of the sacred figures, with the use of tempera and painted on chestnut panel. This information evidence that it is a work from the workshop of Coimbra [14]. The artist frequently adapted his skills to the resource available at the time. An example is the famous Portuguese-Flemish painter, Frei Carlos, who has produced his paintings adapting the concepts of the Portuguese painters.

The main objective of research on easel painting is to understand the structure of the easel paintings in order to plan a conservation strategy, according to the information gathered. Normally, the first step is to identify the painting materials used. The characterization of the materials allows us to understand the structure of the paintings, as well as the cause of the changes, happened on the paintings. Besides, material studies may also reveal previous restoration works done [3, 15]. After gathering enough information on the paintings, a strategy to preserve the paintings, such as the selection of materials suitable for restoration [3], can be decided. Another point to be considered is the creation of an environment suitable to display or store the artwork [5]. The presence of the proteins can be the nutritional source for the growth of microorganism that contributes to the deterioration of the paintings. For instance, the mixture of ovalbumin, collagen, and casein found in the paintings was suggested to be the cause of microbial contamination [11].

1.3 Organic materials in easel paintings

A diversity of organic materials, especially proteinaceous compounds (Figure 1.3), has been used as binders, adhesives and additives in coating layers in easel paintings. Egg ovalbumin, milk casein and animal glue collagen produced from animals' bones, cartilages and skins are among the most commonly found proteins in the artworks [4, 16, 17]. These proteic compounds sometimes used together with siccative oils is known as tempera [4, 18].

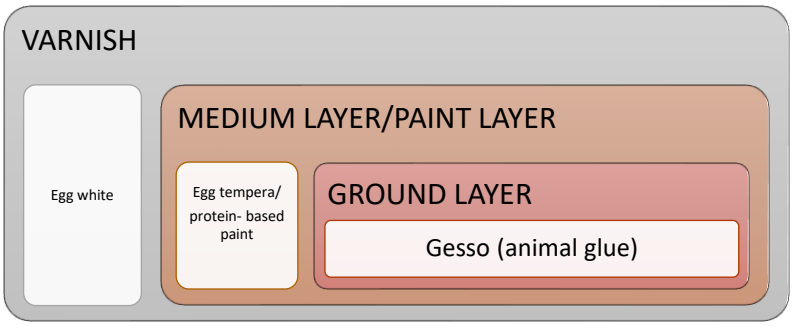

Figure 1.3 Proteinaceous binders commonly used.

Unfortunately, those organic materials are particularly susceptible to the environmental conditions [5] as shown in Figure 1.4. Exposure to the environment cause changes in the organic materials which contribute to composition changes. The surface of the painting, particularly, can degrade under different conditions of lighting, humidity, and temperature [5, 19]. Another factor responsible for structural damages are the degradation compounds produced by pollution [4, 20].

In this way, materials identification, particularly proteins, from paint samples are challenging because:

i. The detection of the different protein materials in these complexes matrices is a difficult task; wide ranges of organic and inorganic materials mixture in the paintings contribute to the complexity of the materials identification [1, 17, 21].
ii. Protein alterated/ degradated [1, 17].

iii. Limited amount of sample; destruction on the artworks must be limited to a minimum [17, 21].

iv. Low protein concentration in the sample [22].

v. Low solubility [4].

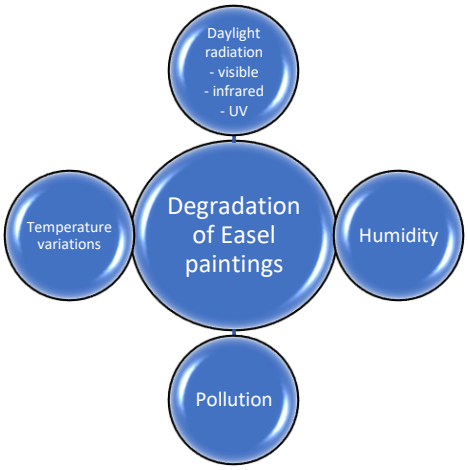

Figure 1.4 Factors contributing to the degradation of easel paintings.

Due to the high importance of the preservation of these artworks, the correct identification of proteinaceous binders is a crucial step for an understanding of the techniques used by the artist, and to provide relevant information for conservation and restoration processes [19]. It is then of paramount importance to develop low invasive analytical methodologies in protein identification in artwork materials that are suitable for protein identification in painting samples.

1.4 Proteinaceous binder detection

The ubiquitous presence of proteins in artworks as binders, adhesives and additives in coating layers makes their identification an important step for characterizing the artist technique and for the development of appropriate conservation and restoration treatments. The pioneer work was initiated by Ostwald [23] in 1936, by using biological dyes such as iodesine or acid

green to stain proteins. The use of iodesine/acid green to stain proteins allowed the identification of some binders for the first time. Solutions of ammonium hydroxide containing iodesine stained tempera and glue red while solutions of methyl violet stained tempera and glue violet. Acid green could stain gelatin and casein and vanillin were also able to stain tempera red or violet [24]. The study of binders in paintings using staining tests were also reported by other studies [25]. Nile blue could stain drying oil effectively while acid fuchsin stained animal glue and egg tempera. Acid fuchsin has already been found to be effective in staining protein through the reaction with the ammonium group of proteins since the early 20th century [24, 25].

The use of other classical colorimetric reactions such as the ninhydrin reaction, the Biuret reaction, the Millon reaction, and the Sakaguchi reaction, among others, have been used for the detection of proteins in paintings [26]. These methods based on the production of visible stains presented limited sensitivity and, depending on the pigment present in the painting sample, produced visible stains that could be difficult to distinguish. Nowadays analytical methods such as high-performance liquid chromatography (HPLC), gas chromatography (GC), combined with mass spectrometric (MS) detection, and thin-layer chromatography infrared spectrometry methods are commonly used in the identification of proteinaceous binders in paintings being capable to distinguish between egg, animal glue and milk proteins [15, 22, 27–33].

Proteomic is used in a broad range of studies like clinical medicine, forensic, food analysis and the origins of life [34, 35]. In the early 2000, the use of proteomic methods was suggested in cultural heritage studies to analyze proteins in artworks including archeological samples [17, 34–37]. Proteomics techniques were adapted to the scientific analysis of archeological microsamples and research work was developed [35, 36] focused on the optimization of the protocols to address the problem of the small quantity of the aged and deteriorated microsamples.

A new technique using Matrix-Assisted Laser Desorption/Ionization-Time of Flight Mass Spectrometry (MALDI-TOF-MS) was used to detect protein components in painting. Painting models were formulated using egg white, lead white pigment, and linseed oil while another

with whole egg, lead white pigment and linseed oil [33]. Application of new protocol of MALDI analysis has also been tried on paint models produced from a mixture of lead white pigment and egg yolk, whole egg, linseed oil or both egg and oil [38] while the further simplification of MALDI protocol was tested on a mixture of inorganic pigments and egg, milk and collagen applied on glass slide [39]. Another study by Romero-Pastor and colleagues [18] tried for the first time the use of PCA on MALDI-TOF-MS-data in cultural heritage using paint models prepared with rabbit glue and rabbit glue with cinnabar or azurite in glue tempera production. Three painting models were prepared based on old medieval recipes.

Nonetheless, there are a few limitations of those methods that need to be considered. Firstly, chromatographic and proteomics techniques involve laborious sample treatment [39] which only experts can implement [4, 40]. It is important to take note that chromatographic methods involve the hydrolysis of the protein in the sample and this can reduce the amount of information (origins of protein, degradation level and interaction between pigment and binder) one can get from the sample [30]. Secondly, expensive instruments are required in performing those techniques [40]. Thirdly, the analysis of the sample using chromatographic and spectroscopic methodology is largely dependent on the characteristics of the sample such as the composition of the sample, level of degradation and contamination [41, 42]. Furthermore, the interpretation of the analysis using chromatographic techniques is difficult if the sample is a complex mixture of organic and inorganics materials [43, 44] and the results have lower specificity [33] when compared with immunological methods.

More recently immunological techniques inspired from biological methods such as Enzyme-Linked ImmunoSorbent Assay (ELISA) [41] or Surface Enhanced Raman Scattering (SERS) nanotags has been successfully used to localize/identify protein binders. The ELISA technique is particularly sensitive and specific in protein identification using antigen-antibody reactions [5, 21, 40, 42]. ELISA is a potential complementary analysis when the information of biological sources of proteins is needed from a sample. The emerging immunological techniques were tested to be used in cultural heritage studies. In the optimization of indirect ELISA to identify proteinaceous binders used in art work, tests have been made [21, 45] on paint models constructed based on old recipes that mimic easel painting/mural painting.

Layers of paint models were prepared by using gypsum and animal glue applied on wood panels. Then, the protein binders like whole egg/egg yolk/milk/bovine glue/rabbit glue were mixed with pigments in the ratio of pigment to binder=3:1. In order to test the dot-ELISA test, Potenza and colleagues [46] have prepared model paintings using egg and rabbit glue mixed with red ochre pigment for tempera layer and applied it on mortar surfaces. Gambino et al. (2013) [47] further study the application of non-competitive dot-blot immunoassay and addressed pigment and aging effects using microsamples of paint replicas prepared in the laboratory; egg white and pigments were mixed and applied on glass slides. In the study by Sciutto et al. (2011) [48], the use of chemiluminescent immunochemical microscope imaging has been tested on ovalbumin and casein followed by testing on collagen [44]. Testing have been done on paint models prepared according to ancient painting recipes in which gypsum and rabbit glue (weight ratio of 19:1) has been applied as ground layer and a mixture of inorganic pigments and rabbit glue (blue smalt: rabbit glue=2:1)/ egg (lead white: egg=20:13)/ casein (red ochre: casein=10:7) as paint layers.

In order to address the challenge of doing on site analysis, one recent study by Zangheri et al (216) [40] tried a newly developed portable analytical device on paint models which were prepared according to ancient painting recipes; gypsum and rabbit glue were applied on wood panel followed by inorganic pigments and egg (egg white: yolk: water= 1:1:1). The combination of immunological techniques and chemiluminescence detection reported the possibility of ovalbumin identification in the paint models as well as from samples of canvas painting, wall painting and painted wood panels. Nevertheless, the main limitation of this method is that it can only detect proteins which are part of the assay [5, 21, 40, 42, 45]. Therefore, negative results from ELISA assays cannot confirm the absence of other proteins. Furthermore, ELISA test is time-consuming [49]. The analysis are also highly costly as materials such as expensive commercially manufactured antibodies specifically tailored for cultural heritage study [41] are needed. Both chromatographic techniques as well as immunological techniques involve expensive equipment and require specialized personnel [5].

In recent years, protein detection based on fluorescence techniques using fluorescent organic compounds has received much attention. Its use for protein detection in paintings was proposed in the end of the 1980s [50]. Thereafter, several dyes like fluorescamine, LISSA, fluorescein isothiocyanate (FITC) and cycloheptaamylose-dansyl chloride complex (DC-C7A) fluorochrome have been introduced [50, 51]. More recently, a ruthenium complex commercial dye, SYPRO Ruby, has also been used for detection of proteins in the works of art, including paintings. These fluorescent dyes interact with different functional groups in the proteins [52, 53] producing fluorescent products. Both fluorescamine and LISSA reacts with primary amines of proteins during fluorescent labelling [24, 54]; the reaction involving primary amines is shown in Figure 1.5.

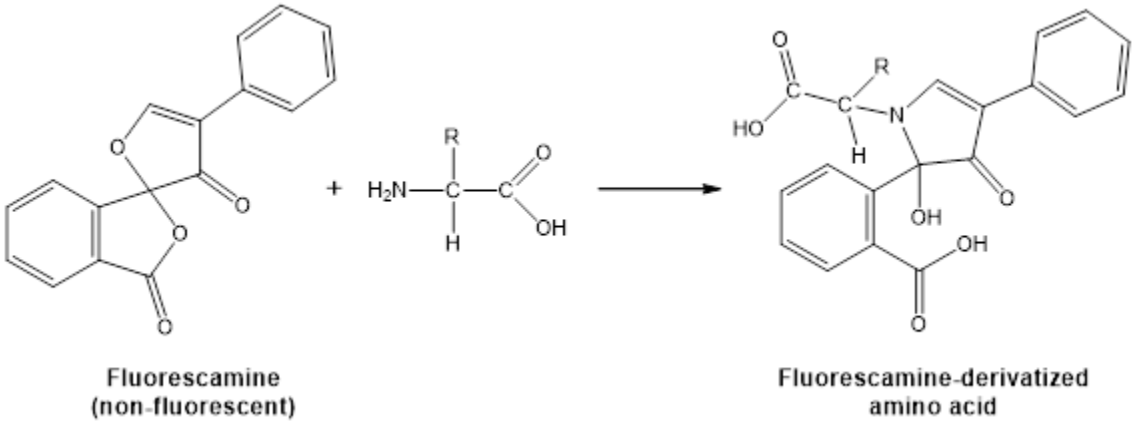

Figure 1.5 Example of fluorescent labelling targeting primary amines of proteins (adapted from Skelley et al., 2003) [54].

In the reaction between FITC and proteins, the sulfhydryl group can also be involved. The same happens with DC-C7A in which the sulfonyl chlorides/isothiocyanates of DC-C7A react with the primary amines and thiols of the proteins [24, 55]. Sypro Ruby is a noncovalent stain adapted from the biomedical field for protein identification through protein mapping, using gel electrophoresis [24, 56]. Staining using Sypro Ruby have been tried on paints [56], a polychromy section of an altarpiece [37, 57], sculptures [58] and on easel painting samples [52]; proteins commonly used in art work (egg, animal glue, fish glue) could be successfully

detected. These fluorescent dye, however, are very expensive and must be used with parsimony [59].

The applicability of a particular molecule as a fluorescent dye is highly dependent on its photophysical and photochemical properties like UV−vis absorption and fluorescence spectra, molar extinction coefficients, quantum efficiencies, Stokes shifts, pH and thermal stabilities among others [60]. Many coumarins (benzopyranones) and coumarin derivatives fit these conditions, which make it particularly adequate for use in fluorescent labelling [61]. The use of coumarin derivatives as fluorescent dyes will be discussed in the following section. The identification of proteinaceous components in paintings remains a challenging task and much effort have been made to develop simpler and less time consuming approaches [39, 40, 46, 62]. Table 1.1 shows a list of some recent research on current methods used in protein detection in art.

Table 1.1 Examples of research using different methodologies to detect proteins in art.

Methodology	**Samples**	**Authors**
Immunofluorescence	Proteins in paint media	Ramírez-Barat et al., 2001 [63]
In-situ Pyrolysis and Silylation	Proteinaceous binders	Chiavari et al., 2003 [64]
Combined GC/MS	Proteinaceous materials in paint microsample	Andreotti et al., 2006 [15]
Enzyme-linked immunosorbent assay and immunofluorescence microscopy	Protein-based materials	Heginbotham et al., 2006 [65]
Proteomics	Proteins in Renaissance paintings	Tokarski et al., 2006 [36]
Chemiluminescence imaging detection combined with optical microscopy	Protein components in painting	Dolci et al., 2008 [66]

Immunofluorescence microscopy	Proteins in painting	Vagnini et al., 2008 [1]
Gas chromatography/mass spectrometry	Organic paint media	Colombini et al., 2010 [22]
Proteomic strategies	Proteinaceous binders in paintings	Leo et al., 2009 [17]
FT-NIR spectroscopy	Organic components in painting materials	Vagnini et al., 2009 [1]
Enzyme-linked immunosorbent assay (ELISA) and immuno-fluorescence microscopy (IFM) techniques	Proteins in ancient paint media	Cartechini et al., 2010 [41]
Liquid chromatography–tandem mass spectrometry	Protein binders in historical paints	Fremout et al., 2010 [30]
GC/MS	Proteinaceous materials from paint microsample	Lluveras et al., 2010 [43]
Surface enhanced Raman scattering (SERS) nanotags	Avian egg, animal glue, or casein binders	Arslanoglu et al. ,2011 [67]
Enzyme-linked immunosorbent assay (ELISA)	Bovine milk (or casein) and chicken albumen	Palmieri et al., 2011 [45]
Indirect Enzyme-Linked Immunosorbent Assay (ELISA) method	Proteinaceous binding media and adhesives	Schultz and Petersen, 2011 [42]
Multiplexed chemiluminescent immunochemical imaging technique	Organic components in the complex stratigraphy of paintings	Sciutto et al., 2011 [48]
Radiographs and technical photographs, x-ray fluorescence	Materials in the portraits executed between	Soares et al. 2012 [3]

	the 16th and 19th centuries from National Library of Portugal (BNP)	
Dot-blot immunoassay	Egg white	Gambino et al. 2013 [47]
Enzyme-linked immunosorbent assay (ELISA)	Animal glue and hen-egg yolk	Palmieri et al. 2013 [21]
Chemiluminescent imaging detection	Animal glues	Sciutto et al., 2013 [44]
MALDI-MS	Lipid- and protein-based binders	Calvano et al. 2015 [39]
XRF, optical microscopy, Raman spectroscopy, and SEM-EDX	Pigments and fillers on the paintings by Giorgio Marini	Bordalo et al. 2016 [68]
Combined surface analysis and microanalytical techniques	Materials of the underdrawings of the Flemish-Portuguese easel paintings	Valadas et al. 2016 [13]
Chemiluminescent immunochemical contact imaging	Chicken ovalbumin	Zangheri et al. 2016 [40]
Scanning electron microscopy analyses, Energy-dispersive X-ray spectroscopy, μ-X-ray diffraction, μ-Raman, μ-FTIR and optical microscopy, immunological assays	Painting materials of the easel paintings by Giorgio Marini	Salvador et al. 2017 [11]

1.5 Use of coumarin derivatives

Coumarins/benzo-α-pyrones/2H-chromen-2-one/1-benzopyran-2-one are large family of compounds, consisting of a fusion of a pyrone and a benzene ring, with the pyrone carbonyl at position 2 (Figure 1.6) [69].

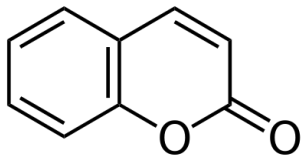

Figure 1.6 Chemical structure of coumarin.

Coumarins possess a variety of biological activity including antibacterial, anticancer, anticoagulant, antifungal, antihelmintic, anti-HIV, anti-inflammatory, antimicrobial, antioxidant, antiviral, estrogenic, dermal photosensitising, vasodilator, molluscucidal, sedative and hypnotic, analgesic and hypothermic activity [70–78]. Studies reported the used of coumarin derivatives in different fields like biology, chemistry, medicine, and pharmacology [79]. It has been applied as anesthetic in laboratory experiments, for fixing odors in perfume, in flavoring and in synthetic vanilla production, as a constituent of lavender oil, and as a natural source of essential antioxidants [80, 81].

Coumarin derivatives represent one of the most important chemical classes of fluorescent organic compounds, being one of the most extensively investigated and commercially significant groups of organic fluorescent materials [6, 70, 71, 82–84]. Some of its substituted derivatives can emit strong fluorescent light [84, 85]. It has been applied in fields such as biological science, environmental monitoring, clinical chemistry, DNA sequencing and genetic analysis by fluorescence in situ hybridization (FISH) [86]. Due to the outstanding photophysical properties of coumarin, it is used in:

i. High-performance liquid chromatography
ii. Studying heterogeneous chemical systems and media

iii. Generating fluorescent derivatives

iv. Probing proteins [69, 86]

Coumarin derivatives provide some of the most important commercial fluorescent brightening agents and appropriately substituted compounds are also used as highly effective fluorescent dyes on synthetic fibers and in daylight fluorescent pigments, conveying a vivid brilliance to a range of paint and printing ink applications. In addition, fluorescent coumarins may be used in a range of applications which specifically exploit their light emission properties, including non-destructive flaw detection, tunable dye lasers, emission layers in organic light-emitting diodes (OLED) and solar energy collectors. The most commonly-encountered fluorescent coumarins either absorb in the UV region emitting blue light (FBAs) or are yellow dyes emitting a green fluorescence [70, 87, 88]. Although several derivatives that both absorb and emit at long wavelengths are known, there is much interest in the molecular design and synthesis of new coumarins derivatives which would extend the available range of long-wavelength emitting fluorescent materials [87, 88].

In particular, coumarins that react with target biomolecules, metals or reactive groups have been extensively exploited as fluorescent labels [89–94]. Examples include the coumarins that have amine reactive moieties, tetrafluorophenyl (TFP) or N-hydroxysuccinimide (NHS) esters, which are effective dyes for biolabelling of molecules possessing primary amine groups [60, 95–97].

It is known that the 4-sulfotetrafluorophenyl coumarin esters, like coumarin 392 STP ester, bonds covalently with amino acids [98], particularly with the lysine side chain amine, providing an efficient labelling. Coumarin392STP, the coumarin derivative fluorophore that was studied in this work, possesses very interesting physicochemical characteristics as a large Stokes shift, pH-independence of absorbance and emission and excellent photo-stability [99]. Other properties of this coumarin derivative include a high fluorescent quantum yield, and easiness to synthesize, and its possession of photophysical and spectroscopic properties which can be easily tailored according to the desired application [6, 70]. These properties,

together with its low cost, point to the possibility of C392TFP to become a fluorescent dye with a wide range of applications in bioimaging and biolabelling.

This work proposes using the coumarin derivative chromophore (Coumarin 392 4-sulfotetrafluorophenyl coumarin ester) [6] to develop a new simple, fast and affordable protocol to detect and identify protein binders used in easel paintings. Figure 1.7 shows a model of C392STP labelling a protein. The proteinaceous extracted from the paints are made react with the coumarin chromophore that binds to the proteins and its fluorescent properties allow an easy detection and identification of the proteins separated by gel electrophoresis. Furthermore, the step of electrophoresis gel staining is not needed in the identification process.

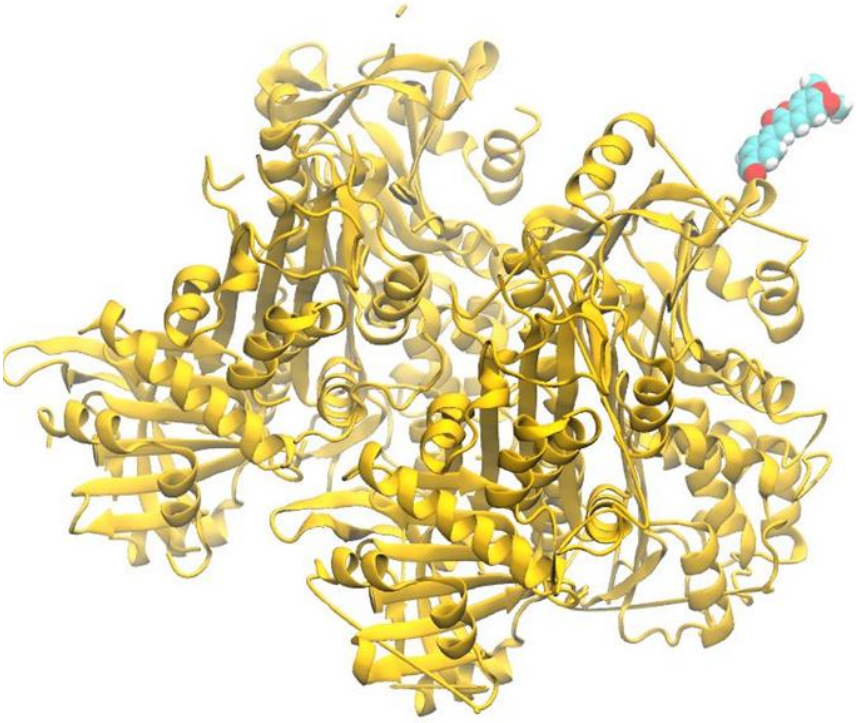

Figure 1.7 Model of C392STP labelling a protein (ovalbumin).

1.6 Theoretical quantum calculation

Quantum chemistry is based on the application on chemistry of methods derived from the laws of quantum mechanics [100]. A few years after the introduction of the Schrödinger equation, the Hartree-Fock approach was introduced and it has been widely used in the quantum chemistry research [101]. Not long after, post-Hartree Fock ab initio method, based on the wave function, has been introduced to address the question on the correlation between electrons [101].

Parallelly, Density Functional Theory (DFT) which is based on Hohenberg-Kohn [102], and Kohn and Sham [103] theorems were also proposed [101, 104, 105]. It is also known as static DFT and formally has the form of an effective one-particle Schrödinger equation [104]. Since then, DFT has been used widely in modeling the ground states of molecules [106, 107]. DFT methods have an increasing popularity in first principles quantum chemical calculations that explore the electronic structure [84, 108–110]. Less CPU time is required when compared with conventional ab initio calculations, it computes the results with greater accuracy than the Hartree-Fock Theory and solvent effect can be taken into account [84, 108, 110]. That makes nowadays DFT as the leading method in theoretical quantum chemical calculation for electronic structure exploration [109].

A few years later, time dependent DFT (TD-DFT), an extension of DFT, has been proposed by Runge and Gross [111]. The TD-DFT method has been proposed for the exploration of electronic excited-states energies [84, 112]. It is formulated in the form of an effective two-particle equation [104] which can be used to calculate the transition energies, dipole moments and emitting geometries [113]. It is now established that TD-DFT theory is an accurate method for analyzing structural, thermodynamic, kinetic and spectroscopic properties [84, 114–120] providing good results with a lower computational cost [101, 105, 121] when compared with other approaches. Parac and Grimme (2002) [122] have shown the applicability of TD-DFT on calculating excitation energies of large molecules.

There are in the literature many examples of DFT and TD-DFT calculations on coumarin and coumarin derivatives, a few of them reported in Table 1.2. In one study 30 coumarin derivatives were studied to investigate molecular properties such as the energy of the highest occupied molecular orbital (HOMO) and the lowest unoccupied molecular orbital energy (LUMO), the energy gap and the dipole moment, by using DFT together with the B3LYP functional and the 6-31G* basis set [81]. Also, a recent work has produced benchmarking studies that explored the spectroscopic characteristic of the absorption spectra of 25 coumarin derivatives [123, 124].

In the study, DFT and TDDFT methods with different functionals and basis set have been used to study the absorption spectra of a diversity of simple coumarins and furanocoumarins derivatives. The calculated spectra were well estimated when comparing to the experimental spectra. The properties of solvated coumarins have also been studied using TDDFT calculations [125–127]. The combination of the functionals and the polarizable continuum model (PCM) was found useful in the study of solvent effects. It is known that PCM is able to give a good estimation of solvent effects [128] with solvatochromic and Stokes' shift calculated presenting good agreement with experimental values [126]. The choice of the functional is largely dependent on the type of the coumarin, the accuracy required, and the computational cost allocated [125, 128].

Table 1.2 Key references of theoretical quantum chemical calculations on coumarin derivatives.

Subjects	**Methodology**	**Authors**
Coumarins 151 and 120	Time-Dependent Density Functional Theory (TDDFT) calculations against CASSCF, CASPT2 (both single and multistate versions), CIS, and ZINDO	Cave 2002 [129]
Coumarin derivatives	Density Functional Theory framework (DFT) at Becke–Lee–Yang–Parr functional (B3LYP)/6-311+G(2d,2p) basis set	Preat et al., 2005 [120]

Acetyl coumarin	DFT and Hartree- Fock (HF) at 6-31G* and 6-311++G** basis sets	Bahgat 2006 [130]
Coumarin derivatives	PBE0/6-31+G(*d)*	Jacquemin et al. 2006 [84]
Coumarin based dyes	TDDFT with the Baer, Neuhauser, and Livshits BNL RSH functional,	Stein et al. 2009 [131]
7-acetoxy-4-methyl coumarin	Density functional theory at B3LYP/6-311+G** basis set	Arivazhagan et al. 2010 [80]
Coumarin–thiourea conjugate	Ab initio molecular orbital calculations	Shiraisi et al. 2010 [118]
3-cyano-4-methylcoumarin	Density functional theory (DFT) at 6-31G(d,p) basis sets	Chaitanya et al. 2012 [79]
3,4-dihydrocoumarin and 3-methylcoumarin	SQM force field method based on ab initio and DFT calculation at 6-311++G(d,p) basis set	Arivazhagan et al. 2014 [132]
7-Acetoxy-4-(Bromomethyl)Coumarin	DFT calculation at B3LYP/6-311++G(d,p) basis set	Erdogdu et al. 2015 [86]
coumarin 151	TDDFT/EFP1	Ramegowda et al. 2015 [127]
V-shaped bis-coumarins	DFT and TDDFT with the M06-2X hybrid exchange–correlation functional	Šimon Budzák et al. 2016
Coumarin derivatives	Density functional theory (DFT) methods at B3LYP functional and a 6-31G* basis set	Hmamouchi et al. 2016 [81]
Simple coumarins and Furanocoumarins derivatives	DFT functional CAM-B3LYP, WB97XD, HSEH1PBE, MPW1PW91 and TD-B3LYP with 6-31 + G (d,p) basis set	Irfan et al., 2017 [124]

The literature also shows several studies focused on a specific type of coumarins. For instance, properties such as conductivity, solvatochromism, gas-phase spectroscopy, solution-phase spectroscopy and electroabsorption spectroscopy of coumarin 151 [129, 133–135] and coumarin 120 [129, 135, 136] were thoroughly studied. The properties of coumarin 120 and coumarin 151 were investigated using TDDFT calculations founding close agreement with the experimental S1←S0 excitation energies [129]. It is also reported that the PBE0 and the MPW1PW91 hybrid functionals gave the better results presenting results nearer to the experimental values [114, 129]. Barone and colleagues presented the UV-Vis absorption spectrum of 7-amino-coumarin based on TDDFT calculations [126, 137]. According to the calculations, the B3LYP functional provided the more reliable geometry the 7-aminocoumarin, among those functionals tested.

In this work, theoretical quantum chemical calculations based on the DFT and TDDFT have been performed on both the E and the Z isomers of C392STP coumarin, the fluorophore label molecule that we used as a probe to bond proteinaceous binders used in paintings. Calculations were also done on a related compound that mimics the fluorescent coumarin bonded with a protein amino acid amine side chain.

Bibliography

[1] M. Vagnini, L. Pitzurra, L. Cartechini, C. Miliani, B. G. Brunetti, and A. Sgamellotti, "Identification of proteins in painting cross-sections by immunofluorescence microscopy," *Anal. Bioanal. Chem.*, vol. 392, no. 1–2, pp. 57–64, 2008.

[2] A. J. Cruz, "Em busca da imagem original: Luciano Freire e a teoria e a prática do restauro de pintura em Portugal cerca 1900," *Conserv. Património*, vol. 5, pp. 67–83, 2007.

[3] C. M. Soares, R. M. Rodrigues, A. J. Cruz, and C. Rêgo, "Historical and material approach to the paintings at the Portugal National Library: contributions to the history of conservation and restoration of easel painting in the 19th century," *Int. J. Herit. Digit. era*, vol. 1, no. supplement 1, pp. 283–288, 2012.

[4] M. P. Colombini and F. Modugno, "Characterisation of proteinaceous binders in artistic paintings by chromatographic techniques," *J. Sep. Sci.*, vol. 27, no. 3, pp. 147–160, 2004.

[5] J. Arslanoglu, J. Schultz, J. Loike, and K. Peterson, "Immunology and art: Using antibody-based techniques to identify proteins and gums in artworks," *J. Biosci.*, vol. 35, no. 1, pp. 3–10, 2010.

[6] S. M. Martins, P. C. Branco, and A. M. D. L. Pereira, "An Efficient Methodology for the Synthesis of 3-Styryl Coumarins," *J. Braz. Chem. Soc.*, vol. 23, no. 4, pp. 688–693, 2012.

[7] C. Salvador, A. Branco, A. Candeias, and A. T. Caldeira, "Innovative approaches for immunodetection of proteic binders in art," *E-Conservation J.*, no. 5, pp. 1–10, 2017.

[8] "Cambridge Dictionary Online," *Cambridge University Press*, 2008. [Online]. Available: https://dictionary.cambridge.org/dictionary/english/easel. [Accessed: 16-Apr-2018].

[9] "Oxford Dictionary of English," *Oxford University Press*, 2015. [Online]. Available: https://en.oxforddictionaries.com/definition/easel. [Accessed: 16-Apr-2018].

[10] J. R. Allred, "Characterization of Hidden Paint Layer Topography Using a Stereographic XRF Approach," Delft University of Technology, 2017.

[11] C. Salvador, R. Bordalo, M. Silva, T. Rosado, A. Candeias, and A. T. Caldeira, "On the conservation of easel paintings: evaluation of microbial contamination and artists materials," *Appl. Phys. A Mater. Sci. Process.*, vol. 123, no. 1, p. 80, 2017.

[12] E. Albertini, L. Raggi, M. Vagnini, A. Sassolini, A. Achili, G. Marconi, and C. Miliani, "Tracing

the biological origin of animal glues used in paintings through mitochondrial DNA analysis," *Anal. Bioanal. Chem.*, vol. 399, no. 9, pp. 2987–2995, 2011.

[13] S. Valadas, R. Freire, A. Cardoso, J. Mirao, P. Vandenabeele, O. J. Caetano, and A. Candeias, "New insight on the underdrawing of 16th Flemish-Portuguese easel paintings by combined surface analysis and microanalytical techniques," *Micron*, vol. 85, pp. 15–25, 2016.

[14] "Museu Nacional Machado de Castro, Coimbra," 2019. [Online]. Available: http://www.museumachadocastro.gov.pt/en-GB/4 coleccoes/painting/ContentDetail.aspx?id=438.

[15] A. Andreotti, M. Bonaduce, M. P. Colombini, G. Gautier, F. Modugno, and E. Ribechini, "Combined GC/MS analytical procedure for the characterization of glycerolipid, waxy, resinous, and proteinaceous materials in a unique paint microsample," *Anal. Chem.*, vol. 78, no. 13, pp. 4490–4500, 2006.

[16] W. Fremout, S. Kuckova, M. Crhova, J. Sanyoya, S. Saverwyns, R. Hynek,…, and L. Moens, "Classification of protein binders in artist's paints by matrix-assisted laser desorption/ionisation time-of-flight mass spectrometry: An evaluation of principal component analysis (PCA) and soft independent modelling of class analogy (SIMCA)," *Rapid Commun. Mass Spectrom.*, vol. 25, no. 11, pp. 1631–1640, 2011.

[17] G. Leo, L. Cartechini, P. Pucci, A. Sgamellotti, G. Marino, and L. Birolo, "Proteomic strategies for the identification of proteinaceous binders in paintings," *Anal. Bioanal. Chem.*, vol. 395, no. 7, pp. 2269–2280, 2009.

[18] J. Romero-Pastor, N. Navas, S. Kuckova, A. Rodríguez-Navarro, and C. Cardell, "Collagen-based proteinaceous binder-pigment interaction study under UV ageing conditions by MALDI-TOF-MS and principal component analysis," *J. Mass Spectrom.*, vol. 47, no. 3, pp. 322–330, 2012.

[19] M. Elias, N. Mas, and P. Cotte, "Review of several optical non-destructive analyses of an easel painting. Complementarity and crosschecking of the results," *J. Cult. Herit.*, vol. 12, no. 4, pp. 335–345, 2011.

[20] H. E. Ahmed and Y. E. Ziddan, "A new approach for conservation treatment of a silk textile

in Islamic Art Museum , Cairo," *J. Cult.*, vol. 12, pp. 412–419, 2011.

[21] M. Palmieri, M. Vagnini, L. Pitzurra, B. G. Brunetti, and L. Cartechini, "Identification of animal glue and hen-egg yolk in paintings by use of enzyme-linked immunosorbent assay (ELISA)," *Anal Bioanal Chem*, vol. 405, pp. 6365–6371, 2013.

[22] M. P. Colombini, A. Andreotti, I. Bonaduce, F. Modugno, and E. Ribechini, "Analytical strategies for characterizing organic paint media using gas chromatography/mass spectrometry," *Acc. Chem. Res.*, vol. 43, no. 6, pp. 715–727, 2010.

[23] W. Ostwald, "Iconoscopic studies I: Microscopic identification of homogenous binding mediums," *Tech. Stud. F. Fine Art*, vol. 4, no. 3, pp. 135–44, 1936.

[24] S. Dallongeville, N. Garnier, C. Rolando, and C. Tokarski, "Proteins in Art, Archaeology, and Paleontology: From Detection to Identification," *Chem. Rev.*, vol. 116, no. 1, pp. 2–79, 2016.

[25] J. Plesters, "Cross-sections and Chemical Analysis of Paint Samples," *Stud. Conserv.*, vol. 2, no. 3, pp. 110–157, 1956.

[26] M. C. Gay, "Essais D'Identification Et De Localisation Des Liants Picturaux Par Des Colorations Specifique Sur Coupe Mince," *Ann. du Lab. Rech. des Museés Fr.*, pp. 8–24, 1970.

[27] A. Lluveras, I. Bonaduce, A. Andreotti, and M.P. Colombini, "GC/MS Analytical Procedure for the Characterization of Glycerolipids, Natural Waxes, Terpenoid Resins, Proteinaceous and Polysaccharide Materials in the Same Paint Microsample Avoiding Interferences from Inorganic Media," *Anal. Chem.*, vol. 82, no. 1, pp. 376–386, 2010.

[28] M. T. Doménech-Carbó, "Novel analytical methods for characterising binding media and protective coatings in artworks," *Anal. Chim. Acta*, vol. 621, no. 2, pp. 109–139, 2008.

[29] R. Checa-Moreno, E. Manzano, G. Mirón, and L. F. Capitan-Vallvey "Comparison between traditional strategies and classification technique (SIMCA) in the identification of old proteinaceous binders," *Talanta.*, vol. 75, no. 3, pp. 697-704, 2008.

[30] W. Fremout, M. Dhaenens, S. Saverwyns, J. Sanyova, P. Vandenabeele, D. Deforce, and L. Moens, "Tryptic peptide analysis of protein binders in works of art by liquid chromatography-tandem mass spectrometry," *Anal. Chim. Acta*, vol. 658, no. 2, pp. 156–162, 2010.

[31] S. Kuckova, M. Crhova, L. Vankova, A. Hnizda, R. Hynek, and M. Kodicek, “Towards proteomic analysis of milk proteins in historical building materials,” *Int. J. Mass Spectrom.*, vol. 284, no. 1–3, pp. 42–46, 2009.

[32] A. Nevin, D. Comelli, G. Valentini, D. Anglos, A. Burnstock, S. Cather, and R. Cubeddu, “Time-resolved fluorescence spectroscopy and imaging of proteinaceous binders used in paintings,” *Anal. Bioanal. Chem.*, vol. 388, no. 8, pp. 1897–1905, 2007.

[33] C. Tokarski, E. Martin, C. Rolando, and C. Cren-Olivé, “Identification of Proteins in Renaissance Paintings by Proteomics,” *Anal. Chem.*, vol. 78, no. 5, pp. 1494–1502, 2006.

[34] S. Have, Y. Ahmad, and A. I. Lamond, “Analytical & Bioanalytical Proteomics – Current Novelties and Future Directions,” no. 3, pp. 1–6, 2011.

[35] R. Vinciguerra, A. De Chiaro, P. Pucci, G. Marino, and L. Birolo, “Proteomic strategies for cultural heritage : From bones to paintings,” *Microchem. J.*, vol. 126, pp. 341–348, 2016.

[36] C. Tokarski, E. Martin, C. Rolando, M. Post-traductionnelles, and A. Cedex, “Identification of Proteins in Renaissance Paintings by Proteomics John the Baptist , St . Sebastian (XVth century), and,” *Analysis*, vol. 78, no. 5, pp. 1494–1502, 2006.

[37] S. Dallongeville, M. Richter, S. Schäfer, M. Kühlenthal, N. Garnier, C. Rolanda, and, C. Tokarski, “Proteomics applied to the authentication of fish glue: application to a 17th century artwork sample,” *Analyst*, vol. 138, no. 18, p. 5357, 2013.

[38] C. D. Calvano, I. D. Van Der Werf, and F. Palmisano, “Fingerprinting of egg and oil binders in painted artworks by matrix-assisted laser desorption ionization time-of-flight mass spectrometry analysis of lipid oxidation by-products,” *Anal Bioanal Chem*, vol. 400, no. 7, pp. 2229–2240, 2011.

[39] C. D. Calvano, I. D. Van Der Werf, F. Palmisano, and L. Sabbatini, “Identification of lipid- and protein-based binders in paintings by direct on-plate wet chemistry and matrix-assisted laser desorption ionization mass spectrometry,” *Anal. Bioanal. Chem.*, vol. 407, no. 3, pp. 1015–1022, 2015.

[40] M. Zangheri, G. Sciutto, M. Mirasoli, S. Prati, R. Mazzeo, A. Roda, and M. Guardigli, “A portable device for on site detection of chicken ovalbumin in artworks by chemiluminescent immunochemical contact imaging,” *Microchem. J.*, vol. 124, pp. 247–

255, 2016.

[41] L. Cartechini, M. Vagnini, M. Palmieri, L.Pitzurra, T. Mello, J. Mazurek, and G. Chiari, “Immunodetection of proteins in ancient paint media,” *Acc. Chem. Res.*, vol. 43, no. 6, pp. 867–876, 2010.

[42] J. Schultz and K. Petersen, “Antibody-Based Techniques to Distinguish Proteins and Identify Sturgeon Glue in Works of Art,” in *Proceedings of Symposium 2011 – Adhesives and Consolidants for Conservation*, 2011, pp. 1–13.

[43] A. Lluveras, I. Bonaduce, A. Andreotti, and M. P. Columbini, “GC/MS analytical procedure for the characterization of glycerolipids, natural waxes, terpenoid resins, proteinaceous and polysaccharide materials in the same paint microsample avoiding interferences from inorganic media,” *Anal. Chem.*, vol. 82, no. 1, pp. 376–386, 2010.

[44] G. Sciutto, L.S. Dolci, M. Guardigli, M. Zangheri, S. Prati, R. Mazzeo, and A. Roda, “Single and multiplexed immunoassays for the chemiluminescent imaging detection of animal glues in historical paint cross-sections,” *Anal. Bioanal. Chem.*, vol. 405, no. 2–3, pp. 933–940, 2013.

[45] M. Palmieri, M. Vagnini, L. Pitzurra, P. Rocchi, B.G. Brunetti, A. Sgamellotti, and L. Cartechini, “Development of an analytical protocol for a fast, sensitive and specific protein recognition in paintings by enzyme-linked immunosorbent assay (ELISA),” *Anal. Bioanal. Chem.*, vol. 399, no. 9, pp. 3011–3023, 2011.

[46] M. Potenza, G. Sabatino, F. Giambi, L. Rosi, A. M. Papini, and L. Dei, “Analysis of egg-based model wall paintings by use of an innovative combined dot-ELISA and UPLC-based approach,” *Anal. Bioanal. Chem.*, vol. 405, no. 2–3, pp. 691–701, 2013.

[47] M. Gambino, F. Cappitelli, C. Cattò, A. Carpen, P. Principi, L. Ghezzi, … and F. Villa, “A simple and reliable methodology to detect egg white in art samples,” *J. Biosci.*, vol. 38, no. 2, pp. 397–408, 2013.

[48] G. Sciutto, L.S. Dolci, A. Buragina, S. Prati, M. Guardigli, R. Mazzeo, and A. Roda, “Development of a multiplexed chemiluminescent immunochemical imaging technique for the simultaneous localization of different proteins in painting micro cross-sections,” *Anal. Bioanal. Chem.*, vol. 399, no. 9, pp. 2889–2897, 2011.

[49] M. C. H. Janssen, A. E. Heebels, M. De Metz, H. Verbruggen, H. Wollersheim, S. Janssen, … and I. R. O. Novakova, “Reliability of five rapid D-Dimer Assays Compared to ELISA in the Exclusion of Deep Venous Thrombosis,” *Thromb. Haemost.*, vol. 77, no. 2, pp. 262–266, 1997.

[50] R. Wolbers and G. Landrey, “The use of direct reactive fluorescent dyes for the characterization of binding media in cross sectional examinations,” 1987.

[51] J. M. Messinger, “Ultraviolet-Fluorescence Microscopy of Paint Cross Sections: Cycloheptaamylose-Dansyl Chloride Complex as a Protein-Selective Stain,” *J. Am. Inst. Conserv.*, vol. 31, no. 3, pp. 267–274, 2013.

[52] D. Magrini, S. Bracci, and I. C. A. Sandu, “Fluorescence of Organic Binders in Painting Cross-sections,” *Procedia Chem.*, vol. 8, pp. 194–201, 2013.

[53] I. C. A. Sandu, S. Schäfer, D. Magrini, S. Bracci, and C. A. Roque, “Cross-Section and Staining-Based Techniques for Investigating Organic Materials in Painted and Polychrome Works of Art: A Review,” *Microsc. Microanal.*, vol. 18, no. 04, pp. 860–875, 2012.

[54] A. M. Skelley, F. J. Grunthaner, J. L. Bada, and R. A. Mathies, “Mars Organic Detector III : A Versatile Instrument for Detection of Bio-organic Signatures on Mars,” in *SPIE Proceedings*, 2003, no. April, pp. 59–67.

[55] J. M. Messinger, “Ultraviolet-Fluorescence Microscopy of Paint Cross Sections : Cycloheptaamylose-Dansyl Chloride Complex as a Protein-Selective Stain,” *J. Am. Inst. Conserv.*, vol. 31, no. 3, pp. 267–274, 1992.

[56] I. C. A. Sandu, A.C.A. Roque, P. Matteini, S. Schä fer, G. Agati, C.R. Correia, and J.F.F.P Viana, “Fluorescence recognition of proteinaceous binders in works of art by a novel integrated system of investigation,” *Microsc. Res. Tech.*, vol. 75, no. 3, pp. 316–324, 2012.

[57] I. C. A. Sandu, E. Nurta, R. Veiga, V.S.F. Wall, M. Pereira, S. Kuckova, and T. Busani, “An innovative, interdisciplinary, and multi-technique study of gilding and painting techniques in the decoration of the main altarpiece of Miranda do Douro Cathedral (XVII-XVIIIth centuries, Portugal),” *Microsc. Res. Tech.*, vol. 76, no. 7, pp. 733–743, 2013.

[58] S. Kuckova, I. C. A. Sandu, M. Crhova, R. Hynek, I. Fogas, and S. Schafer, “Protein identification and localization using mass spectrometry and staining tests in cross-sections

of polychrome samples," *J. Cult. Herit.*, vol. 14, no. 1, pp. 31–37, 2013.

[59] R. J. Simpson, "Fluorescent Staining of Proteins with SYPRO Ruby," pp. 2006–2009, 2006.

[60] X. Liu, J. M. Cole, and K. S. Low, "Solvent effects on the uv-vis absorption and emission of optoelectronic coumarins: A Comparison of three empirical solvatochromic models," *J. Phys. Chem. C*, vol. 117, no. 28, pp. 14731–14741, 2013.

[61] A. R. Katritzky and N. Tamari, "Fluorescent amino acids: advances in protein-extrinsic fluorophores," *Org. Biomol. Chem.*, vol. 7, no. 4, pp. 627–634, 2009.

[62] P. Přikryl, L. Havlíčkova, V. Pacáková, J. Hradilová, K. Štulík, and P. Hofta, "An evaluation of GC-MS and HPLC-FD methods for analysis of protein binders in paintings," *J. Sep. Sci.*, vol. 29, no. 17, pp. 2653–2663, 2006.

[63] B. Ramírez Barat and S. de la Viña, "Characterization of proteins in paint media by immunofluorescence: a note on methodological aspects," *Stud. Conserv.*, vol. 46, no. 4, pp. 282–288, 2001.

[64] G. Chiavari, G. Lanterna, C. Luca, M. Matteini, S. Prati, and I. C. A. Sandu, "Analysis of proteinaceous binders by in-situ pyrolysis and silylation," *Chromatographia*, vol. 57, no. 9–10, pp. 645–648, 2003.

[65] A. Heginbotham, V. Millay, and M. Quick, "The use of immunofluorescence microscopy and enzyme-linked immunosorbent assay as complementary techniques for protein identification in artists' materials," *J. Am. Inst. Conserv.*, vol. 45, no. 2, pp. 89–105, 2006.

[66] L. S. Dolci, G. Sciutto, M. Guardigli, M. Rizzoli, S. Prati, R. Mazzeo, and A. Roda, "Ultrasensitive chemiluminescent immunochemical identification and localization of protein components in painting cross-sections by microscope low-light imaging," *Anal. Bioanal. Chem.*, vol. 392, no. 1–2, pp. 29–35, 2008.

[67] J. Arslanoglu, S. Zaleski, and J. Loike, "An improved method of protein localization in artworks through SERS nanotag-complexed antibodies," *Anal. Bioanal. Chem.*, vol. 399, no. 9, pp. 2997–3010, 2011.

[68] R. Bordalo, C. Bottaini, C. Moricca, and A. Candeias, "Material Characterisation of a Florentine painter in Portugal in the Late 19th century: paintings by Giorgio Marini," *Int. J. Conserv. Sci.*, vol. 7, no. 4, pp. 967–980, 2016.

[69] B. D. Wagner, “The use of coumarins as environmentally-sensitive fluorescent probes of heterogeneous inclusion systems,” *Molecules*, vol. 14, no. 1, pp. 210–237, 2009.

[70] S. Martins, P. S. Branco, M. C. Delatorre, M. A. Sierra, and A. Pereira, “New methodology for the synthesis of 3-substituted coumarins via palladium-catalyzed site-selective cross-coupling reactions,” *Synlett*, no. 19, pp. 2918–2922, 2010.

[71] A. R. Das, A. Medda, and R. Singha, “Synthesis of biologically potent new 3-(heteroaryl)aminocoumarin derivatives via Buchwald-Hartwig C-N coupling,” *Tetrahedron Lett.*, vol. 51, no. 7, pp. 1099–1102, 2010.

[72] Y. L. Garazd, E. M. Kornienko, L. N. Maloshtan, M. M. Garazd, and V. P. Khilya, “Modified coumarins. 17. Synthesis and anticoagulant activity of 3,4-cycloannelated coumarin D-glycopyranosides,” *Chem. Nat. Compd.*, vol. 41, no. 5, pp. 508–512, 2005.

[73] J. R. Hwu, R. Singha, S.C. Hong, Y.H. Chang, A.R. Das, I. Vliegen, … and J. Neyts., “Synthesis of new benzimidazole-coumarin conjugates as anti-hepatitis C virus agents,” *Antiviral Res.*, vol. 77, no. 2, pp. 157–162, 2008.

[74] O. Kayser and H. Kolodziej, “Antibacterial activity of simple coumarins: Structural requirements for biological activity,” *Zeitschrift fur Naturforsch. - Sect. C J. Biosci.*, vol. 54, no. 3–4, pp. 169–174, 1999.

[75] C. A. Kontogiorgis and D. J. Hadjipavlou-Litina, “Synthesis and antiinflammatory activity of coumarin derivatives,” *J. Med. Chem.*, vol. 48, no. 20, pp. 6400–6408, 2005.

[76] J. Neyts, E. Clercq, R. Singha, Y.H. Chang, A.R. Das, S.K. Chakraborty, … and J.R. Hwu, “Structure - Activity Relationship of New Anti-Hepatitis C Virus Agents: Heterobicycle - Coumarin Conjugates,” *J. Med. Chem*, vol. 52, no. 5, pp. 1486–1490, 2009.

[77] D. T. H. Phuong Thien Thuong, Tran Manh Hung, Tran Minh Ngoc and J. S. C. and K. B. Byung Sun Min, Seung Jun Kwack, Tae Suk Kang, “Antioxidant Activities of Coumarins from Korean Medicinal Plants and their Structure–Activity Relationships,” *Phyther. Res.*, vol. 24, pp. 101–106, 2010.

[78] M. Suzuki, K. Nakagawa-Goto, S. Nakamura, H. Tokuda, S.L. Morris-Natschke, M. Kozuka, and K.H. Lee, “Cancer preventive agents. Part 5. Anti-tumor-promoting effects of coumarins and related compounds on Epstein-Barr virus activation and two-stage mouse

skin carcinogenesis," *Pharm. Biol.*, vol. 44, no. 3, pp. 178–182, 2006.

[79] N. Udaya Sri, K. Chaitanya, M. V. S. Prasad, V. Veeraiah, and A. Veeraiah, "FT-IR, FT-Raman and UV-Vis spectra and DFT calculations of 3-cyano-4-methylcoumarin," *Spectrochim. Acta - Part A Mol. Biomol. Spectrosc.*, vol. 97, pp. 728–736, 2012.

[80] M. Arivazhagan, K. Sambathkumar, and S. Jeyavijayan, "Density functional theory study of FTIR and FT-Raman spectra of 7-acetoxy-4-methyl coumarin," *Indian J. Pure Appl. Phys.*, vol. 48, no. 10, pp. 716–722, 2010.

[81] R. Hmamouchi, M. Larif, S. Chtita, A. Adad, M. Bouachrine, and T. Lakhlifi, "Predictive modelling of the LD 50 activities of coumarin derivatives using neural statistical approaches: Electronic descriptor-based DFT," *J. Taibah Univ. Sci.*, vol. 10, no. 4, pp. 451–461, 2016.

[82] J. Gordo, J. Avó, A. J. Parola, J. C. Lima, A. Pereira, and P. S. Branco, "Convenient synthesis of 3-vinyl and 3-styryl coumarins," *Org. Lett.*, vol. 13, no. 19, pp. 5112–5115, 2011.

[83] C. R. Reddy, B. Srikanth, N. Narsimha Rao, and D. S. Shin, "Solid-supported acid-catalyzed C3-alkylation of 4-hydroxycoumarins with secondary benzyl alcohols: access to 3,4-disubstituted coumarins via Pd-coupling," *Tetrahedron*, vol. 64, no. 51, pp. 11666–11672, 2008.

[84] D. Jacquemin, E.A. Perpète, G. Scalmani, M.J. Frisch, X. Assfeld, I. Ciofini, and C. Adamo, "Time-dependent density functional theory investigation of the absorption, fluorescence, and phosphorescence spectra of solvated coumarins," *J. Chem. Phys.*, vol. 125, no. 16, 2006.

[85] J. R. Heldt, J. Heldt, M. Stoń, and H. A. Diehl, "Photophysical properties of 4-alkyl- and 7-alkoxycoumarin derivatives. Absorption and emission spectra, fluorescence quantum yield and decay time," *Spectrochim. Acta Part A Mol. Biomol. Spectrosc.*, vol. 51, no. 9, pp. 1549–1563, 1995.

[86] Y. Erdogdu, S. Saglam, and Ö. Dereli, "Theoretical (DFT) and experimental (FT-IR, FT-Raman, FT-NMR) investigations on 7-Acetoxy-4-(bromomethyl)coumarin," *Opt. Spectrosc.*, vol. 119, no. 3, pp. 411–423, 2015.

[87] R. M. Christie and C. H. Lui, "Studies of fluorescent dyes: Part 1. An investigation of the

electronic spectral properties of substituted coumarins," *Dye. Pigment.*, vol. 42, no. 1, pp. 85–93, 1999.

[88] R. M. Christie, K. M. Morgan, and M. S. Islam, "Molecular design and synthesis of N-arylsulfonated coumarin fluorescent dyes and their application to textiles," *Dye. Pigment.*, vol. 76, no. 3, pp. 741–747, 2008.

[89] H. Li, L. Cai, and Z. Chen, "Coumarin-Derived Fluorescent Chemosensors," *Adv. Chem. Sensors*, pp. 121–150, 2012.

[90] G. Wenska, M. Insińska, and B. Skalski, "Synthesis and solvatochromism of 2-(N-Pyridinio)-pyrimidin-4-olate and related betaines derived from uracils," *Pol. J. Chem.*, vol. 74, no. 5, pp. 659–671, 2000.

[91] A. Gandioso, R. Bresoli-Obach, A. Nin-Hill, M. Bosch, M. Palau Requena, A. Galindo Muñoz, and V. Marchán Sancho, "Redesigning the Coumarin Scaffold into Small Bright Fluorophores with Far-Red to Near-Infrared Emission and Large Stokes Shifts Useful for Cell Imaging," *J. Org. Chem.*, vol. 83, no. 3, pp. 1185–1195, 2018.

[92] H. Schill, S. Nizamov, F. Bottanelli, J. Bierwagen, V. N. Belov, and S. W. Hell, "4-Trifluoromethyl-substituted coumarins with large stokes shifts: Synthesis, bioconjugates, and their use in super-resolution fluorescence microscopy," *Chem. - A Eur. J.*, vol. 19, no. 49, pp. 16556–16565, 2013.

[93] J. Chen, W. Liu, B. Zhou, G. Niu, H. Zhang, J. Wu, and P.Wang, "Coumarin- and rhodamine-fused deep red fluorescent dyes: Synthesis, photophysical properties, and bioimaging in vitro," *J. Org. Chem.*, vol. 78, no. 12, pp. 6121–6130, 2013.

[94] R. P. Bhusal, P. Yun Cho, S. A. Kim, H. Park, and H. S. Kim, "Synthesis of green emitting coumarin bioconjugate for the selective determination of flu antigen," *Bull. Korean Chem. Soc.*, vol. 32, no. 5, pp. 1461–1462, 2011.

[95] B. Wetzl, M. Gruber, B. Oswald, A. Dürkop, B. Weidgans, M. Probst, and, O.S. Wolfbeis, "Set of fluorochromophores in the wavelength range from 450 to 700 nm and suitable for labeling proteins and amino-modified DNA," *J. Chromatogr. B Anal. Technol. Biomed. Life Sci.*, vol. 793, no. 1, pp. 83–92, 2003.

[96] I. Bora, S. A. Bogh, M. Santella, M. Rosenberg, T. J. Sørensen, and B. W. Laursen,

"Azadioxatriangulenium: Synthesis and Photophysical Properties of Reactive Dyes for Bioconjugation," *European J. Org. Chem.*, vol. 2015, no. 28, pp. 6351–6358, 2015.

[97] Z. Gao, Y. Hao, M. Zheng, and Y. Chen, "A fluorescent dye with large Stokes shift and high stability: synthesis and application to live cell imaging," *RSC Adv.*, vol. 7, no. 13, pp. 7604–7609, 2017.

[98] K. R. Gee, E. A. Archer, and H. C. Kang, "4-Sulfotetrafluorophenyl (STP) esters: New water-soluble amine-reactive reagents for labeling biomolecules," *Tetrahedron Lett.*, vol. 40, no. 8, pp. 1471–1474, 1999.

[99] M. González-Pérez, S. Y. Ooi, S. Martins, J. P. P. Ramalho, A. Pereira, and A. T. Caldeira, "Gaining insight into the photophysical properties of a coumarin STP ester with potential for bioconjugation," *New J. Chem.*, vol. 42, no. 20, pp. 16635–16645, 2018.

[100] J. B. Foresman and A. Frisch, *Exploring Chemistry with Electronic Structure Methods G*, Third Edit. Gaussian, 2015.

[101] A. Dreuw and M. Head-gordon, "Single-Reference ab Initio Methods for the Calculation of Excited States of Large Molecules," *Chem. Rev.*, vol. 105, pp. 4009–4037, 2005.

[102] P. Hohenberg and W. Kohn, "Inhomogeneous Electron Gas," *Phys. Rev.*, vol. 136, no. 3B, pp. B864–B871, 1964.

[103] W. Kohn and L. J. Sham, "Self-Consistent Equations Including Exchange and Correlation Effects," *Phys. Rev.*, vol. 140, no. 4A, pp. A1133–A1138, 1965.

[104] G. Onida, L. Reining, and A. Rubio, "Electronic excitations : density-functional versus many-body Green ' s-function approaches," *Rev. Mod. Phys.*, vol. 74, pp. 601–659, 2002.

[105] M. E. Casida, "Time-dependent density-functional theory for molecules and molecular solids," *J. Mol. Struct. THEOCHEM*, vol. 914, no. 1–3, pp. 3–18, 2009.

[106] C. Adamo and D. Jacquemin, "The calculations of excited-state properties with Time-Dependent Density Functional Theory," *Chem. Soc. Rev.*, vol. 42, pp. 845–856, 2013.

[107] M. Van Faassen and K. Burke, "Time-dependent density functional theory of high excitations: To infinity, and beyond," *Phys. Chem. Chem. Phys.*, vol. 11, no. 22, pp. 4437–4450, 2009.

[108] J. B. Foresman and A. Frisch, "Exploring Chemistry With Electronic Structure Methods.pdf,"

Exploring Chemistry with Electronic Structure Methods. p. 302, 1996.

[109] I. Y. Zhang, J. Wu, and X. Xu, "Extending the reliability and applicability of B3LYP," *Chem. Commun.*, vol. 46, no. 18, pp. 3057–3070, 2010.

[110] A. Tomberg, *Gaussian 09W Tutorial. An introduction to computational chemistry using G09W and Avogadro software*. 2013.

[111] E. Runge and E. K. Gross, "Density-functional theory for time-dependent systems," *Phys. Rev. Lett.*, vol. 52, no. 12, p. 997, 1984.

[112] K. Burke, J. Werschnik, and E. K. U. Gross, "Time-dependent density functional theory: Past, present, and future," *J. Chem. Phys.*, vol. 123, no. 6, p. 062206, 2005.

[113] D. Jacquemin and B. Mennucci, "Excited-state calculations with TD-DFT : from benchmarks to simulations in complex environments," *Phys. Chem. Chem. Phys.*, vol. 13, pp. 16987–16998, 2011.

[114] C. Adamo and V. Barone, "Toward reliable density functional methods without adjustable parameters: The PBE0 model," *J. Chem. Phys.*, vol. 110, no. 13, pp. 6158–6170, 1999.

[115] M. Cossi and V. Barone, "Time-dependent density functional theory for molecules in liquid solutions," *J. Chem. Phys.*, vol. 115, no. 10, pp. 4708–4717, 2001.

[116] E. J. Baerends, G. Ricciardi, A. Rosa, and S. J. A. Van Gisbergen, "A DFT/TDDFT interpretation of the ground and excited states of porphyrin and porphyrazine complexes," *Coord. Chem. Rev.*, vol. 230, no. 1–2, pp. 5–27, 2002.

[117] C. J. Jo and H. P. Lu, "Time-Dependent Density Functional Theory (TDDFT) Study of the Excited Charge-Transfer State Formation of a Series of Aromatic Donor - Acceptor Systems," *J. Am. Chem. Soc.*, vol. 125, no. d, pp. 252–264, 2003.

[118] Y. Shiraishi, S. Sumiya, and T. Hirai, "A coumarin – thiourea conjugate as a fluorescent probe for Hg (II) in aqueous media with a broad pH range 2 – 12," *Org. Biomol. Chem.*, vol. 8, pp. 1310–1314, 2010.

[119] K. B. Wiberg, A. E. De Oliveira, and G. Trucks, "A comparison of the electronic transition energies for ethene, isobutene, formaldehyde, and acetone calculated using RPA, TDDFT, and EOM-CCSD. Effect of basis sets," *J. Phys. Chem. A*, vol. 106, no. 16, pp. 4192–4199, 2002.

[120] J. Preat, D. Jacquemin, and E. A. Perpe, “Theoretical investigations of the UV spectra of coumarin derivatives,” *Chem. Phys. Lett.*, vol. 415, pp. 20–24, 2005.

[121] M. R. Silva-junior and W. Thiel, “Benchmark of Electronically Excited States for Semiempirical Methods: MNDO, AM1, PM3, OM1, OM3 , INDO/S , and INDO/S2,” *J. Chem. Theory Comput.*, vol. 6, pp. 1546–1564, 2010.

[122] M. Parac and S. Grimme, “Comparison of multireference Møller-Plesset theory and time-dependent methods for the calculation of vertical excitation energies of molecules,” *J. Phys. Chem. A*, vol. 106, no. 29, pp. 6844–6850, 2002.

[123] A. M. Asiri, “Synthesis and characterisation of new coumarin derivatives as ultraviolet absorbers,” *Pigment resin Technol.*, vol. 32, no. 5, pp. 326–330, 2003.

[124] M. Irfan, J. Iqbal, B. Eliasson, K. Ayub, U. Ali, and S. U. Khan, “Benchmark study of UV / Visible spectra of coumarin derivatives by computational approach,” *J. Mol. Struct.*, vol. 1130, pp. 603–616, 2017.

[125] A. D. Laurent and D. Jacquemin, “TD-DFT Benchmarks : A Review,” *Int. J. Quantum Chem.*, vol. 113, pp. 2019–2039, 2013.

[126] A. Pedone, “Role of Solvent on Charge Transfer in 7-Aminocoumarin Dyes: New Hints from TD-CAM-B3LYP and State Specific PCM Calculations,” *J. Chem. Theory Comput.*, vol. 9, pp. 4087–4096, 2013.

[127] M. Ramegowda, “Spectrochimica Acta Part A : Molecular and Biomolecular Spectroscopy A TDDFT / EFP1 study on hydrogen bonding dynamics of coumarin 151 in water,” *Spectrochim. ACTA PART A Mol. Biomol. Spectrosc.*, vol. 137, pp. 99–104, 2015.

[128] D. Jacquemin and E. A. Perpe, “Extensive TD-DFT Benchmark : Singlet-Excited States of Organic Molecules Organic Molecules,” *J. Chem. Theory Comput.*, vol. 5, pp. 2420–2435, 2009.

[129] R. J. Cave, K. Burke, and E. W. Castner, “Theoretical Investigation of the Ground and Excited States of Coumarin 151 and Coumarin 120,” *J. Phys. Chem. A*, vol. 106, pp. 9294–9305, 2002.

[130] K. Bahgat, “Scaled quantum chemical studies of the structural and vibrational spectra of acetyl coumarin,” *Cent. Eur. J. Chem.*, vol. 4, no. 4, pp. 773–785, 2006.

[131] T. Stein, L. Kronik, R. Baer, T. Stein, L. Kronik, and R. Baer, “Prediction of charge-transfer excitations in coumarin-based dyes using a range- separated functional tuned from first principles Prediction of charge-transfer excitations in coumarin-based dyes using a range-separated functional tuned from first principle,” *J. Chem. Phys.*, vol. 131, p. 244119, 2009.

[132] M. Arivazhagan, R. Kavitha, and V. P. Subhasini, “Spectroscopic and quantum chemical electronic structure investigations of 3,4-dihydrocoumarin and 3-methylcoumarin,” *Spectrochim. Acta - Part A Mol. Biomol. Spectrosc.*, vol. 130, pp. 502–515, 2014.

[133] B. A. Pryor, P. M. Palmer, P. M. Andrews, M. B. Berger, and M. R. Topp, “Spectroscopy of Jet-Cooled Water Complexes with Coumarin 151 : Observation of Vibronically Induced Conformational Barrier Crossing,” *J. Phys. Chem. A*, vol. 102, pp. 3284–3292, 1998.

[134] A. Mühlpfordt, R. Schanz, N. P. Ernsting, and S. Grimme, “Coumarin 153 in the gas phase : Optical spectra and quantum chemical calculations Coumarin 153 in the gas phase : optical spectra and quantum chemical calculations,” *Phys. Chem. Chem. Phys.*, vol. 1, pp. 3209–3218, 1999.

[135] A. Samanta and R. W. Fessenden, “Excited-State Dipole Moment of 7-Aminocoumarins as Determined from Time-Resolved Microwave Dielectric Absorption Measurements,” *J. Phys. Chem. A*, vol. 104, pp. 8577–8582, 2000.

[136] N. A. Nemkovich, H. Reis, and W. Baumann, “Ground and excited state dipole moments of coumarin laser dyes: Investigation by electro-optical absorption and emission methods,” *J. Lumin.*, vol. 71, no. 4, pp. 255–263, 1997.

[137] F. Muniz-miranda, A. Pedone, G. Battistelli, M. Montalti, J. Bloino, and V. Barone., “Benchmarking TD-DFT against Vibrationally Resolved Absorption Spectra at Room Temperature : 7-Aminocoumarins as Test Cases,” *J. Chem. Phys.*, vol. 11, pp. 5371–5384, 2015.

Chapter 2 THEORETICAL QUANTUM CHEMICAL CALCULATIONS

Part of the results have been published in:

- **S. Y. Ooi**, A. T. Caldeira, A. Pereira, and J. P. P. Ramalho, Abstract of "Labelling of proteinaceous binders: Density functional theory and time dependent density functional theory calculation on some coumarin derivatives," XIX National Congress of Biochemistry, pp. 87, 2016.

- M. González-Pérez, **S. Y. Ooi**, S. Martins, J. P. P. Ramalho, A. Pereira, and A. T. Caldeira, "Gaining insight into the photophysical properties of a coumarin STP ester with potential for bioconjugation," New J. Chem., vol. 42, no. 20, pp. 16635–16645, 2018.

2.0 Overview

This chapter aims to explore the electronic and spectroscopic characteristics of the coumarin derivative chromophore, Coumarin 392 4-sulfotetrafluorophenyl coumarin ester, C392STP (sodium (*E/Z*)-4-(4-(2-(6,7-dimethoxy-coumarin-3-yl) vinyl) benzoyl)-2,3,5,6-tetrafluorobenzenesulfonate) and of a simple model of C392STP bonded to an amino acid, (*E/Z*)-4-(2-(6,7- dimethoxycoumarin-3-yl)vinyl)-N-propylbenzamide.

Theoretical quantum chemical calculations based on the Density Functional Theory (DFT) and Time Dependent Density Functional Theory (TD-DFT) have been performed firstly on free C392STP. The same method was used to investigate (*E/Z*)-4-(2-(6,7- dimethoxycoumarin-3-yl)vinyl)-N-propylbenzamide. The spectroscopic characteristics of the free C392STP have been studied in several solvents. The DFT and TD-DFT calculations confirm the experimental trends in absorption wavelengths and are in good agreement with experimental absorption spectra.

2.1 Introduction

Nowadays, DFT calculations are the most commonly used methods in quantum chemistry [1, 2]. The most significant advantage of DFT methods when compared with the Hartree-Fock approach relays on a significant increase in accuracy without a substantial additional increase in computational time. It time dependent extension, the time-dependent density functional theory (TD-DFT), originally proposed by Runge and Gross [3], is also, probably, the most used approach for the theoretical calculation of electronic absorption spectra and excited-state properties [4–7].

The popularity of TD-DFT relay on its accuracy on the evaluation of excited state energies, on being much less computationally demanding when compared with ab initio wave function methods, its rapidity and applicability to large molecules [8–10] and also its relative simplicity of implementation [4]. It is known that DFT methods can predict with good accuracy the structure and spectroscopic properties of coumarins [11]. Thus, DFT calculations were

performed to gain more insight into the geometric and electronic properties of C392STP and (*E/Z*)-4-(2-(6,7- dimethoxycoumarin-3-yl)vinyl)-N-propylbenzamide.

Additionally, the accuracy is also depended on the environment of the model system. The use of continuum models is particularly attractive, due to its low computational cost when compared with methods that represent explicitly the surrounding solvent molecules. In continuum models, the model is divided into a solute part, lying inside a cavity, surrounded by the solvent part represented as a structureless material, characterized by some parameters like its dielectric constant, molar volume, the polarizability, etc. The polarizable continuum model (PCM) is one of the most widely used methods to bulk solvent effects [12–19]. In this approach, the solvent reaction field is represented as a set of charges, induced by the solute charge distribution, dispersed all over the solute cavity surface and has been found an essential tool to explore solvent effects and evaluate solvatochromic shifts for absorption and fluorescence.

In this chapter, the interaction between the target molecule and the solvent were considered by using the polarizable continuum model (PCM) [8, 9, 20-21]. In the first step, we used the theoretical methods to study the C392STP coumarin (Figure 2.1).

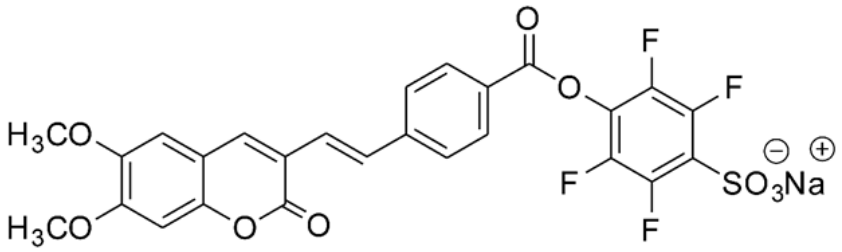

Figure 2.1 Structural formulas of the C392STP, sodium (*E/Z*)-4-(4-(2-(6,7-dimethoxy-coumarin-3-yl) vinyl) benzoyl)-2,3,5,6-tetrafluorobenzenesulfonate.

By doing this, we can gain a better understanding of the geometry, electronic structure and spectral features of the compound.

In the labeling process the chromophore, C392STP, bonds covalently with some amino acids [22] as depicted in Figure 2.2.

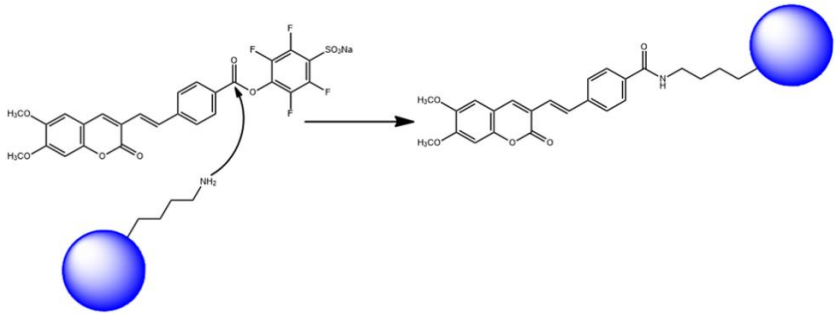

Figure 2.2 Reaction between C392STP and a protein side chain amino acid amine group.

To mimic the bonding of the coumarin chromophore with an amino acid we studied the (*E/Z*)-4-(2-(6,7- dimethoxycoumarin-3-yl)vinyl)-N-propylbenzamide, coumarin derivative (Figure 2.3), which results from the reaction of C392STP and propylamine. Based on the results, we can estimate the potential of C392STP as a chromophore probe to bind proteinaceous binders used in easel paintings.

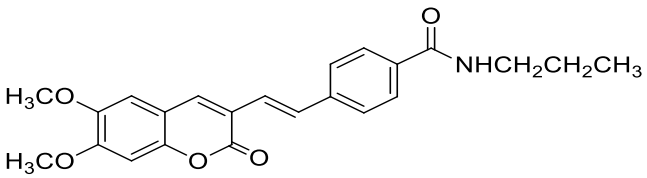

Figure 2.3 Chemical structure of (*E/Z*)-4-(2-(6,7- dimethoxycoumarin-3-yl)vinyl)-N-propylbenzamide.

2.2 Theoretical quantum chemical calculation

Theoretical quantum chemical calculations at DFT and TD-DFT level have been performed on the C392STP coumarin chromophore. Optimization of the molecular structures was performed with the widely used B3LYP hybrid functional together with the 6-31G (d,p) basis set. Subsequent frequency analysis was done to confirm the optimized geometries were in a minimum energy configuration by showing no imaginary frequencies. Next, TD-DFT was used for calculating the low-lying excited states and electronic transitions by using the hybrid PBE0 functional with the 6-311+g (2d, p) basis set. The equations were solved for 20 excited states. Initially, the conformational landscape of C392STP was explored in water. After that, the optimization of the geometry was also done in several other solvents including THF, acetone, dioxane, methanol by means of the implicit polarized continuum model (PCM) [13] in order to mimic the experimental conditions and also with an explicit water model.

After the calculations on the C392STP coumarin, we have studied the (*E/Z*)-4-(2-(6,7-dimethoxycoumarin-3-yl)vinyl)-N-propylbenzamide, coumarin derivative. Similar theoretical quantum chemical calculations at DFT and TD-DFT level have been performed on this coumarin derivative. Optimization of the molecular structures was performed by using the B3LYP hybrid functional with the 6-31G (d,p) basis set, followed by frequency analysis. Similarly, in order to mimic the experimental conditions, the optimization of the coumarin derivative geometry was done in acetonitrile solvent by means of the implicit polarized continuum (PCM) [13]. Next, TD-DFT was used for calculating the low-lying excited states and electronic transitions of the systems, by using the hybrid PBE0 functional together with the much larger 6-311+g (2d, p) basis set. The equations were solved for 20 excited states. All calculations were performed using the Gaussian 09 and Gaussian 16 software Packages [23].

2.3 Results and discussions

2.3.1 Study of the free coumarin derivative chromophore C392STP

The C392STP coumarin derivative chromophore can exist in two conformations, either as a *E* or a *Z* isomers. In real samples, depending on the synthesis conditions, coumarin compounds can appear as a mixture of E and Z isomers in different percentages.

The minimum-energy molecular geometry (Figure 2.4) has been computed through DFT calculations at B3LYP/6-31+G(d)/PCM level for both *E* and *Z* isomers, and the optimized geometries calculated in the solvent of THF are depicted in Figure 2.4.

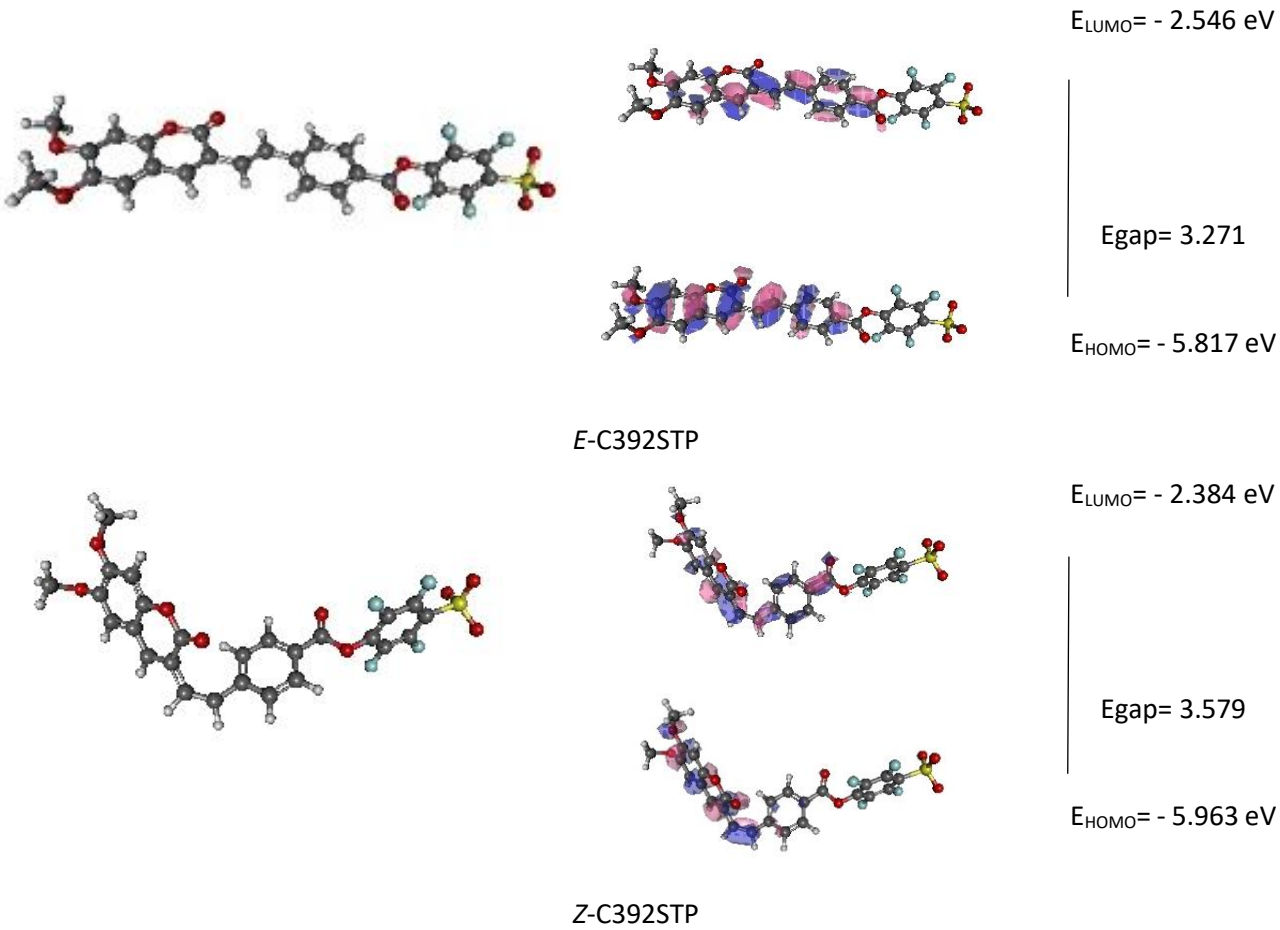

Figure 2.4 Optimized molecular geometry for *E*-C392STP and *Z*-C392STP in THF at the B3LYP/6-31+G(d) level and the HOMO and LUMO orbitals.

It was found that the E isomer has a nearly coplanar structure (with efficient pi conjugation) while the Z isomer is twisted out of plane of the carbon-carbon double bond (steric hindrance). In the case of *E*-C392STP, the calculated eigen values of LUMO and HOMO are – 5.817 eV and -2.546 eV respectively, with an energy gap of 3.271 eV (Figure 2.4). The HOMO orbital spread over the entire molecule while the LUMO orbital concentrates at the pyrone carbonyl group and benzene ring. This suggests that charge transfer can occur between the pyrone carbonyl group and benzene ring moiety, and the entire molecule through the C-C double bond. In the case of *Z*-C392STP, the calculated eigen values of LUMO and HOMO are – 5.963 eV and -2.384 eV respectively, with an energy gap of 3.579 eV. The spreading of the LUMO and HOMO orbitals on the molecule is similar for the *Z*-392STP isomer case. The optimized geometries were found to be similar in other solvents. Calculated energies for both isomers at the B3LYP/6-31+G(d) theory level of the C392STP coumarin in different solvents have been compared in Table 2.1. Based on the calculated energies values obtained, the *E* isomer has in all cases a lower energy as compare with the *Z* isomer. The energy difference is between 7.0 to 8.5 kcal/mol, depending on the solvent. These results show that the *E* isomer is the most stable form for both compounds as expected since the bulky groups on the same side on the *Z* isomer cause repulsive interactions forcing the aromatic ring out-of-plane. Also in experiments, the *E* isomer is the most abundant species as it is more stable when compared with the *Z* isomer. Based on the ^{1}H-RMN spectra, the *E* isomer constitutes 84% of the total while the *Z* isomer is 16 % which will be discussed in section 3.1.

Table 2.1 Calculated energies for the *E*-392STP and *Z*-C392STP isomers in different solvents at the B3LYP/6-31+G(d) theory level.

Solvent	**Energy (a.u)**		**ΔE (kcal mol^{-1})**
	E isomer	*Z* isomer	
Dioxane	-2474.4763	-2474.4629	8.41
THF	-2474.5127	-2474.5002	7.41
Acetone	-2474.5240	-2474.5120	7.53
Methanol	-2474.5264	-2474.5146	7.86
Water	-2474.5289	-2474.5172	7.33

Photophysical properties of the C392STP coumarin were explored through in silico calculations. The TD-DFT methodology has been used and the two isomers of the C392STP coumarin have been studied in dioxane, THF, acetone, methanol, and water modeled by the PCM model. A mixed implicit/explicit model, including explicit water molecules, has been studied as well.

The calculated lowest energy, oscillator strength (f) and the major contributions for the transitions for both isomers in different solvents were shown in Table 2.2. The lowest energy transitions of the C392STP coumarin, corresponding to the S0⟶S1 transition, is the most intense presenting the higher oscillator strength, for the both conformers, and it is similar in the different solvents. This lowest energy transition of the C392STP coumarin is mainly of HOMO⟶LUMO character in THF, methanol, water and in the explicit water model while is mainly of HOMO-1⟶LUMO character in dioxane and acetone (Figure 2.5).

Table 2.2 Calculated properties of the C392STP coumarin in different solvents at the PBE0/311+G(2d,p) level of theory.

	State	Wavelength, λ/nm	Oscillator strength (f)	Major transitions
Dioxane				
	S_1	*404*	*1.755*	*H-1->LUMO (99%)*
E	S_2	*318*	*0.026*	*H-4->LUMO (80%)*
	S_3	*317*	*0.121*	*H-1->L+1 (81%)*
	S_1	*378*	*0.916*	*H-1->LUMO (99%)*
Z	S_2	*323*	*0.0001*	*H-2->LUMO (83%)*
	S_3	*319*	*0.022*	*H-4->LUMO (45%)*
THF				
	S_1	409	1.773	H->L (99%)
E	S_2	324	0.046	H->L+1 (90%)
	S_3	320	0.085	H-2->L (86%)
	S_1	384	0.870	H->L (99%)
Z	S_2	324	0.093	H->L+1 (89%)
	S_3	314	0.175	H-2->L (84%)
Acetone				
	S_1	*407*	*1.770*	*H-1->LUMO (99%)*
E	S_2	*319*	*0.053*	*H-1->L+1 (83%)*
	S_3	*317*	*0.088*	*H-5->LUMO (76%)*
	S_1	*381*	*0.955*	*H-1->LUMO (99%)*
Z	S_2	*329*	*0.001*	*H-2->LUMO (92%)*
	S_3	*323*	*0.005*	*H-3->LUMO (86%)*
Methanol				
	S_1	410	1.753	H->L (99%)
E	S_2	326	0.031	H->L+1 (89%)
	S_3	321	0.106	H-1->L (85%)
	S_1	388	0.847	H->L (99%)
Z	S_2	327	0.124	H->L+1 (92%)
	S_3	315	0.172	H-1->L (86%)
H_2O				
	S_1	411	1.753	H->L (99%)
E	S_2	326	0.030	H->L+1 (89%)
	S_3	321	0.109	H-1->L (42%)
	S_1	389	0.842	H->L (99%)
Z	S_2	327	0.132	H->L+1 (92%)
	S_3	315	0.175	H-1->L (87%)
H_2O explicit				
	S_1	406	1.826	H->L (99%)
E	S_2	329	0.045	H->L+1 (94%)
	S_3	316	0.046	H-1->L (85%)
	S_1	375	0.786	H->L (99%)
Z	S_2	324	0.123	H->L+1 (92%)
	S_3	309	0.130	H-1->L (86%)

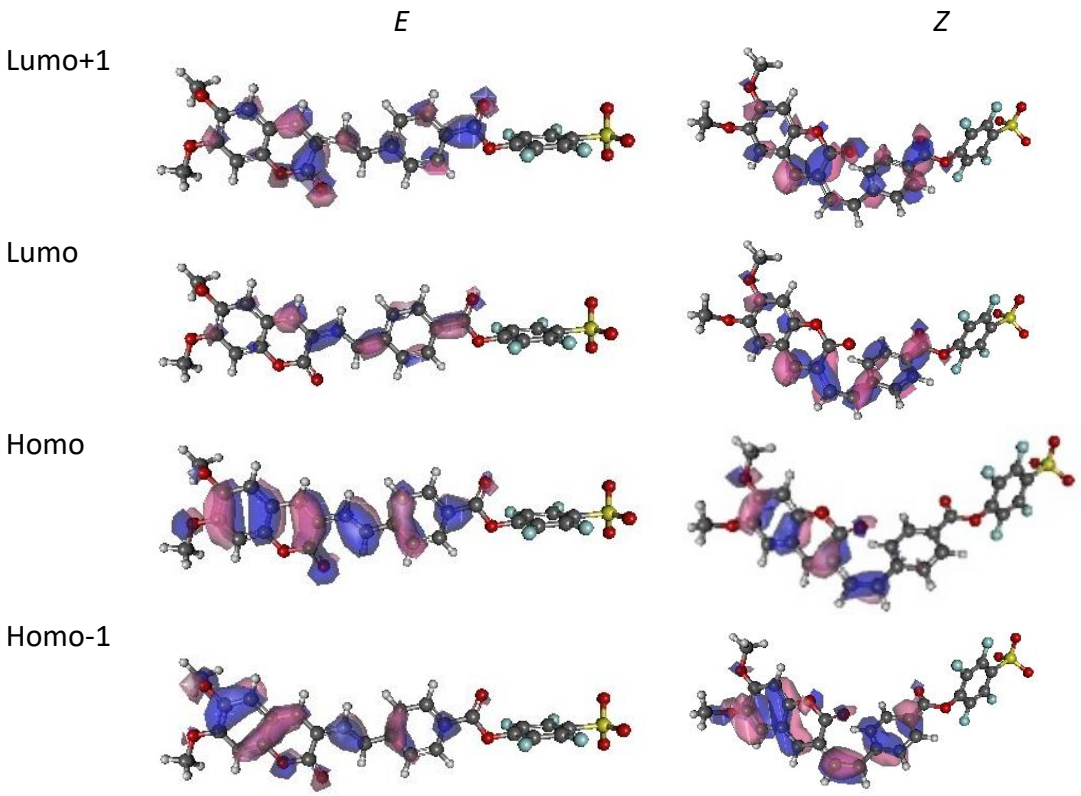

Figure 2.5 Schematic drawings of the frontier molecular orbitals of both isomers involved in the most important transitions for *E*- and *Z*-C392STP in acetone.

Simulated absorption spectra of the isomers in some solvents, comparing with experimental spectra, are shown in Figure 2.6 and the calculated absorption data of the lowest energy transition in table 2.3. The calculated lowest energy transition in non-aqueous solvents shows very good agreement with the experimentally measured wavelengths of the coumarin derivative chromophore absorption [24]. However, the model is not capable of reproducing the blue shift that occurs in water. This can be attributed to the use of a continuum model for a solvent in which specific interactions between the solute and the solvent may need special considerations. Therefore, an explicit solvent cluster model was also used to model the absorption spectra of the isomers in aqueous solutions.

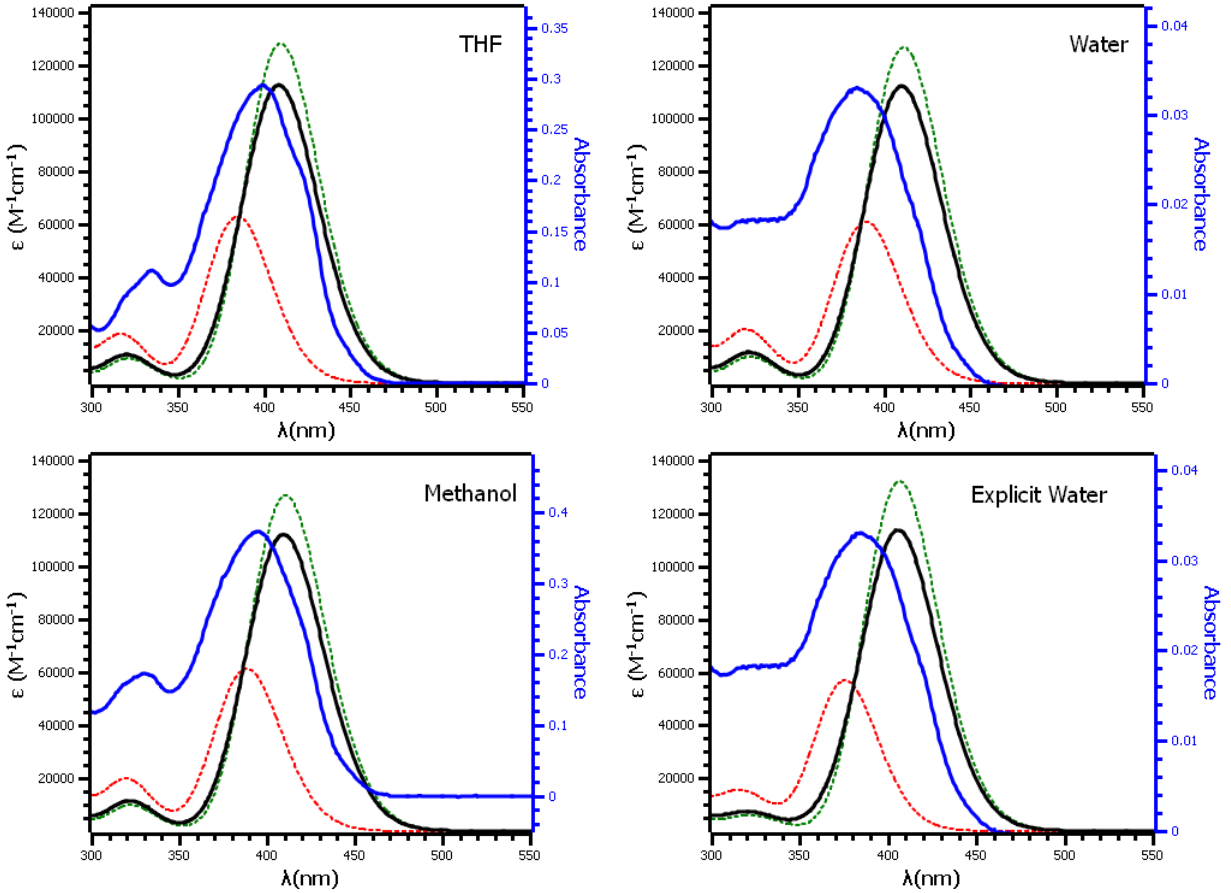

Figure 2.6 Calculated UV-Vis spectra for the Z and E isomers of C392STP (green and red, respectively) and for their mixture (E/Z 84:16) (black) and comparison with the experimental (blue) spectra in THF, methanol and water. Adapted from González-Pérez et al. [24].

Table 2.3 Calculated absorption data of the lowest energy transition for *E* and *Z* isomers in different solvents.

Solvents	**E isomer**		**Z isomer**		**E/Z mixture**	**Experimental** [24]
	λ (nm)	**f**	**λ (nm)**	**f**	**λ[a] (nm)**	**λ, FWHM[b] (nm)**
Dioxane	404	1.755	378	0.916	-	-
THF	409	1.773	384	0.870	408	399,68
Acetone	407	1.770	381	0.955	-	-
Methanol	410	1.753	388	0.847	409	396,69
Water	411	1.753	389	0.824	410	385,74
Explicit water	406	1.826	375	0.786	405	-

In order to investigate the properties of C392STP coumarin in water, theoretical calculation using the model of coumarin with nine explicit water molecules were performed. The coumarin–water complex was optimized, and its absorption spectra was calculated by TD-DFT, embedded in a PCM water medium (Figure 2.7).

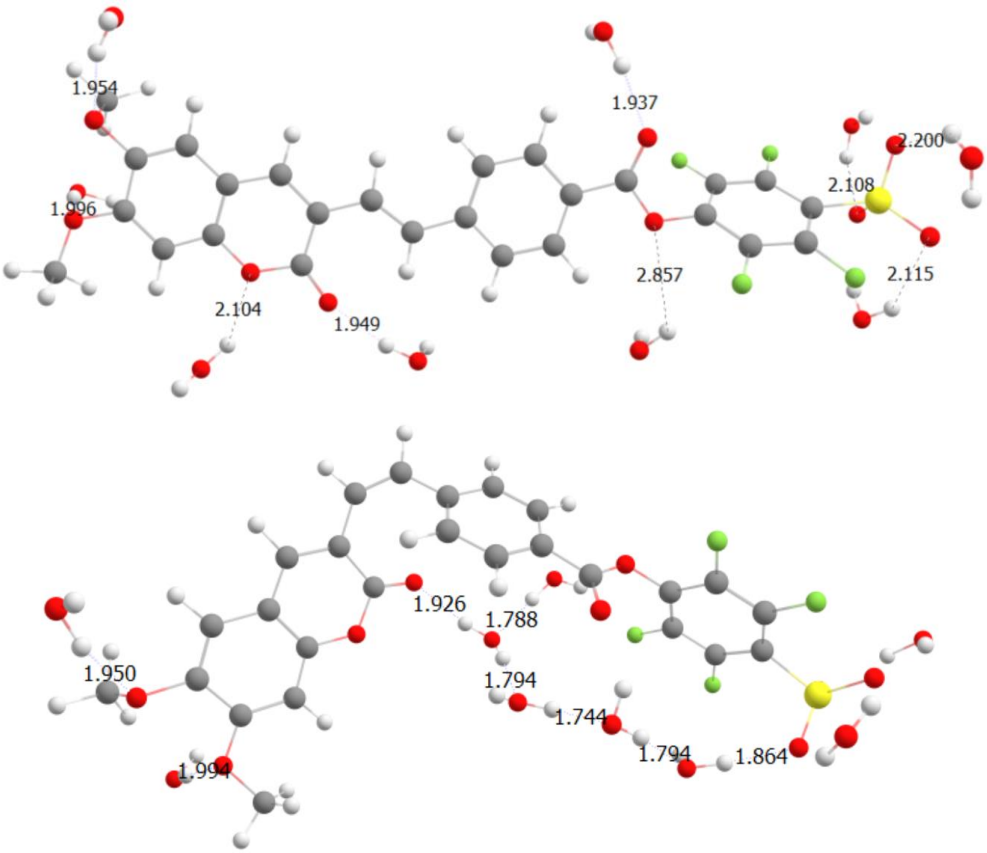

Figure 2.7 Optimized molecular geometry for *E*-C392STP (up) and *Z*-C392STP (down) in the PCM/water explicit model, at the B3LYP/6-31+G(d) level.

The results of optimization with explicit water molecules showed that at least seven hydrogen bonds are formed with *E*-392STP, two intermolecular CO---H-O are formed between the methoxy oxygens of the C392STP and water hydrogens, one intermolecular C=O---H-O bond and one O---H-O between the coumarin moiety and hydrogen of water molecules, one intermolecular C=O---H-O hydrogen bond between the carbonyl group and the hydrogen of one water molecule and three SO---H-O bonds between the sulphonate oxygens and water hydrogens. The *Z*-392STP only shows six hydrogen bonds between the coumarin and waters,

probably due to its more compact shape. When compared with the continuum model, the mixed PCM/explicit water model excitation corresponding to the $S_0 \rightarrow S_1$ transition shifts to higher energies than in non-aqueous solvents (Table 2.3), as observed experimentally, although with a smaller blue shift than in the experiment.

The DFT calculations of electronic structure confirm the experimental trends in the UV wavelength absorption and are in good agreement with the experimental absorption spectra. The properties of C392STP coumarin were further explored by calculating the infrared spectrum. Figure 2.8 compares the calculated infrared spectra and the infrared spectra of C392STP coumarin chromophore. Through the theoretical calculations, one band measured at 1265 cm^{-1} can be assigned to the CO stretching vibrations as the range of the CO stretching vibration ester of aromatic acids is around 1250 to 1300 cm^{-1}. On the other hand, peaks were observed at the range between 2916 and 3068 cm^{-1} which were assigned to the CH stretching vibrations of the aromatic ring. The calculated IR peaks of CH stretching, found between 2916 and 3068 cm^{-1}, are comparable with the experimental IR peaks found in the range of 2849 and 3016 cm^{-1}.

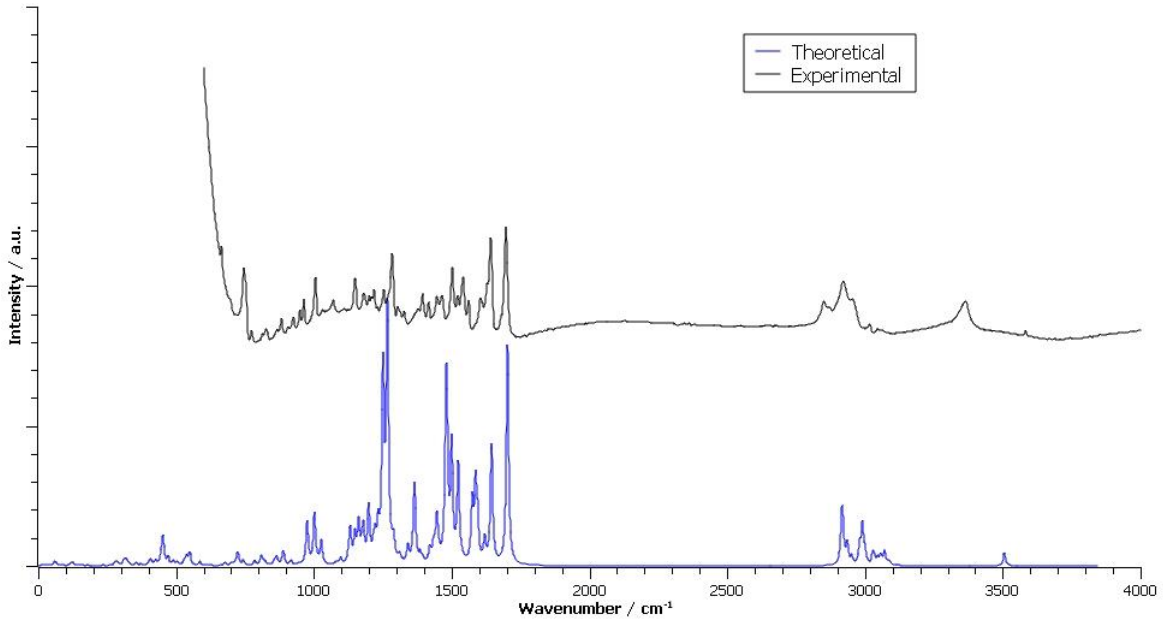

Figure 2.8 Theoretical and experimental IR spectra of sodium (*E/Z*)-4-(4-(2-(6,7-dimethoxy-coumarin-3-yl) vinyl) benzoyl)-2,3,5,6-tetrafluorobenzenesulfonate.

2.3.2 Study of (*E/Z*)-4-(2-(6,7- dimethoxycoumarin-3-yl)vinyl)-N-propylbenzamide

The C392STP coumarin can react with the primary amines of proteins amino acids during the fluorescent labelling process. By forming a covalent bond, C392STP coumarin bonds with the amino acid amine and lose its' 2,3,5,6-tetrafluorobenzene sulfonate group, producing the resulting fluorescent amino acid. To model this process, C392STP coumarin react with propylamine to produce (*E/Z*)-4-(2-(6,7- dimethoxycoumarin-3-yl)vinyl)-N-propylbenzamide, as represented in Figure 2.9. The reaction is further discussed in the section 3.3.

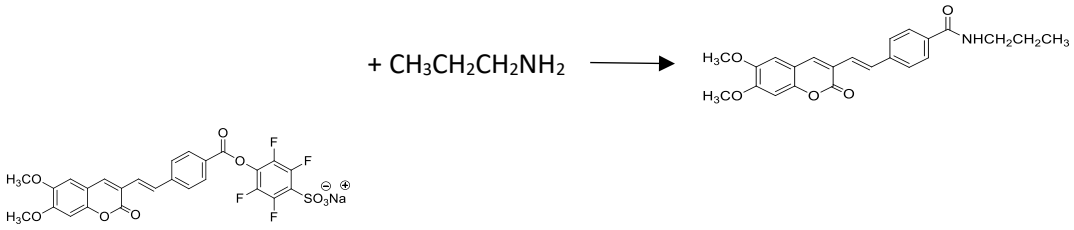

Figure 2.9 Reaction of C392STP coumarin and propylamine to produce (*E*)-4-(2-(6,7-dimethoxycoumarin-3-yl)vinyl)-N-propylbenzamide

The optimized molecular geometries of the chromophore isomers determined at the B3LYP/6-31G(d,p) theory level using acetonitrile as solvent are reported in Figure 2.10.

Figure 2.10 Optimized molecular geometry of the E and Z conformers of the coumarin derivative in acetonitrile at B3LYP/6-31G(d,p) level.

Contrary to the *Z* isomer, the *E* isomer is mostly planar, suggesting an efficient pi conjugation though the molecule. An energy difference of 7.7 kcal/mol between the *E* and *Z* isomers calculated at the same theory level, including ZPE corrections was found, with the E isomer showing the lower energy. These results show that the E isomer is the most stable form for both compounds as expected similarly to the case of the C392STP coumarin.

Figure 2.11 shows the highest occupied molecular orbital (HOMO) and HOMO-1 and the lowest unoccupied molecular orbital (LUMO) and LUMO+1 in acetonitrile for the both isomers. The frontier orbitals present typical π character, delocalized over the entire molecule with less significance for the propyl moiety, and are similar for both isomers. The main difference is that while in the *E* case the orbitals are spread for all the conjugated moiety, for the *Z* isomer the orbitals are slightly more localized on the coumarin part. From the TD-DFT calculations with the 6-311+g(2d, p) basis set the 20 lowest energy transitions were obtained. The TD-DFT calculated E and Z isomers absorption spectra in acetonitrile solution are reported in Figure 2.12 as well as the experimentally determined spectrum of the compound. The first experimental absorption band is located around 392 nm while the second absorption band is observed at 324 nm. When comparing the calculated spectra of the *E* and *Z* isomers the lower energy band of the *Z* isomer is shifted to higher energies due to sterical hindrance that forces the aromatic ring out-of-plane, resulting in a reduction on conjugation.

In real samples, depending on the synthesis conditions, the coumarin compounds can appear as a mixture of *E* and *Z* isomers in different percentages. In the present case, NMR experimental data (Appendix) shows that the *E* isomer is the most abundant form (around 100%) after synthesis and purification. Comparing the *E* isomer spectra with the experimental one, the lower energy absorption band is only slightly red-shifted and the agreement between the theoretical calculated and experimental spectra is remarkable.

To gain insight into the origin of the absorption spectra and the nature of the electronic transitions, the calculated transitions in terms of energy, oscillator strength, and the most important molecular orbital involved, together with the experimental absorption maxima, are depicted in Table 2.4. The lowest-energy transition corresponds to an S0⟶S1 transition

and originates from a $\pi \rightarrow \pi^*$ transition being mainly associated with a HOMO→LUMO transitions, for the both isomers.

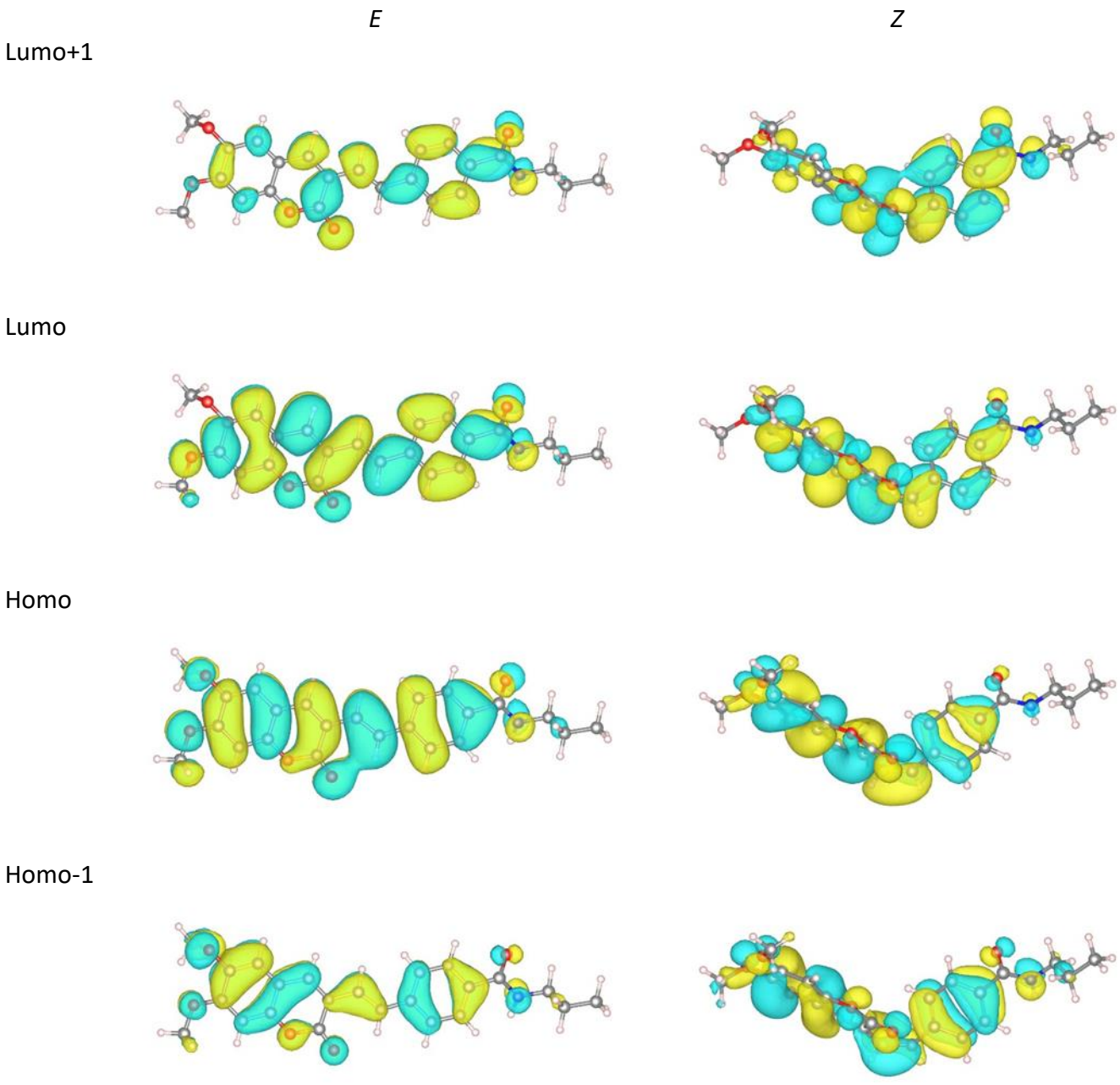

Figure 2.11 Schematic drawings of the frontier molecular orbitals of the both isomers involved in the most important transitions.

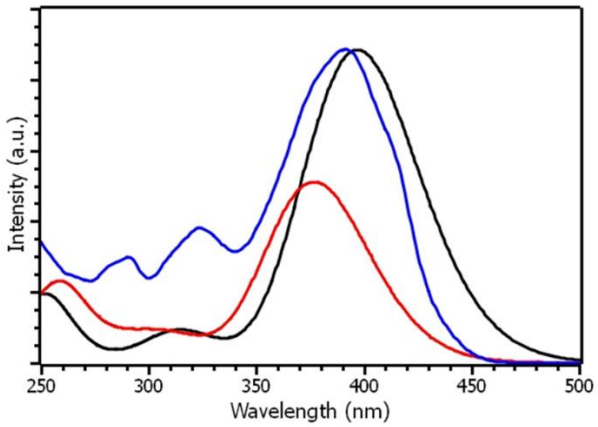

Figure 2.12 Comparison between the experimental (blue line) and the calculated absorption spectra of the coumarin *E* (black) and *Z* (red) isomers.

It is followed by two excited states close in energy (S2 and S3), presenting small oscillator forces and are mainly associated with HOMO-1→LUMO and HOMO→ LUMO+1 transition, for the both isomers.

The infrared spectra of (*E*)-4-(2-(6,7- dimethoxycoumarin-3-yl)vinyl)-N-propylbenzamide is shown in Figure 2.13. Calculated IR peakss are observed between 1513 and 1631 cm^{-1}. The peaks in the range of 1510 to 1650 cm^{-1} suggested the N-H bending vibration of amines. Peaks are also observed from 1674 to 1758 cm^{-1} which suggests –C=O stretching vibrations (Amide-I band). In our case, the CH stretching vibrations of aromatic rings was observed at 3050-3125 cm^{-1}. In previous research, the CH stretching were also found at 3046–3109 cm^{-1} (3-(bromoacetyl)coumarin), 3051–3120 cm^{-1} (3-acetyl-7-methoxycoumarin) [25], 3172, 3092 and 3064 cm^{-1} (6-methyl-4-bromomethylcoumarin) [26], 3172 and 3079 cm^{-1} (7-methyl-4-bromomethylcoumarin) [27], 3159, 3087, 3067 and 3043 cm^{-1} (6 and 7-Chloro-4-bromomethylcoumarin) [28] respectively. The present DFT calculation predicts the N-H bending vibration of amine in the range between 1513 and 1631 cm^{-1}. Additionally, the C=O stretching vibrations of amide-I band is predicted at 1674 to 1758cm^{-1}. The N-H bending vibrations and C=O stretching vibrations are comparable between the theoretical predicted IR peaks and the experimental measured spectra.

Table 2.4 Experimental and calculated spectral properties of the coumarin isomers at hybrid Pbe0 functional with 6-311+g (2d, p) theory level.

	State	Wavelength (nm)	*f*	Major MO → MO transitions	Experimental
***E* isomer**	S1	396.81	1.627	HOMO→LUMO (99%)	392
	S2	316.43	0.068	H-1→LUMO (83%) H-3→LUMO (3%) H-2→LUMO (4%) HOMO→L+1 (2%) HOMO→L+3 (3%)	324
	S3	313.91	0.101	HOMO→L+1 (90%) H-1→LUMO (4%)	
***Z* isomer**	S1	376.65	0.940	HOMO→LUMO (99%)	
	S2	316.82	0.044	H-1→LUMO (85%) HOMO→L+1 (8%)	
	S3	308.38	0.095	H-2→LUMO (10%) HOMO→L+1 (79%) H-1→LUMO (5%)	

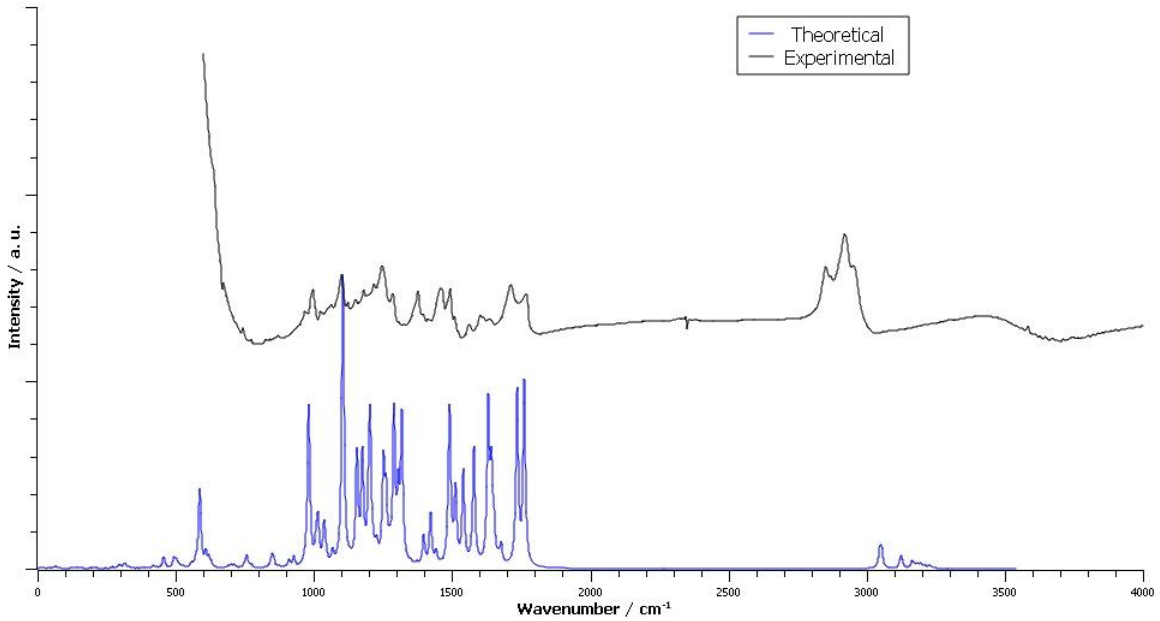

Figure 2.13 Experimental and calculated IR spectra of (*E*)-4-(2-(6,7- dimethoxycoumarin-3-yl)vinyl)-N-propylbenzamide.

2.4 Conclusion

The electronic structure and spectral features of the potential chromophore proposed for the new fluorescent labelling methodology, C392STP coumarin, was presented. Characteristics of C392STP in different solvents were also explored. Furthermore, the characteristics of a related compound intended to mimic the chromophore-amino acid complex has been investigated as well. To gain a better understanding of the electronic structure and spectral features of the chromophore-amino acid complex, DFT and TD-DFT calculations on both the *E* and *Z* conformers of this coumarin derivative have been performed. The TD-DFT calculations for both C392STP coumarin and (E/Z)-4-(2-(6,7- dimethoxycoumarin-3-yl)vinyl)-N-propylbenzamide have presented a good agreement with the experimental absorption spectra and a comprehensive assignment of the main spectral features of the studied compounds was done. In the following chapter, the C392STP chromophore was tested as a label both with commercial proteins and with extracted proteins from natural products.

Bibliography

[1] J. B. Foresman and A. Frisch, “Exploring Chemistry With Electronic Structure Methods.pdf,” *Exploring Chemistry with Electronic Structure Methods*. p. 302, 1996.

[2] A. Tomberg, *Gaussian 09W Tutorial. An introduction to computational chemistry using G09W and Avogadro software*. 2013.

[3] E. Runge and E. K. Gross, “Density-functional theory for time-dependent systems,” *Phys. Rev. Lett.*, vol. 52, no. 12, p. 997, 1984.

[4] M. E. Casida, “Time-Dependent density functional response theory for molecules,” *Recent Adv. Density Funct. Methods (Part I)*, pp. 155–192, 1995.

[5] R. E. Stratmann, G. E. Scuseria, and M. J. Frisch, “An efficient implementation of time-dependent density-functional theory for the calculation of excitation energies of large molecules,” *J. Chem. Phys.*, vol. 109, no. 19, p. 8218, 1998.

[6] A. Dreuw and M. Head-gordon, “Single-Reference ab Initio Methods for the Calculation of Excited States of Large Molecules,” *Chem. Rev.*, vol. 105, pp. 4009–4037, 2005.

[7] F. Furche, R. Ahlrichs, C. Wachsmann, E. Weber, A. Sobanski, F. Vögtle, and S. Grimme, “Circular dichroism of helicenes investigated by time-dependent density functional theory,” *J. Am. Chem. Soc.*, vol. 122, no. 8, pp. 1717–1724, 2000.

[8] D. Jacquemin, E.A. Perpète, G. Scalmani, M.J. Frisch, X. Assfeld, I. Ciofini, and C. Adamo, “Time-dependent density functional theory investigation of the absorption, fluorescence, and phosphorescence spectra of solvated coumarins,” *J. Chem. Phys.*, vol. 125, no. 16, 2006.

[9] D. Jacquemin, E. A. Perpe, C. Adamo, and E. N. Supe, “Accurate Simulation of Optical Properties in Dyes,” *Acc. Chem. Res.*, vol. 42, no. 2, pp. 326–334, 2009.

[10] C. Adamo and D. Jacquemin, “The calculations of excited-state properties with Time-Dependent Density Functional Theory,” *Chem. Soc. Rev.*, vol. 42, pp. 845–856, 2013.

[11] G. Signore, R. Nifosì, L. Albertazzi, and R. Bizzarri, “A Novel Coumarin Fluorescent Sensor to Probe Polarity Around Biomolecules A Novel Coumarin Fluorescent Sensor to Probe Polarity Around Biomolecules,” *J. Biomed. Nanotechnol.*, vol. 5, pp. 722–729, 2009.

[12] R. McWeeny, “Methods of Molecular Quantum Mechanics,” 1992.

[13] M. Cossi and V. Barone, “Time-dependent density functional theory for molecules in liquid solutions,” *J. Chem. Phys.*, vol. 115, no. 10, pp. 4708–4717, 2001.

[14] M. Cossi, V. Barone, B. Mennucci, and J. Tomasi, “Ab initio study of ionic solutions by a polarizable continuum dielectric model,” *Chem. Phys. Lett.*, vol. 286, pp. 253–260, 1998.

[15] B. Mennucci, E. Cancès, and J. Tomasi, “Evaluation of Solvent Effects in Isotropic and Anisotropic Dielectrics and in Ionic Solutions with a Unified Integral Equation Method: Theoretical Bases, Computational Implementation, and Numerical Applications,” *J. Phys. Chem. B*, vol. 101, no. 49, pp. 10506–10517, 1997.

[16] B. Mennucci and J. Tomasi, “Continuum solvation models: A new approach to the problem of solute’s charge distribution and cavity boundaries,” *J. Chem. Phys.*, vol. 106, no. 12, pp. 5151–5158, 1997.

[17] E. Cancès, B. Mennucci, and J. Tomasi, “A new integral equation formalism for the polarizable continuum model: Theoretical background and applications to Isotropic and anisotropic dielectrics,” *J. Chem. Phys.*, vol. 107, no. 8, pp. 3032–3041, 1997.

[18] B. Mennucci, R. Cammi, and J. Tomasi, “Analytical free energy second derivatives with respect to nuclear coordinates: Complete formulation for electrostatic continuum solvation models,” *J. Chem. Phys.*, vol. 110, no. 14, pp. 6858–6870, 1999.

[19] J. Tomasi, B. Mennucci, and E. Cancès, “The IEF version of the PCM solvation method: an overview of a new method addressed to study molecular solutes at the QM ab initio level - ScienceDirect,” *J. Mol. Struct.*, vol. 464, pp. 211–226, 1999.

[20] D. Jacquemin and B. Mennucci, “Excited-state calculations with TD-DFT : from benchmarks to simulations in complex environments,” *Phys. Chem. Chem. Phys.*, vol. 13, pp. 16987–16998, 2011.

[21] A. D. Laurent and D. Jacquemin, “TD-DFT Benchmarks : A Review,” *Int. J. Quantum Chem.*, vol. 113, pp. 2019–2039, 2013.

[22] K. R. Gee, E. A. Archer, and H. C. Kang, “4-Sulfotetrafluorophenyl (STP) esters: New water-soluble amine-reactive reagents for labeling biomolecules,” *Tetrahedron Lett.*, vol. 40, no. 8, pp. 1471–1474, 1999.

[23] M. J. Frisch and A. Tomberg, “Gaussian 09W Tutorial,” *an Introd. To Comput. Chem. Using*

G09W Avogadro Softw., p. 34, 2009.

[24] M. González-Pérez, S. Y. Ooi, S. Martins, J. P. P. Ramalho, A. Pereira, and A. T. Caldeira, "Gaining insight into the photophysical properties of a coumarin STP ester with potential for bioconjugation," *New J. Chem.*, vol. 42, no. 20, pp. 16635–16645, 2018.

[25] R. J. Cave, K. Burke, and E. W. Castner, "Theoretical Investigation of the Ground and Excited States of Coumarin 151 and Coumarin 120," *J. Phys. Chem. A*, vol. 106, pp. 9294–9305, 2002.

[26] V. Sortur, J. Yenagi, J. Tonannavar, V. B. Jadhav, and M. V. Kulkarni, "Fourier transform-infared and Raman spectra, ab inition calculations and assignments fo 6-methyl-4-bromomethylcoumarin," *Spectrochim. Acta Part A Mol. Biomol. Spectrosc.*, vol. 64, no. 2, pp. 301–307, 2006.

[27] V. Sortur, J. Yenagi, J. Tonannavar, V. B. Jadhav, and M. V. Kulkarni, "Vibrational assignments for 7-methyl-4-bromomethylcoumarin, as aided by RHF and B3LYP/6-31G* calculations," *Spectrochim. Acta Part A Mol. Biomol. Spectrosc.*, vol. 71, no. 2, pp. 688–694, 2008.

[28] J. Tonannavar, J. Yenagi, V. Sortur, V. Jadhav, and M. Kulkarni, "Vibrational spectra, normal modes, ab initio and DFT calculations for 6-Chloro-7-Chloro-4-bromomethylcoumarins," *Spectrochim. Acta Part A Mol. Biomol. Spectrosc.*, vol. 77, no. 2, pp. 351–358, 2010.

Chapter 3 FLUORESCENT LABELLING METHODOLOGY DEVELOPMENT

Part of the results have been published in:

- **S. Y. Ooi**, C. Salvador, A. Candeias, A. Pereira, J. P. P. Ramalho, and A. T. Caldeira, Abstract of “Development of a simple method in the identification of proteinaceous binders in art,” TECHNART 2017 Non-destructive and microanalytical techniques in art and cultural heritage, pp. 235, 2017.

3.0 Overview

This chapter describes the steps in developing the new fluorescent labelling methodology using C392STP, in order to increase the detection signals of proteins. Initially, we have developed and optimized the method by using commercial proteins such as BSA (A2153), ovalbumin (A5378), casein (C3400) and collagen (C9879). The optimized method was also used to test proteins extracted from hen's egg yolk and white, bovine milk and rabbit skin. The electrophoretic profiles showed similar characteristic band profiles between the extracted and the commercial proteins. These results evidence the potential to apply this optimized methodology as an effective and useful analytical tool in the identification of protein binders in samples obtained from easel paintings.

3.1 Introduction

Easel paintings emerged in the Middle Ages and since then have been one of the most important art expressions, constituting today's relevant Cultural Heritage assets with important historical and cultural values. These artworks contain a diversity of organic materials, namely proteic compounds. The proteinaceous binders are commonly produced from egg, milk or animal skin and bones. Unfortunately, the detection of different protein materials in these complex matrices is a difficult task. Moreover, wide ranges of organic and inorganic materials mixture in the paintings also contribute to the complexity of the materials identification [1]. It is then of paramount importance to develop analytical methodologies in protein identification for artwork materials investigation that can be applied as low invasive approaches and that are suitable for protein identification in painting samples.

In the remaining part of this chapter, the description of this new simple, fast and affordable protocol to detect and identify protein binders used in easel paintings was done. A coumarin derivative chromophore, C392STP (sodium (E/Z)-4-(4-(2-(6,7-dimethoxy-coumarin-3-yl) vinyl) benzoyl)-2,3,5,6-tetrafluorobenzenesulfonate) was used as a fluorescent label to identify and distinguish the different protein binders used in easel

paintings' samples. The C392STP is a fluorescent amine-reactive coumarin synthesized by our research group [2]. The 4-sulfotetrafluorophenyl (STP) ester synthesis is chosen because it is easy to synthesize with high yield and due to its high amine reactivity. It is also highly soluble in water compared to *N*-hydroxysuccinimidyl (NHS) esters and is unlikely to suffer hydrolysis when compared with succinimidyl esters and pentafluorophenyl (PFP) esters. The mentioned properties of C392STP make it very useful for biomolecules (containing amine groups) labelling. The synthesis of C392STP produces a mixture of *E* and *Z* isomers in different percentages. The ^{1}H-RMN experimental data (Supplementary info, Figure 1) showed that the ratio of *E* isomer to *Z* isomer is 84:16. The *E* isomer has two doublets, at 7.41 and 7.72 ppm with a 16.3 Hz coupling constant characteristic of this kind of isomer and two singlets at 7.30 and 7.61 ppm from the *Z* isomer.

The C392STP coumarin derivative was synthesized in high yield, with a simple, effective and low cost reaction, according to the synthetic pathway (Figure 3.1) and described below:

Synthesis of (E)-methyl 4-(2-(6,7-dimethoxycoumarin-3-yl)vinyl)benzoate (A)

Under a nitrogen atmosphere, a mixture of 6,7-dimethoxy-3-vinylcoumarin (73) (250 mg, 1.077 mmol), methyl 4-iodobenzoate (256 mg, 0.979 mmol), Pd(PPh3)4 (57 mg, 0.049 mmol) and CH3CO2Ag (180 mg, 1.077 mmol) in DMF (3 mL) was stirred at 80ºC for a period of 72 h. After cooling to r.t., the reaction mixture was diluted with CH_2Cl_2, and washed with H_2O. The organic layer was dried (Na_2SO_4), filtered, and concentrated under vacuum. The residue was purified by flash column chromatography on silica gel (230 400 mesh; CH_2Cl_2/EtOAc gradient) to yield (*E*)-methyl 4-(2-(6,7-dimethoxy-coumarin-3-yl)vinyl)benzoate (330 mg, 0.900 mmol, 92%). ^{1}H NMR (400 MHz, $CDCl_3$) δ (ppm): 3.92 (3H, s, OCH_3), 3.94 (3H, s, OCH_3), 3.96 (3H, s, OCH_3), 6.85 (1H, s, H-8), 6.89 (1H, s, H-5), 7.18 (1H, d, J=16.3, H-1'), 7.58 (2H, d, J=8.0, H-4', H-8'), 7.62 (1H, d, J=16.3, H-2'), 7.77 (1H, s, H-4), 8.02 (2H, d, J=8.0, H-5', H-7'). ^{13}C NMR (100 MHz, CDCl3) δ: 52.3 (COOCH3), 56.5 (OCH3), 56.6 (OCH3), 99.8 (C-8), 107.9 (C-5), 112.3 (C-4a), 121.5 (C-3), 125.2 (C-1'), 126.8 (C-5', C-7'), 129.5 (C-6'), 130.2 (C-4', C-8'), 131.4 (C-2'), 138.6 (C-4), 141.7 (C-3'), 146.8 (C-6), 149.2 (C-8a), 153.1 (C-7), 160.7 (C-2), 167.0 (CO2CH3). MS-TOF(+) calc. for C21H18O6Na $[M+Na]^+$ 389.09956 found 389.0989. FTIR ν^{max}(cm^{-1}): 2953,

2922, 2852, 1713, 1603, 1561, 1523, 1449, 1397, 1287, 1258, 1221, 1185, 1156, 1113, 1008, 968, 870, 816, 752.

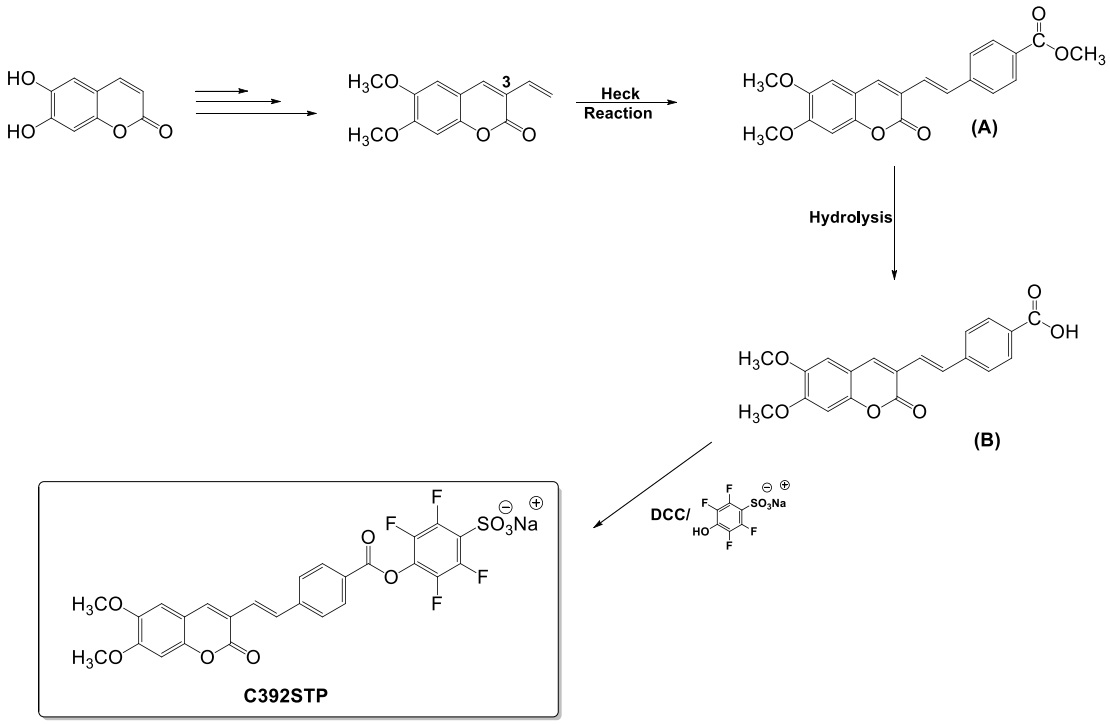

Figure 3.1 Synthesis of sodium (*E/Z*)-4-(4-(2-(6,7-dimethoxycoumarin-3-yl)vinyl)-benzoyl)-2,3,5,6-tetrafluoro-benzenesulfonate (C392STP).

Synthesis of ((E)-4-(2-(6,7-dimethoxycoumarin-3-yl)vinyl)-benzoic acid (B)

To a mixture of (E)-methyl 4-(2-(6,7-dimethoxycoumarin-3-yl)vinyl)benzoate (250 mg, 0.682 mmol) in 1,4-dioxane (3.41 mL) was added 1 M sodium hydroxide (3.41 mL, 3.41 mmol). The reaction was stirred at 60ºC for about 2 h. After cooling to r.t., the reaction was acidified with HCl (10%) solution. The reaction mixture was diluted with CH_2Cl_2, and washed with H_2O. The organic layer was dried (Na_2SO_4), filtered, and concentrated under vacuum. The residue was purified by flash column chromatography on silica gel (230 400 mesh; CH_2Cl_2/MeOH gradient) to yield (E)-4-(2-(6,7-dimethoxy-coumarin-3-yl)vinyl)benzoic acid (216 mg, 0.614 mmol, 90%). ^{1}H NMR (400 MHz, DMSO-d^6) δ (ppm): 3.83 (3H, s, OCH_3), 3.88 (3H, s, OCH_3), 7.11 (1H, s, H-8), 7.23 (1H, s, H-5), 7.29 (1H, d, J=16.3, H-1'), 7.64 (1H, d, J=16.3, H-2'), 7.68 (2H, d, J= 8.2, H-4', H-8'), 7.94 (2H, d, J= 8.2, H-5', H-7'), 8.22 (1H, s, H-4), 12.97 (1H, s, CO2H).

^{13}C NMR (100 MHz, DMSO-d^{6}) δ (ppm):.55.9 (OCH3), 56.3 (OCH3), 99.8 (C-8), 108.6 (C-5), 111.8 (C-4a), 119.9 (C-3), 125.5 (C-1'), 126.6 (C-5', C-7'), 129.9 (C-4', C-6', C-8'), 130.1 (C-2'), 140 (C-4), 141.2 (C-3'), 146.2 (C-6), 148.6 (C-8a), 152.9 (C-7), 159.8 (C-2), 167.1 (CO2H). MS-TOF(+) calc. for C20H16O6Na [M+Na]$^{+}$ 375.08391 found 375.0845. FTIR ν^{max}(cm^{-1}): 2950, 2921, 28511725, 1682, 1600, 1557, 1503, 1459, 1423, 1406, 1383, 1312, 1286, 1256, 1175, 1146, 1039, 1021, 995, 970, 961, 926, 875, 837, 797, 757, 697.

Synthesis of sodium (*E/Z*)-4-(4-(2-(6,7-dimethoxycoumarin-3-yl)vinyl)-benzoyl)-2,3,5,6-tetra-fluorobenzenesulfonate (C392STP)

To a mixture of (*E*)-4-(2-(6,7-dimethoxycoumarin-3-yl)vinyl)benzoic acid (200 mg, 0.568 mmol), 4-sulfotetrafluorophenol sodium salt (163 mg, 0.607 mmol) and *N*,*N*'-dicyclohexylcarbodiimide (137 mg, 0.664 mmol) in CH3CN (8 mL) and DMF (2 mL) was stirred at room temperature for a period of 18 h. The reaction mixture was evaporated to dryness and the residue was purified by flash column chromatography on silica gel (230–400 mesh; CH_2Cl_2/MeOH gradient) to yield sodium (*E/Z*)-4-(4-(2-(6,7-dimethoxycoumarin-3-yl)vinyl)benzoyl)-2,3,5,6-tetrafluorobenzenesulfonate (335 mg, 0.556 mmol, 98%).E-isomer: ^{1}H NMR (400 MHz, DMSO-d^{6}) δ (ppm): 3.83 (3H, s, OCH_3), 3.88 (3H, s, OCH_3), 7.12 (1H, s, H-8), 7.24 (1H, s, H-5), 7.41 (1H, d, J=16.3, H-1'), 7.72 (1H, d, J=16.3, H-2'), 7.84 (2H, d, J= 8.2, H-4', H-8'), 8.18 (2H, d, J= 8.2, H-5', H-7'), 8.27 (1H, s, H-4). *Z*-isomer: ^{1}H NMR (400 MHz, DMSO-d^{6}) δ (ppm): 3.83 (3H, s, OCH3), 3.88 (3H, s, OCH3), 7.10 (1H, s, H-8), 7.23 (1H, s, H-5), 7.30 (1H, s, H-1'), 7.61 (1H, s, H-2'), 7.66 (2H, d, J= 8.0, H-4', H-8'), 7.94 (2H, d, J= 8.0, H-5', H-7'), 8.22 (1H, s, H-4). ^{13}C NMR (100 MHz, DMSO-d6) δ (ppm): 56.0 (OCH_3), 56.3 (OCH3), 99.8 (C-8), 108.7 (C-5), 111.8 (C-4a), 119.7 (C-3), 124.7 (C-1'), 126.5 (C13'), 127.3 (C-5', C-7'), 129.2 (C-2'), 129.9 (C6') 131.1 (C-4', C-8'), 140,0 (C12', C14'), 141.0 (C-4), 141.5 (C10'), 143.8 (C-3'), 144.3 (C11', C15'),146.3 (C-6), 148.8 (C-8a), 153.1 (C-7), 159.8 (C-2), 162.0 (COO). MS-TOF(-) calc. for C26H15NO9F4S [M-H]$^{-}$ 579.037841 found 579.0378. FTIR ν^{max}(cm^{-1}): 2952, 2921, 2852, 1769, 1712, 1602, 1561, 1493, 1461, 1376, 1285, 1246, 1217, 1181, 1151, 1100, 996, 639. UV (CH_3CN) λ^{max} (nm): 197, 293, 332, 392.

Our previous study has reported its' potential as chromophore. Evaluation has been made on its' potential for producing singly fluorescent-labeled oligonucleotides and assessment of their performance as RNA-FISH probes [3]. The properties of this coumarin derivative such as its effectiveness and high fluorescent quantum yields, as well as its low price and easy to synthesize makes it particularly suitable for labelling. Another advantage of this family of compounds is that it possesses photo physical and spectroscopic properties which can be easily tailored according to the desired application [4–6]. It is known that C392STP bonds covalently with amino acids [7]. The proteinaceous content extracted from the paints can then react effectively with the coumarin chromophore, producing fluorescent proteins that can be separated and identified by gel electrophoresis, with the advantage of the gel staining step not being necessary in the identification process. The following of this chapter addressed the questions: Can C392STP label the commercial proteins? Is C392STP able to label the proteins extracted from animal material?

3.2 Materials and methodology

3.2.1 Materials

All the commercial reagents such as acetic acid (PanReac), BSA, ovalbumin, casein, collagen from bovine achilles tendon, gelatin from cold water fish skin (all from Sigma-Aldrich), acrylamide (Sigma-Aldrich), bisacrylamide (Sigma-Aldrich), bromophenol blue (Sigma-Aldrich), glycerol (Merck), Tris-HCl buffer (VWR) were used as it was received. The buffer was prepared in distilled water with Na_2CO_3 (6398, Merck) (0.1 mol) and $NaHCO_3$ (6329, Merck) (0.1 mol), pH 8.2. On the other hand, rabbit glue was prepared in the lab using the natural glue (extracted from the rabbit skin) which is stored in solid state.

3.2.2 Fluorescent labelling of commercial proteins

In this section, the method was tested with commercial proteins such as BSA (A2153), ovalbumin (A5378), casein (C3400) and collagen (C9879). In the first step, the commercial

proteins are allowed to react with C392STP. The reactions were prepared by mixing C392STP (0.00234 g, 1.0 mmol, 20.0 equiv) and the commercial proteins, in different protein: chromophore ratios and at two different temperatures, in sodium bicarbonate buffer (4.0 ml) and stirred for a period of 24 hour (Table 3.1). In the case of collagen, C392STP (1) (0.00234 g, 1.0 mmol, 20.0 equiv) was mixed with collagen (14.62 mg/ml) in acetic acid (0.1M) (4.0 mL) and was stirred at 40°C for a period of 24 h.

Table 3.1 Optimization process of fluorescent labelling methodology.

	Test				
	1	**2**	**3**	**4**	**5**
	BSA/Ovalbumin/ Casein/Collagen/Fish gelatin	**Ovalbumin/Casein**			**Collagen**
Proportion of protein: chromophore	1:20	1:20	5:20	10:20	5:20
Reaction temperature (°C)	R.T.	40	40	40	40

R.T. – room temperature

3.2.3 Test of the optimized method by using the proteins extracted from hen's egg, bovine milk and animal glue

3.2.3.1 Protein extraction

Extraction of ovalbumin was based on isoelectric precipitation using TCA. This method uses a quantity of egg white/yolk (10 ml), separately, on three centrifugation steps of 10 minute at 3000 rpm. Firstly, 10 ml H_20 was used to help the dissolution and clean some of the impurities. Then, 10 ml of trichloroacetic acid (5%) was added to promote the proteins precipitation and followed by another washing step. The extracted proteins were resuspended in 10 ml of H_2O [8].

Extraction of casein was made by precipitation with hydrochloric acid, by mixing 10 ml of bovine milk with 10 ml of H_2O and adding 2 ml hydrochloric acid (2 %). It was then centrifuged

at 2000 rpm for 5 minutes (obtaining 2 ml of protein crude). The supernatant was discarded, and the precipitate was washed with H_2O and centrifuged at 2000 rpm for 10 minutes. The supernatant was discarded, and the final crude was resuspended in 4 ml of distilled water [8].

Rabbit glue was prepared in the lab using commercial rabbit glue (Sennelier) in water with a ratio of 1:9 and then placing over a bain-marie (55ºC) during 30 min. Subsequently, the samples were incubated overnight at 25°C and then mixed with a glass stirring rod to ensure homogeneity. The glue solution was ready to use and stored at 5°C. The fluorescent labelling with C392STP was then performed on the rabbit glue.

3.2.3.2 Bonding of the extracted proteins with C392STP

The previously described procedure in section 3.2.2 has been applied on the extracted proteins, a mixture of C392STP (0.00234 g, 1.0 mmol, 20.0 equiv) and the proteins extract, in sodium bicarbonate buffer (4.0 ml), was stirred for a period of 24 hour.

3.2.3.3 Spectroscopy analysis

Before the labeling process, the experimental UV-Vis absorption spectra of the free C392STP was recorded in acetonitrile at room temperature. The experimental UV-Vis absorption spectra of the unbonded commercial proteins, unbonded extracted proteins, the fluorescent commercial proteins and the fluorescent extracted proteins were also recorded using a Thermo Electron Corporation (Nicolet Evolution 300) spectrophotometer. All the commercial proteins were measured in the solution of sodium bicarbonate buffer except collagen which was measured in the solution of the mixture of acetic acid and sodium bicarbonate buffer. The Infrared spectra of the unbonded commercial proteins and the fluorescent commercial proteins were obtained with an Infrared spectrometer Bruker Hyperion 3000. The infrared spectra were acquired with a spectral resolution of 8 cm^{-1}, 32 scans, in the infrared region between 4000 and 650 cm^{-1}.

3.2.3.4 *Electrophoretic Separation by PAGE*

The electrophoretic profiles of the proteins and the proteins bonded to the coumarin derivative chromophore were analyzed by PAGE (Polyacrylamide gel electrophoresis). The gel of the PAGE was prepared according to the composition of concentration and resolution gels showed in Table 3.2. After the polymerization of gel [Acrylamide: Bisacrylamide (30: 0.8)] was completed, electrophoresis was prepared using the MiniPROTEAN equipment from Bio-Rad.

Table 3.2 Composition of concentration and resolution gels in PAGE.

Composition of gels for PAGE	Concentration gel (2.5%)	Resolution gel (4%)
Acrylamide: Bisacrylamide (8: 0.8) (mL)	1.562	7
Concentration buffer (Tris- HCl 0.5 M pH 6.8) (mL)	1.250	-
Resolution Buffer (Tris- HCl 3M, pH 8.8) (mL)	-	1.750
TEMED (µL)	5	9.8
H_2O (mL)	1.933	4.540
Ammonium persulphate 1.5% (mL)	0.250	0.700

The gel was placed on the support and the electrophoresis buffer (Tris 25 mM with glycine 0.192 M, pH 8.3) was added. Samples were prepared by mixing 15 µL of sample with 10 µL of loading buffer (20 µg/mL of bromophenol blue and 10% of glycerol at 87% in Tris-HCl buffer 62.5 mM, pH 6.8) and were applied in the wells (25 µL per well). In addition, NZY Colour Protein Marker II (Nzytech) with molecular weight (MW) between 11 and 245 kDa was used as the molecular marker and was applied in the wells of the acrylamide gel ends. Electrophoretic run was started at a potential difference of 110 V until the bromophenol blue travel throughout the gel. The gels were visualized in a UV chamber (Molecular Imager, Gel Doc - XR+ Imaging System, Bio-Rad), analyzed and results recorded using the Image Lab 5.0 software (Copyright 2013, Bio-Rad Laboratories).

3.3 Results and discussions

The C392STP new fluorescent dye was synthesized in our lab, as a mixture of *E* (84%) and *Z* (16%) isomers [3]. In the chromophore C392STP reaction with propylamine (Figure 3.2 and described below), performed to mimic the reaction that occurs with proteins, particularly with the lysine amino acid, only the *E*-isomer is observed in the products. The ^{1}H NMR experimental data of 4-(2-(6,7-dimethoxy-coumarin-3-yl) vinyl)-*N*-propylbenzamide (Supplementary info, Figure 2), show that the *E* isomer is the most abundant form (around 100%) after synthesis and purification. The ^{1}H NMR spectrum presents two doublets, at 7.26 and 7.63 ppm, from the double bond protons with a 16.8 Hz coupling constant, characteristic of *E* isomer. These results suggest that the chromophore reaction with proteins will produce only the most stable isomer and with greater bathochromic shift, ie, the *E* isomer.

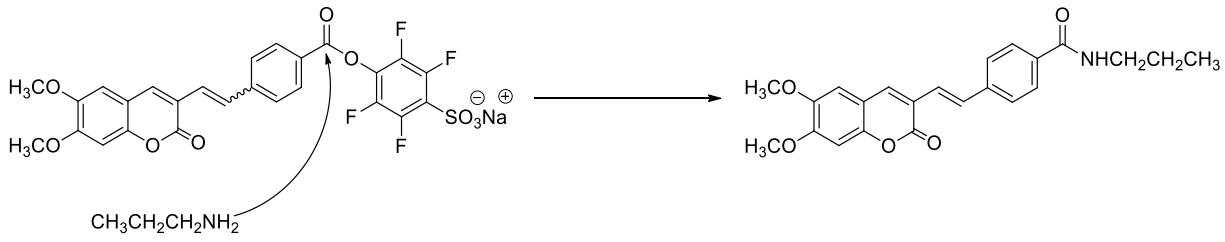

Figure 3.2 Reaction of (*E/Z*)-4-(4-(2-(6,7-dimethoxycoumarin-3-yl)vinyl)benzoyl)-2,3,5,6-tetrafluorobenzenesulfonate and propylamine to produce (*E*)-4-(2-(6,7- dimethoxycoumarin-3-yl)vinyl)-*N*-propylbenzamide.

Reaction of C392STP reaction with propylamine to produce (*E*)-4-(2-(6,7-dimethoxycoumarin-3-yl)vinyl)-*N*-propylbenzamide

A mixture of sodium (*E*)-4-(4-(2-(6,7-dimethoxycoumarin-3-yl)vinyl)benzoyl)-2,3,5,6-tetrafluorobenzenesulfonate (60.2 mg, 0.1 mmol) and propylamine (5.9 mg, 8.2 µL, 0.11 mmol, 1.1 equiv) in 2.0 mL of sodium bicarbonate buffer (pH 8.2) was stirred at 25ºC for a period of 24 h. The reaction mixture was concentrated under vacuum. The residue was

purified by flash column chromatography on silica gel (230 400 mesh; $CHCl_3$/MeOH gradient) to yield (*E*)-4-(2-(6,7- dimethoxycoumarin-3-yl)vinyl)-*N*-propylbenzamide (38.5 mg, 98%). ^{1}H NMR (400 MHz, DMSO-d^6) δ (ppm): 0.89 (3H, t, J=7.6, $NHCH_2CH_2\underline{CH_3}$), 1.53 (2H,m, $NHCH_2\underline{CH_2}CH_3$), 3.22 (2H, m, $NH\underline{CH_2}CH_2CH_3$), 3.83 (3H, s, OCH3), 3.88 (3H, s, OCH3), 7.11 (1H, s, H-8), 7.23 (1H, s, H-5), 7.26 (1H, d, J=16.8, H-1'), 7.63 (1H, d, J=16.8, H-2'), 7.65 (2H, d, J= 6.8, H-4', H-8'), 7.86 (2H, d, J= 6.8, H-5', H-7'), 8.20 (1H, s, H-4), 8.48 (1H, t, J=5.6, $\underline{NH}CH_2CH_2CH_3$)). ^{13}C NMR (100 MHz, DMSO-d^6) δ (ppm):.11.5 ($NHCH_2CH_2\underline{CH_3}$), 22.4 ($NHCH_2\underline{CH_2}CH_3$), 41.0 ($NH\underline{CH_2}CH_2CH_3$), 55.9 (OCH3), 56.3 (OCH3), 99.8 (C-8), 108.6 (C-5), 111.9 (C-4a), 120.0 (C-3), 124.6 (C-1'), 126.4 (C-5', C-7'), 127.8 (C-4', C-8'), 130.4 (C-2'), 133.8 (C-6'), 139.5 (C-3'), 139.7 (C-4), 146.2 (C-6), 148.6 (C-8a), 152.8 (C-7), 159.9 (C-2), 165.6 (CONH). FTIR ν^{max} (cm^{-1}): 3018, 2922, 2851, 1697, 1642, 1605, 1541, 1503, 1284, 1150, 1006, 746. UV (CH_3CN) λ^{max} (nm): 195, 240, 291, 324, 392.

3.3.1 Spectroscopic characteristics

In this section we intend to apply UV-Vis and FTIR spectrometry to identify several proteins after labeling with chromophore C392STP. Considering the photochemical properties of the chromophore C393STP, in UV-Vis spectrometry we expect to obtain different protein profiles between 250 and 500 nm before and after the labeling reaction. In the case of FTIR spectroscopy, considering the complexity of the spectra of the proteins in this type of spectroscopy, we expect to observe different profiles, between 1500 and 1700 cm^{-1} after the labeling reaction. The changes in the referred range will confirm the possible reactions of the lysine residues with the chromophore, as they will produce new amides with different vibrational modes.

3.3.1.1 UV

The experimental UV-Vis spectrum of C392STP is shown in Figure 3.3, and present peaks at 293, 332 and 392 nm.

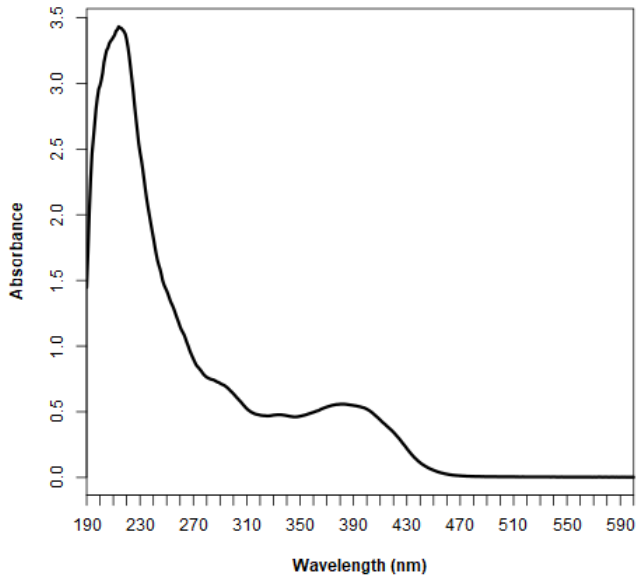

Figure 3.3 UV-Vis spectra of C392STP in acetonitrile.

The UV-Vis spectra of all fluorescent labelled proteins tested (Figure 3.4 to Figure 3.8), show different profiles in the region between 230 to 470 nm, when compared with the UV-Vis spectra of their commercial unlabelled counterparts. Fluorescent BSA presents differentiated peaks at 243, 285 and 381 nm. Similar situations are observed in the UV-Vis spectra of fluorescent ovalbumin, with peaks at 255, 335 and 389 nm, in UV-Vis spectra of fluorescent casein, with peaks at 240 and 374 nm, in UV-Vis spectra of fluorescent collagen, with peaks at 268 and 368 nm and in UV-Vis spectra of fluorescent fish gelatin, with peaks at 245 and 382 nm. The peaks observed in these profiles are not due to the presence of the free chromophore, that absorbs at different wavelengths, which suggest the effectiveness of the labelling reaction of the related proteins.

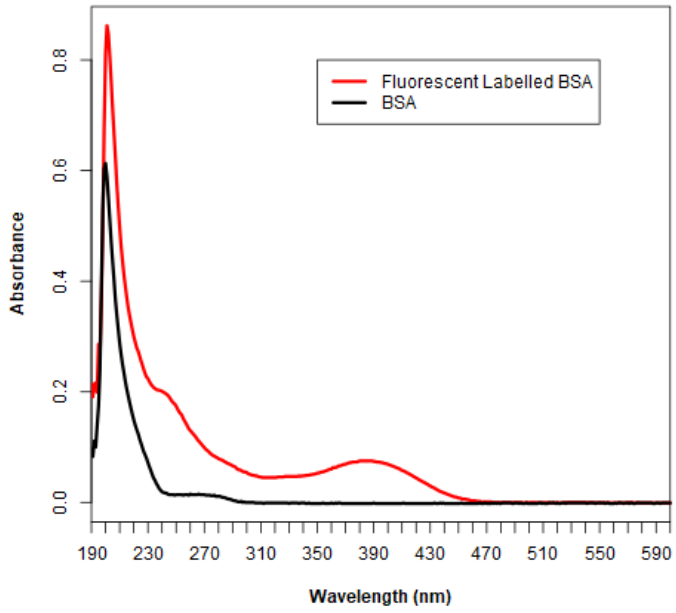

Figure 3.4 UV-Vis spectra of BSA (black) and Fluorescent Labelled BSA (red) in sodium bicarbonate buffer.

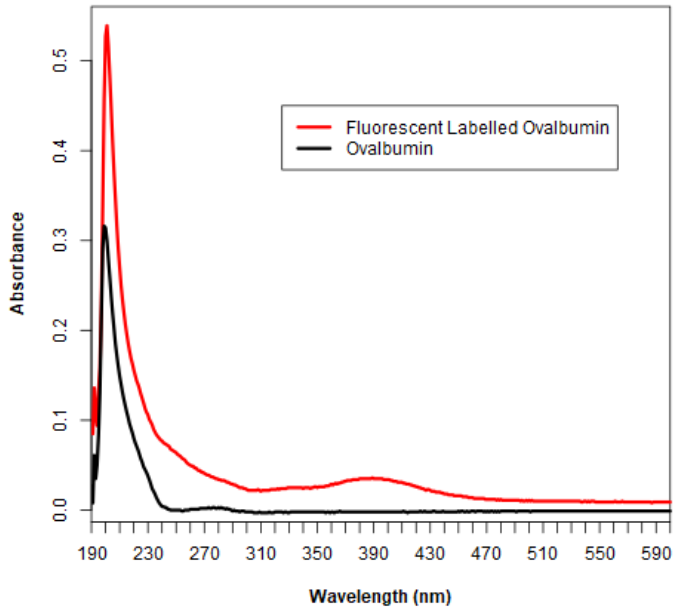

Figure 3.5 UV-Vis spectra of Ovalbumin (black) and Fluorescent Labelled Ovalbumin (red) in sodium bicarbonate buffer.

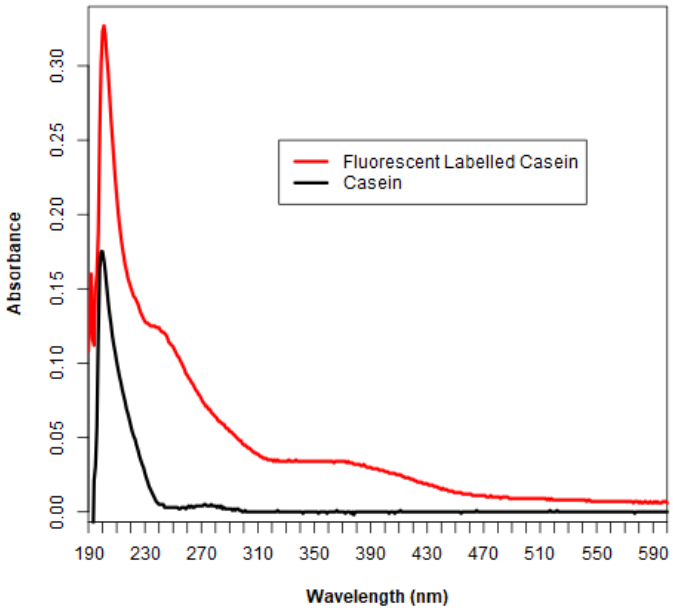

Figure 3.6 UV-Vis spectra of Casein (black) and Fluorescent Labelled Casein (red) in sodium bicarbonate buffer.

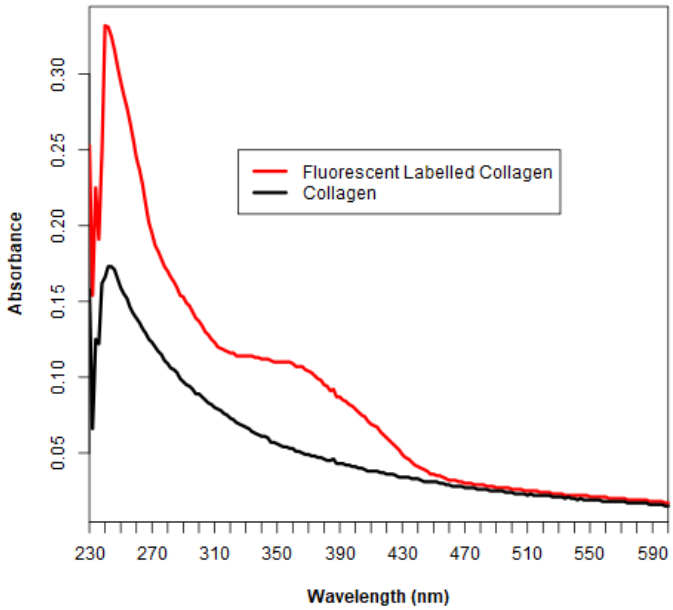

Figure 3.7 UV-Vis spectra of the Collagen (black) and Fluorescent Labelled Collgen (red), was recorded in a mixture of glacial acetic acid (1mL) and sodium bicarbonate buffer solution (4mL), due to its low solubility.

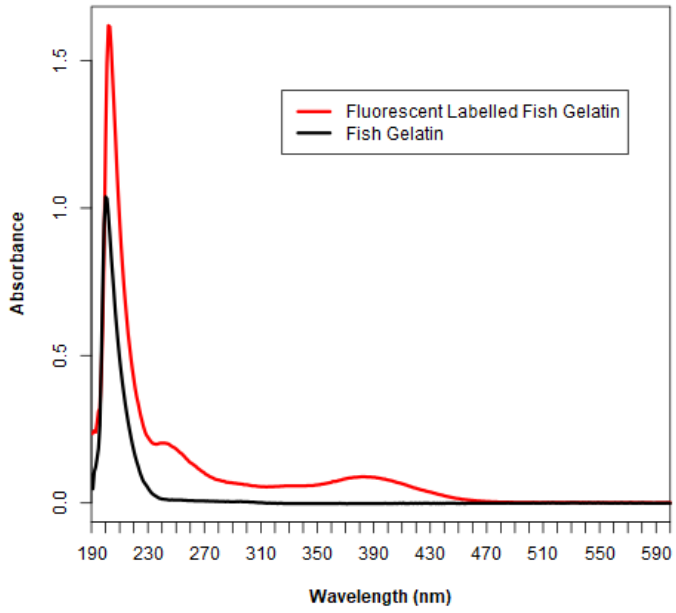

Figure 3.8 UV-Vis spectra of Fish Gelatin (black) and Fluorescent Labelled Fish Gelatin (red) in sodium bicarbonate buffer.

The comparison of the UV-Vis spectra of fluorescent BSA, ovalbumin, casein, collagen and fish gelatin are shown in Figure 3.9. All the fluorescent proteins showed different profiles in the region of 230 to 470 nm.

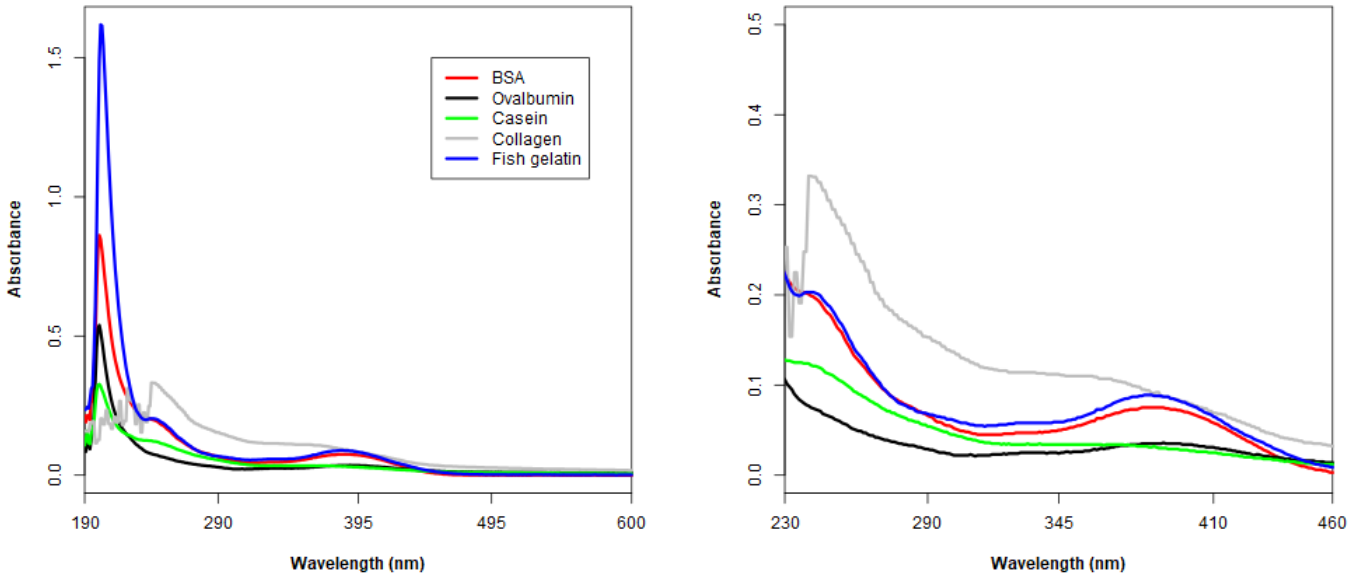

Figure 3.9 UV spectra of the fluorescent labelled BSA (red), ovalbumin (black), casein (green), collagen (grey), fish gelatin (blue) in sodium bicarbonate buffer.

3.3.1.2 FTIR

The infrared spectra of all commercial proteins tested are shown in Figure 3.10 to Figure 3.14. The peaks ranging from 1510 to 1650 cm^{-1} may be attributed to the N-H bending vibration in amines. The peaks between 1630 to 1700 cm^{-1}, and 1510 to 1570 cm^{-1} may be attributed to the –C=O stretching vibrations (Amide-I band) and to the combination bands of N-H deformation and C-N stretching vibrations, respectively, in secondary amides. Changes in the samples of commercial BSA, ovalbumin casein, collagen and fish glue, after the fluorescent labelling with C392STP were detected by infrared spectroscopy.

The infrared spectra of fluorescent BSA show a different profile in the region between 1500 to 1560 cm^{-1} and 1660 to 1700 cm^{-1}. Similar situations are observed in the infrared spectra of fluorescent ovalbumin (1510 to 1560 cm^{-1} and 1625 to 1700 cm^{-1}), in the infrared spectra of fluorescent casein (1500 to 1575 cm^{-1} and 1610 to 1720 cm^{-1}), in the infrared spectra of fluorescent collagen (1500 to 1570 cm^{-1} and 1600 to 1720 cm^{-1}) and in the infrared spectra of fluorescent fish gelatin (1500 to 1560 cm^{-1} and 1600 to 1700 cm^{-1}). These different

profiles in the infrared region of primary amines and secondary amides confirm the effectiveness of the labelling reaction on the related proteins.

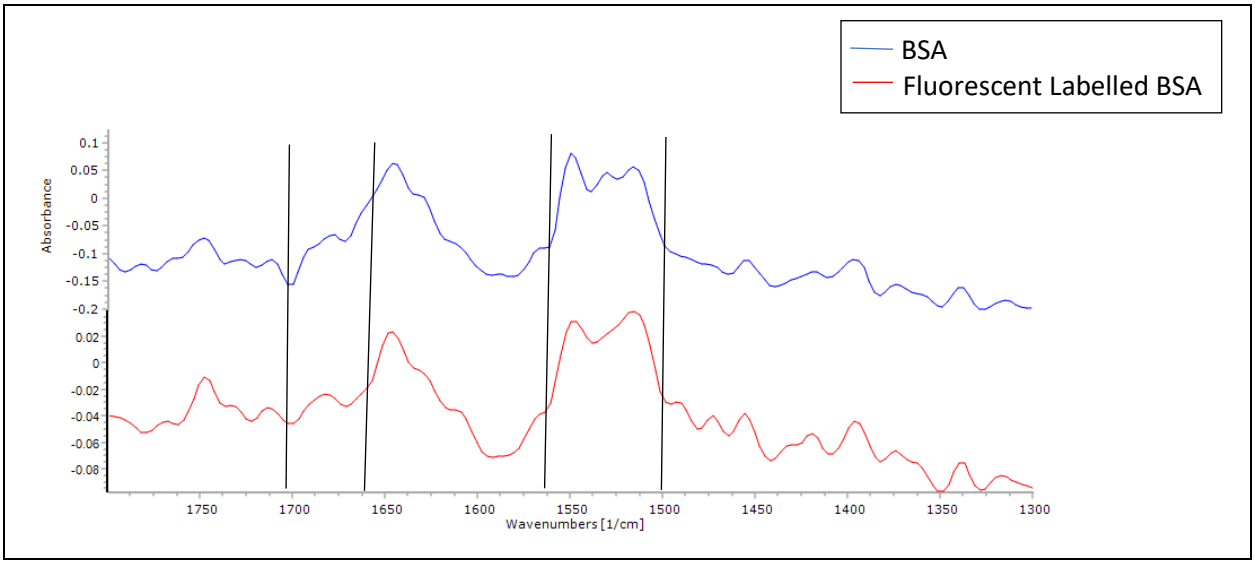

Figure 3.10 FTIR spectra of BSA (blue) and Fluorescent Labelled BSA (red).

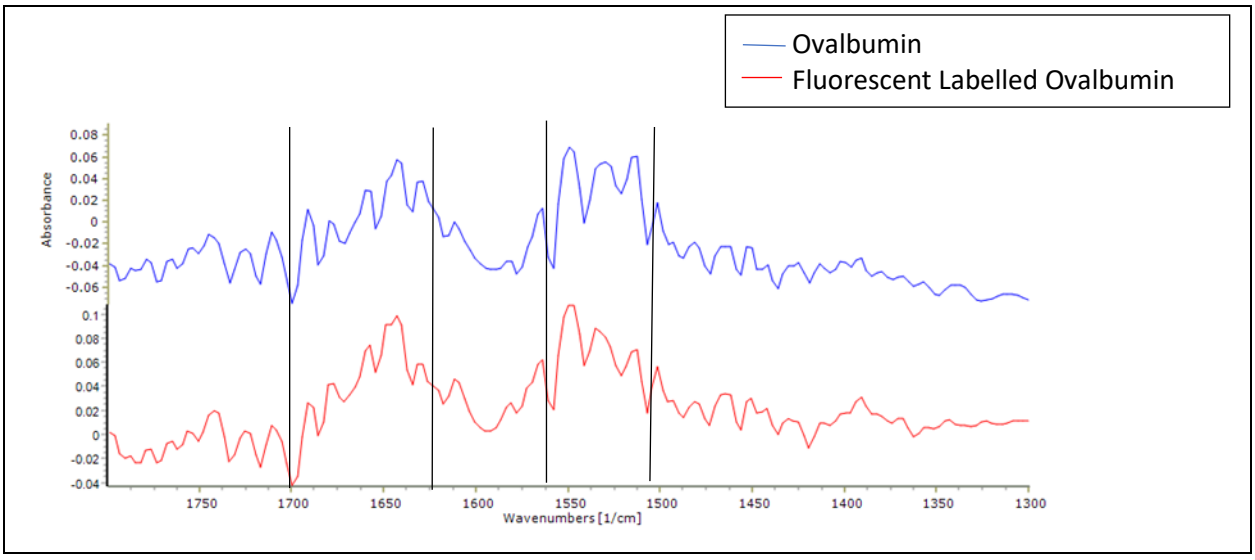

Figure 3.11 FTIR spectra of Ovalbumin (blue) and Fluorescent Labelled Ovalbumin (red).

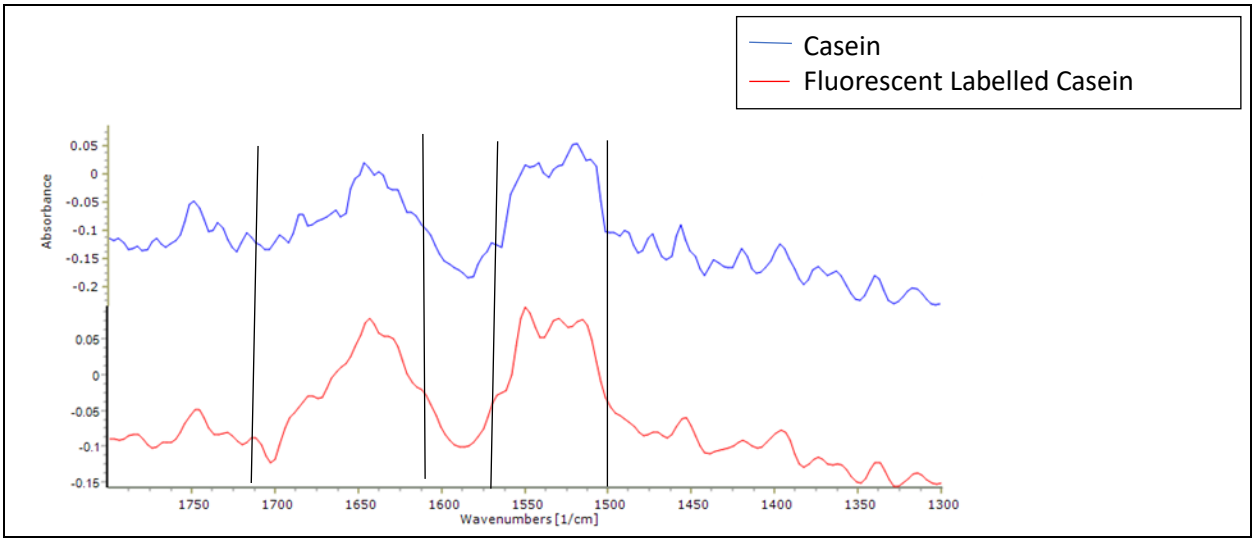

Figure 3.12 FTIR spectra of Casein (blue) and Fluorescent Labelled Casein (red).

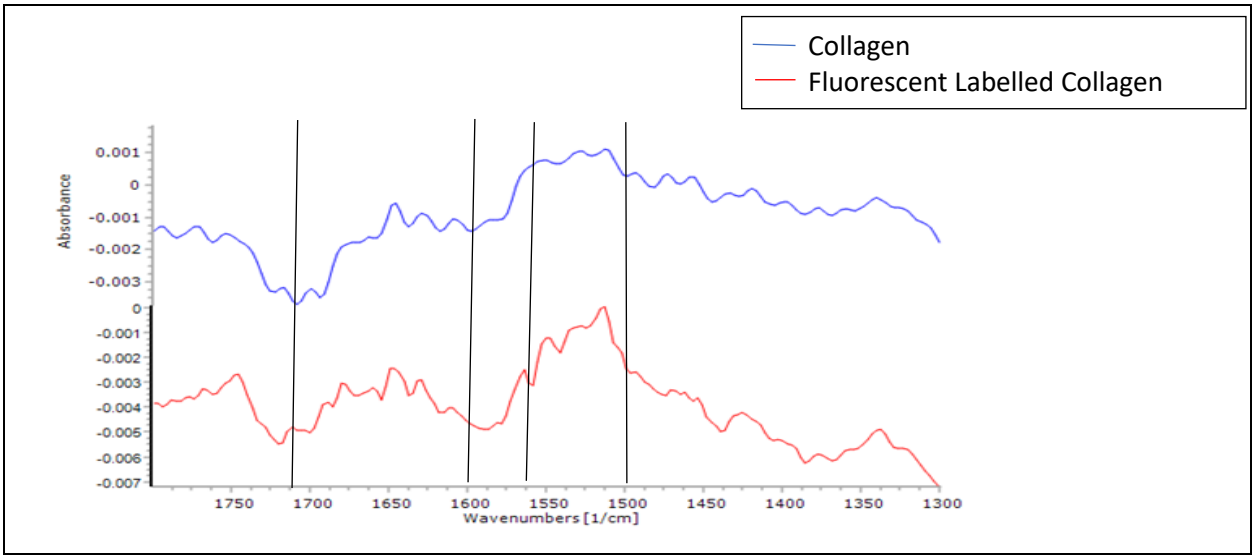

Figure 3.13 FTIR spectra of Collagen (blue) and Fluorescent Labelled Collagen (red).

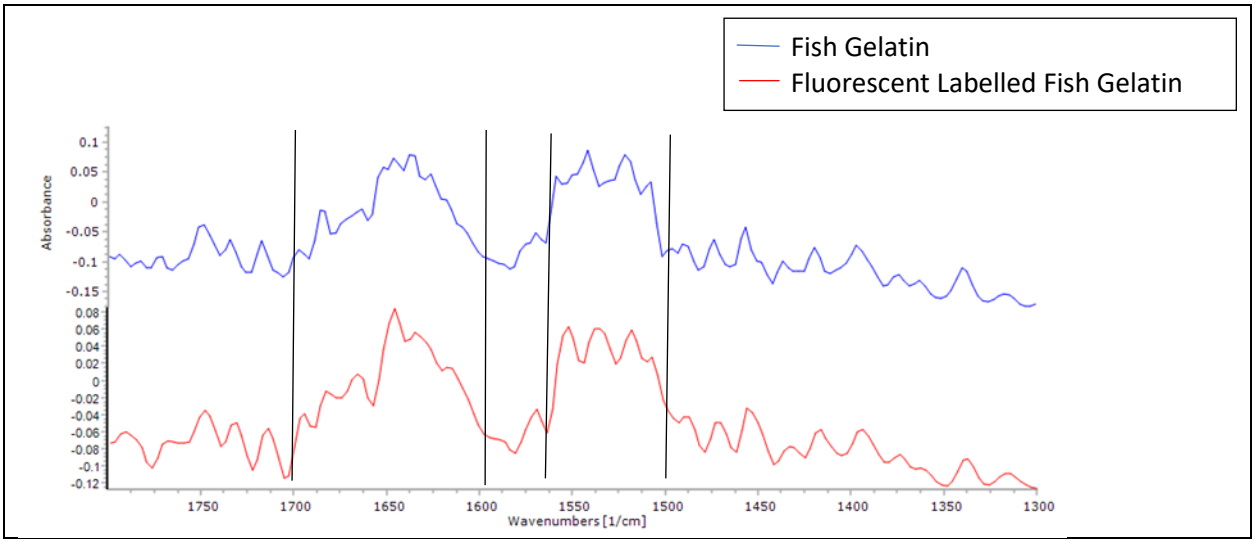

Figure 3.14 FTIR spectra of Fish Gelatin (blue) and Fluorescent Labelled Fish Gelatin (red).

3.3.3 Electrophoretic profiles

To proceed with the identification of the different proteins, electrophoresis was used. Electrophoretic profiles of unbonded proteins and the proteins labeled with C392STP were analyzed for the determination of the characteristic profiles. The PAGE separates the proteins according to their charge and its molecular weight, based on its structure. Through the electrophoresis performed for the commercial proteins (Table 3.3) without the linkage to C392STP, four distinct proteic bands were observed for BSA (200.8, 160.5, 101.4, 52.4 kDa). The result found was similar to the result reported in a previous work which has shown proteic bands of BSA with MW of (198, 132, 66 kDa) [9]. For ovalbumin four distinct proteic bands were observed (64.1, 46.3, 40.0, 36.0 kDa) while casein presented two bands at 66.6 and 38.0 kDa. The lowest concentration that produces clear bands, for both unlabeled commercial ovalbumin and casein, was 0.0625 mg/ml. In the electrophoretogram, it was difficult to observe the band profile corresponding to the unlabelled commercial collagen and fish gelatin (Figure 3.15).

Electrophoresis was also performed with the commercial proteins bonded with C392STP after each step of the optimization process. In test 1, commercial BSA has bonded successfully

with C392STP; four distinct proteic bands, between 35 kDa and 135 kDa, have appeared in the electrophoresis gel. However, the electrophoretic profiles of ovalbumin and casein were not clearly shown. Thus, the optimization process proceeded to test 2, test 3, test 4 and test 5 by increasing the temperature to 40°C with 3 different ratios of C392STP to protein. In this case, four distinct proteic bands, between 20 to 75 kDa, were observed for commercial ovalbumin while three proteic bands, between 35 to 75 kDa, were observed for commercial casein, showing that ovalbumin and casein bond more effectively with C392STP in slightly increased temperature (40°C) conditions. Test 2 was then chosen for the detection of ovalbumin and casein in order to minimize the amount of sample needed. As shown in the electrophoretogram (Figure 3.15) it was difficult to observe the band profile corresponding to the unlabelled commercial collagen. On the other hand, a fluorescent band corresponding to 35 kDa is clearly seen after labelled with coumarin 392 STP ester. From the results, test 5 was efficient in labelling collagen with the proportion of protein:C392STP=5:20. Nevertheless, the electrophoretic profile of fish gelatin showed a fluorescent band with >245 kDa. These electrophoretic profiles (Figure 3.15) confirm the effectiveness of the labelling reaction of the proteins.

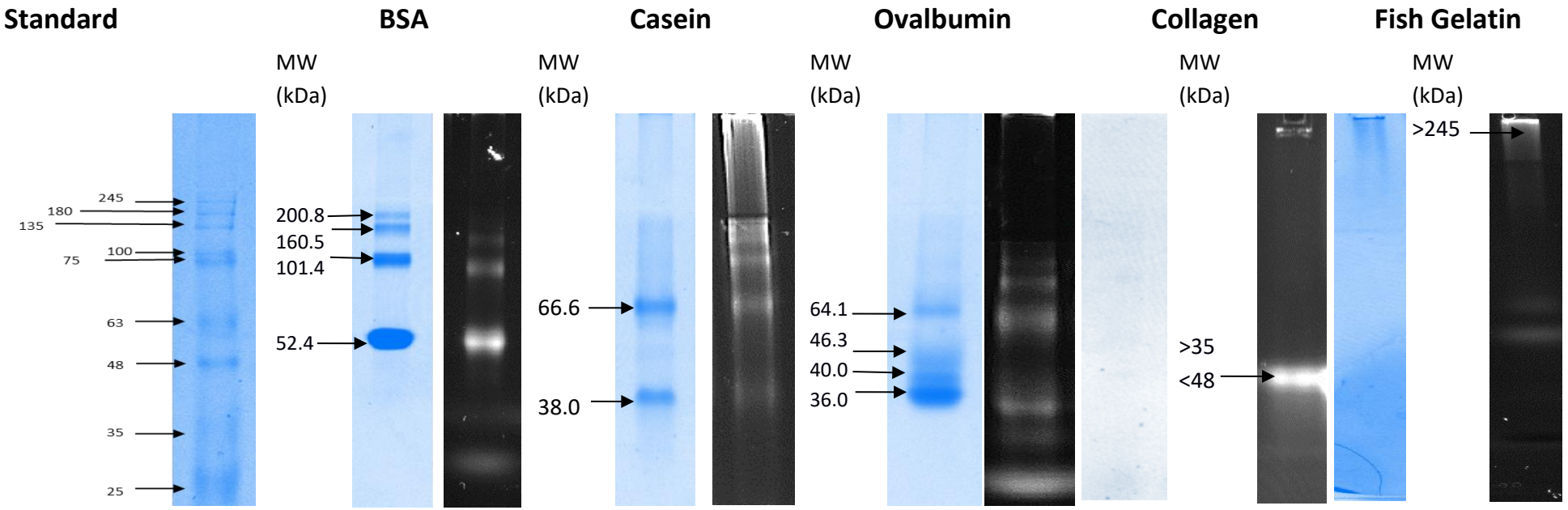

Figure 3.15 Electrophorectogram of commercial BSA, casein, ovalbumin, collagen and fish gelatin without labelling and after fluorescent labelling.

Table 3.3 Molecular weight (kDa) of the commercial proteins displayed in PAGE profiles.

Commercial Proteins	BSA		Ovalbumin		Casein		Collagen
	Unbonded	Fluorescent	Unbonded	Fluorescent	Unbonded	Fluorescent	Fluorescent
	200.8	>100 <135	64.1	>63 <75	66.6	>63 <75	>35 <48
	160.5	>63 <100	46.3	>48 <63	38.0	>48 <63	
	101.4	>63 <75	40.0	>25 <35		>35 <48	
	52.4	>35 <48	36.0	>20 <25			

In the next step, the optimized procedure has been applied on the protein extracted from hen's egg, milk, and rabbit skin. Figure 3.16 shows the electrophorectogram of hen's egg, bovine milk and rabbit glue while Table 3.4 shows the molecular weight of the extracted proteins tested. Ovalbumin extracted from egg yolk present three clear bands at 195.8, 111.7 and 64.0 kDa while one weak band around 48 kDa. On the other hand, two distinct bands were seen for ovalbumin extracted from egg white (177.9, 109.6 kDa) and casein extracted from milk (69.6, 39.9 kDa). Concerning the unlabelled rabbit glue it is possible to detect a diffuse band between 63 and 75 kDa. Branco et al. (2014) also found that rabbit skin glue presents diffuse bands on PAGE [9]. Additionally, in the electrophoresis gel of fluorescent extracted proteins, three clear proteic bands were seen for ovalbumin from egg yolk and casein while four proteic bands were observed for ovalbumin from egg white. On the other hand, for the fluorescent labelled rabbit glue, a clear band is seen between 63 and 75 kDa, evidencing once more the detection capability of this methodology. Comparing the commercial proteins and extracted proteins, the proteic bands appeared around the same positions which means that the molecular weight of both commercial proteins and extracted proteins were similar.

Advantages of this new fluorescent labelling method are that the coumarin derivative ester used can be synthesized easily, at low cost, and has a long wavelength, which is significantly important for biological purposes. Furthermore, it has good solubility in the reaction buffer media. In fact, it was showed that C392STP have a higher water solubility when compared with *N*-hydroxysuccinimidyl (NHS) esters [7]. This is an important characteristic for the application in biological research because it decreases the problem of hydrophobicity of some previously used labelling chromophores [10]. The linkage of proteins with this coumarin chromophore produces clear bands through electrophoresis in native conditions without requiring the step of electrophoresis gel staining making the labelling process simpler and rapid.

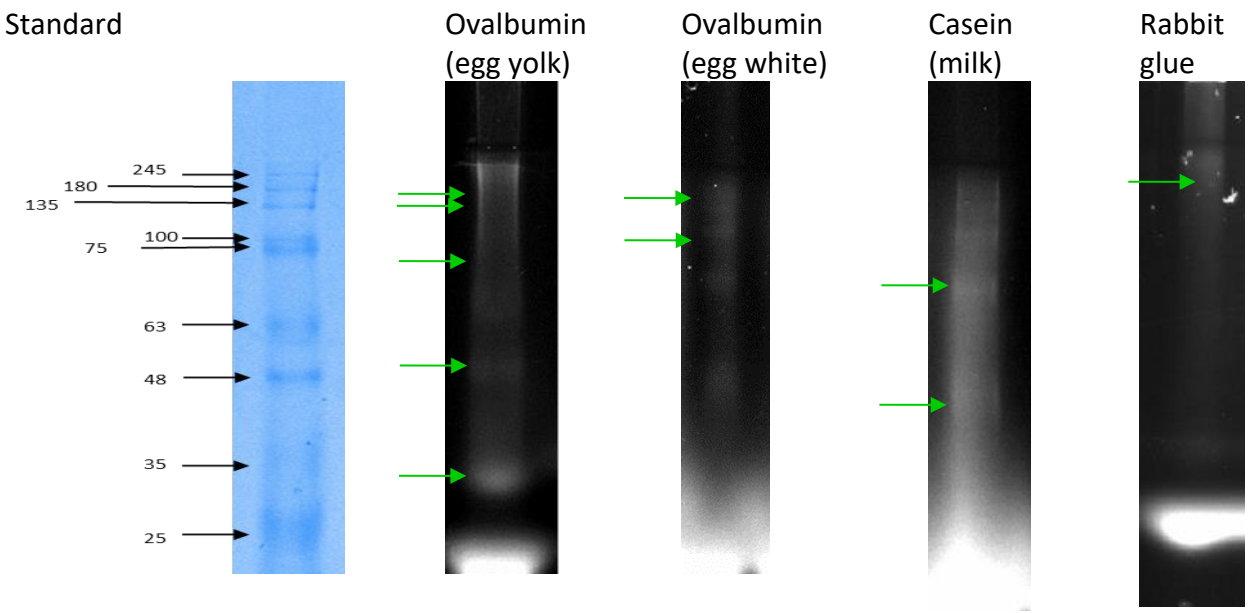

Figure 3.16 Electrophorectogram of extracted proteins [ovalbumin (egg yolk and egg white), casein (milk) and rabbit skin glue].

Table 3.4 Molecular weight (kDa) of the extracted proteins displayed in PAGE profiles.

Ovalbumin				Casein		Collagen	
Unbonded		Fluorescent		Unbonded	Fluorescent	Unbonded	Fluorescent
(egg yolk)	(egg white)	(egg yolk)	(egg white)	Casein (milk)		Rabbit glue	
195.8	177.9	>180	>135 <180	69.6	>63 <75	>63 <75	>63 <75
111.7	109.6	>100 <135	>100 <135	39.9	>35 <48	>63 <75	>63 <75
64.0		>63 <75					
		>48 <63					

3.4 Conclusion

A simple and inexpensive method to detect and identify protein binders, using a coumarin derivative chromophore (C392STP) as a fluorescent label, was presented. It has been applied to commercial proteins and extracted proteins. The proteinaceous samples were made react with the C392STP chromophore. The C392STP bonded to the proteins, and their fluorescent property allows their detection and identification by gel electrophoresis, without the need of the electrophoresis gel staining. The properties of the coumarin derivative used, such as its high fluorescent quantum yields, solubility, low price and synthesis simplicity makes it particularly suitable for this kind of labeling. Furthermore, this family of coumarins owns photo physical and spectroscopic properties that can be easily tailored according to the desired application.

This methodology showed that it is able to identify as well as in detecting the source of the protein. The reported results evidence a great potential of the method as an effective and useful analytical tool in the identification of protein binders in the samples obtained from easel paintings. In the following chapter, the protocol was tested with microsamples from Easel painting's paint models.

Bibliography

[1] M. Vagnini, L. Pitzurra, L. Cartechini, C. Miliani, B. G. Brunetti, and A. Sgamellotti, "Identification of proteins in painting cross-sections by immunofluorescence microscopy," *Anal. Bioanal. Chem.*, vol. 392, no. 1–2, pp. 57–64, 2008.

[2] "A novel amine-reactive coumarin: Evaluation of its potential for produzing singly fluorescent-labeled oligonucleotides and assessment of their performance as RNA-FISH probes (in review)," *New J. Chem.*

[3] M. González-Pérez, S. Y. Ooi, S. Martins, J. P. P. Ramalho, A. Pereira, and A. T. Caldeira, "Gaining insight into the photophysical properties of a coumarin STP ester with potential for bioconjugation," *New J. Chem.*, vol. 42, no. 20, pp. 16635–16645, 2018.

[4] J. Gordo, J. Avó, A. J. Parola, J. C. Lima, A. Pereira, and P. S. Branco, "Convenient synthesis of 3-vinyl and 3-styryl coumarins," *Org. Lett.*, vol. 13, no. 19, pp. 5112–5115, 2011.

[5] S. M. . Martins, P. C. . Branco, and A. M. D. L. . Pereira, "An Efficient Methodology for the Synthesis of 3-Styryl Coumarins," *J. Braz. Chem. Soc.*, vol. 23, no. 4, pp. 688–693, 2012.

[6] S. Martins, P. S. Branco, M. C. Delatorre, M. A. Sierra, and A. Pereira, "New methodology for the synthesis of 3-substituted coumarins via palladium-catalyzed site-selective cross-coupling reactions," *Synlett*, no. 19, pp. 2918–2922, 2010.

[7] K. R. Gee, E. A. Archer, and H. C. Kang, "4-Sulfotetrafluorophenyl (STP) esters: New water-soluble amine-reactive reagents for labeling biomolecules," *Tetrahedron Lett.*, vol. 40, no. 8, pp. 1471–1474, 1999.

[8] C. Salvador, A. Branco, A. Candeias, and A. T. Caldeira, "Innovative approaches for immunodetection of proteic binders in art," *E-Conservation J.*, no. 5, pp. 1–10, 2017.

[9] A. Branco, C. Salvador, A. Fialho, M. Semedo, S. Martins, M.F. Candeias, …, and A.T. Caldeira, "Characterisation and purification of proteic binders used in easel paintings," in *ed. MA Rogerio-Candelera, Science, Technology and Cultural Heritage, CRC Press, London*, 2014, pp. 177–183.

[10] M. S. T. Gonçalves, "Fluorescent labeling of biomolecules with organic probes," *Chem. Rev.*, vol. 109, no. 1, pp. 190–212, 2009.

Chapter 4 APPLICATION OF FLUORESCENT LABELLING METHODOLOGY ON PAINT MODELS

Part of the results have been published in:

- **S. Y. Ooi**, J. P. P. Ramalho, A. Pereira, S. Martins, C. Salvador, & A. T. Caldeira, A simple method for labelling and detection of proteinaceous binders in art using fluorescent coumarin derivatives. Eur. Phys. J. Plus, vol. *134, no.* 2, pp. 71, 2019.

4.0 Overview

This chapter explores the application of fluorescent labelling method on complex matrices. The fluorescent labelling method was tested on proteins extracted from easel painting's paint models. The paint models were made by mixing proteins such as casein, ovalbumin and rabbit glue with different pigments (lead white, chrome yellow and black bone), and submitted to an artificial aging process. The fluorescent labelling was done using the protocol developed in the previous chapter, a mixture of C392STP and the protein extracted from paint model were prepared and stirred for a period of 24 hours before proceeding to electrophoresis. Fluorescent bands were clearly observed on the electrophoresis gel with fluorescent labelling. Results revealed that with fluorescent labelling, proteins extracted from the paint models, in a 6.0 µg/ml concentration could be detected. These extracted proteins, clearly observed in the electrophoretic profiles after fluorescent labelling, were not possible to detect in the conventional electrophoresis performed. The results indicate that fluorescent labelling, followed by electrophoresis can act with high specificity in the identification of proteinaceous binders since it is also possible to detect the proteins extracted from complex matrices.

4.1 Introduction

As described earlier, the proteinaceous compounds such as eggs ovalbumin, milk casein and animal glue collagen produced from animals' bones, cartilages and skins act as binders, adhesives and additives in the coating layer of easel painting [1–5]. They are also mixed with pigments during the painting processes. Binders, that are used as the layer after the draft of artist, can be composed of one kind of protein, a mixture of proteins, a mixture of protein with oil or a mixture of a few types of organic materials [6]. Following a series of original painting process and conservation treatment (with adhesives or coatings), the proteinaceous binder may be a mixture of different proteins. Dealing with the analysis of the composition of this complex mixture of organic materials [6, 7] is even more challenging since it can change over time because of the chemical interactions between the different materials under the

environment where the painting is stored [8, 9]. It is known that the commonly used techniques in proteinaceous materials identification such as chromatographic techniques: high-performance liquid chromatography (HPLC), liquid chromatography and gas chromatography (GC), combined with mass spectrometric (MS), thin-layer chromatography infrared spectrometry), optical methods [1, 10–12] produce signal that is difficult to interpret due to the complexity of matrices and do not allow to identify the biological origins of proteins. On the other hand, the proteomic strategies [6, 7, 13] require expensive equipment and experienced personnel. This chapter was planned to acknowledge the issue of complex matrices in protein identification with the new fluorescent labelling method.

Customarily, a newly developed method is tried on paint models to evaluate the performance of the method. During the development of a protocol which will be applied in cultural heritage studies, testing on paint model is also important because microsamples from paintings are often limited in amount. Painting models are commonly made from proteinaceous binders blended with pigments. In the preparation of paint models, one of the most commonly used protein is ovalbumin from egg [2, 6, 14–18] because ovalbumin is always found as a binder, mixed with pigments or as varnish on top of the paintings. Milk, rabbit glue and bovine glue have also been used in paint model construction to mix with pigments in producing paint layers [2, 14–16].

Through the literature review, it was identified that painters in the 19th century often used pigments such as lead white, yellow ochre, chrome yellow [9, 19, 20]. Thus, three pigments have been chosen for the paint model construction. Lead white, yellow ochre and black bone have been chosen because they are detected in previous research on 19^{th} century Easel paintings in Portugal [9, 19]. From previous research, steps of paint models' preparation started with the extraction of protein (ovalbumin) from egg followed by mixing with pigments and finally applied on glass slide [6, 17]. Another typical proteinaceous binder, rabbit glue, was also used in paint models' preparation of Medieval painting [21]. In the present study we have prepared paint models by mixing proteins: casein, ovalbumin and rabbit glue, with different pigments: lead white, yellow ochre and black bone. The mixture of pigment and binder in a ratio of pigment to binder weight ratio = 3:1 were then applied on the prepared

support and the submitted to an artificial aging process. Subsequently, the fluorescent labelling method was tested on proteins extracted from the paint models. The following of this chapter addressed the fourth research question as below:

1. How does fluorescent labelling assist in identifying the origins of protein binders used in easel paintings when painting matrices are complex with the presence of pigments and has undergone aging processes?

4.2 Methodology

4.2.1 Materials

All the commercial reagents such as acetic acid (PanReac), acrylamide (Sigma-Aldrich), bisacrylamide (Sigma-Aldrich), bromophenol blue (Sigma-Aldrich), glycerol (Merck), Tris-HCl buffer (VWR) were used as they were received. The buffer was prepared in distilled water with Na_2CO_3 (6398, Merck) (0.1 mol) and $NaHCO_3$ (6329, Merck) (0.1 mol), pH 8.2. The rabbit glue was prepared in the lab using the concentrated animal glue (boiling the rabbit skin and bone) which was stored in solid state.

4.2.2 Protein content

Before the fluorescent labelling methodology be applied on paint models, the concentration of samples required were tested using unbonded proteins. The lower concentration needed in order to obtain a clear electrophoretic profile were tested by testing the electrophoretic profiles for commercial casein and commercial ovalbumin at different concentrations. The concentration of protein and the concentrations of C392STP needed were decided and applied on the protein recover from paint models.

4.2.3 Mimitize real conditions using paint models of Easel paintings

4.2.3.1 Paint models' construction with one pigment

Paint models of Easel paintings were prepared by mixing proteins extracted from hen's egg (yolk and white), bovine milk, and rabbit skin glue used as binders, and different pigments. Pigments commonly used in Easel paintings such as lead white, yellow ochre and black bone were chosen (Table 4.1). These are pigments commonly found in painting, for instance the lead white and yellow chrome pigments used in the paint models were found in the paintings from Giorgio Marini [19], studied in the next chapter. The ratio of binders to pigment was 1:3. Mixtures layers with thickness between 50-150 µm (Figure 4.1) were applied on glass supports. The Easel painting paint models were then placed in aging chamber for 1 month to undergo the aging process artificially. The aging process was carried out in 3 cycles, each cycle consisting of 5 days in a relative humidity of 85 % and a temperature of 45°C followed by 5 days in a relative humidity of 30 % and a temperature of 12°C.

Table 4.1 Constitution of paint models.

	Proteic binders	**Pigments**
PM1	Whole egg	Lead white: $2(PbCO_3).\ Pb(OH)_2$ (10 g)
PM2		Yellow ochre: FeO(OH)
PM3		Black bone: $Ca_5(OH)(PO_4)_3$ and C
PM4	Bovine milk	Lead white: $2(PbCO_3).\ Pb(OH)_2$ (10 g)
PM5		Yellow ochre: FeO(OH)
PM6		Black bone: $Ca_5(OH)(PO_4)_3$ and C
PM7	Rabbit skin glue	Lead white: $2(PbCO_3).\ Pb(OH)_2$ (10 g)
PM8		Yellow ochre: FeO(OH)
PM9		Black bone: $Ca_5(OH)(PO4)_3$ and C

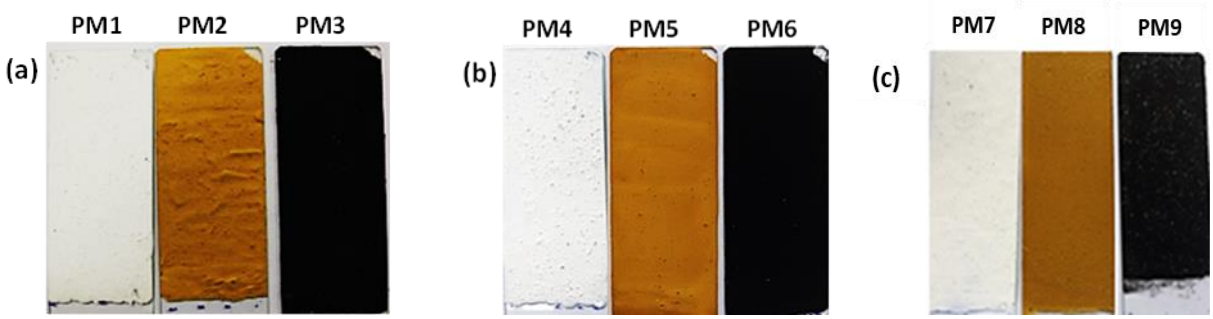

Figure 4.1 Easel painting models prepared using (a) hen's egg, (b) bovine milk, and (c) rabbit skin glue, as binder with different pigments, lead white, yellow ochre and black bone.

4.2.3.2 Paint models' construction with three pigments

These paint models consist of protein binders and a mixture of different pigments. We have prepared three paint models, each with one kind of protein and three different pigments (Figure 4.2).

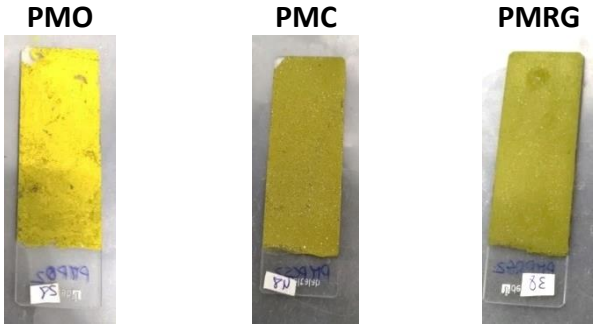

(a) Ovalbumin lead white + chrome yellow + black bone

(b) Casein lead white + chrome yellow + black bone

(c) Rabbit glue lead white + chrome yellow + black bone

Figure 4.2 Easel painting models prepared using (a) hen's egg, (b) bovine milk, and (c) rabbit skin glue, as binder with three different pigments, lead white, chrome yellow and black bone.

The mixtures of 1 portion of protein and 3 portions of pigments were applied on glass support to form paint layer with thickness between 50–150 µm. All the paint models prepared were placed in the aging chamber to mimic the aging process artificially. The aging conditions

consisted on 5 days in a relative humidity of 85% and a temperature of 45°C followed by 5 days in a relative humidity of 30% and a temperature of 12 °C for a cycle. This cycle was repeated for 3 times.

4.2.3.3 Bonding of extracted proteins with the coumarin chromophore

The samples were obtained from the paint models microsamples. Then, each sample was suspended in 1 ml of sodium bicarbonate buffer. The proteins were extracted in three cycles consisting of a sonification step during 1h and an incubation step at 37°C with orbital agitation during 1h, followed by an overnight incubation at 37°C as described by Salvador et al., 2017 [9].

The proteinaceous content which was extracted from the paint microsamples was determined using the Bradford method [22]. Commercial BSA (A2153) was prepared in concentrations ranging from 1 to 40 µg/ml as the standard solution. The total protein content of the microsamples was expressed as g of BSA equivalents per milligram of microsample [23], [24]. After determining the protein content extracted, they were bonded with C392STP using the developed fluorescent labelling method. The reactions were prepared by mixing the C392STP at the concentration of 0.025 mg/ml and the proteins recovered from the paint models in sodium bicarbonate buffer with a total volume of (1.0 ml) and stirred for a period of 24 h (Table 4.2).

4.3 Results and discussions

4.3.1 Fluorescent labelling

Results showed that it was possible to detect the electrophoretic signals of commercial casein, commercial ovalbumin and rabbit glue without fluorescent labelling at concentrations above 0.0625 mg/ml. Likewise, different concentrations of C392STP were tested for labelling this amount of protein (Figure 4.3). The labelled protein produced was

then submitted to electrophoresis and based on the fluorescent bands observed, the concentration of 0.25 mg/ml of C392STP was chosen for labelling.

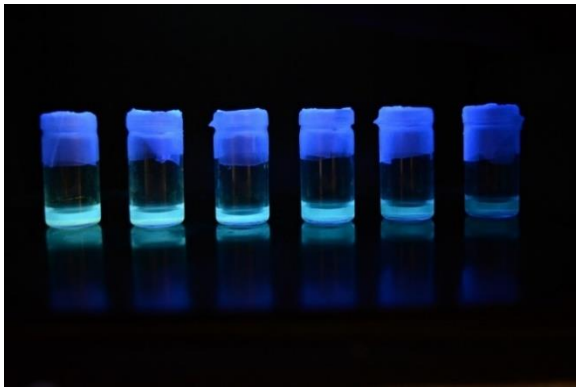

Figure 4.3 Fluorescent proteins with different concentrations of chromophore.

This methodology was tested on the paint models prepared as previously described. Considering the objective of reducing the amount of microsample and C392STP for fluorescent labelling, 0.25 mg/ml of C392STP was applied on the fluorescent labelling of protein recovered from different paint models, reactions 1-12 (Table 4.2).

Table 4.2 Fluorescents labelling between paint models and C392STP.

Reactions	Paint models with one pigment		
Reaction 1	100 µl protein extract recovered from PM1	0.25 ml C392STP (0.25 mg/ml)	0.75 ml buffer
Reaction 2	100 µl protein extract recovered from PM2		
Reaction 3	100 µl protein extract recovered from PM3		
Reaction 4	100 µl protein extract recovered from PM4		
Reaction 5	100 µl protein extract recovered from PM5		
Reaction 6	100 µl protein extract recovered from PM6		
Reaction 7	100 µl protein extract recovered from PM7		
Reaction 8	100 µl protein extract recovered from PM8		
Reaction 9	100 µl protein extract recovered from PM9		
	Paint models with 3 pigments		
Reaction 10	100 µl protein extract recovered from PMC	0.25 ml C392STP (0.25 mg/ml)	0.75 ml buffer
Reaction 11	100 µl protein extract recovered from PMO		
Reaction 12	100 µl protein extract recovered from PMRG		

4.3.2 Electrophoretic profiles of paint models with one pigment

As mentioned in section 4.2.1.3, proteins were extracted from the paint models (PM1-PM9) and labelled with C392STP. The range of protein concentration was between 6.42 µg/ml and 33.58 µg/ml (Figure 4.4). To proceed with the identification of the proteins, electrophoresis was used for the determination of the characteristic profiles. Figure 4.5 shows the electrophoresis gel obtained from the extracted proteins from the paint microsamples. Fluorescent band were observed at >25 <35 kDa for extracted ovalbumin (PM1-PM3), which was in line with the band observed from fluorescent commercial ovalbumin and fluorescent ovalbumin from egg yolk. Additionally, a clear fluorescent band was found at >100 <135 kDa for the extracted casein from the paint model.

The electrophoretic profile showed similar characteristic band profiles for the extracted and the commercial proteins. Fluorescent bands were observed at the same area (>25 <35 kDa) for the paint models which contained the same protein (ovalbumin) and different pigments (PM1, PM2 and PM3) while fluorescent bands were also observed at the same area (>100 <135 kDa) for the paint models containing casein with different pigments (PM4, PM5, PM6). On the other hand, the electrophoretic profiles of rabbit glue and fluorescent rabbit glue extracted from the paint microsamples (PM7, PM8, PM9) showed coincident patterns, permitting to identify collagen proteinaceous binders in the painting matrices. The fluorescent bands, characteristics of proteins were clearly visible even after the accelerated aging process that can promote complex modifications of the proteinaceous binders.

The results showed that is possible to extract and detect these proteic binders from different matrices in the presence of several different pigments. The protein content at the concentrations ranged from 6.42 µg/ml – 17.42 µg/ml (ovalbumin paint models), 10.10 µg/ml – 27.95 µg/ml (casein paint models) and 6.49 µg/ml – 33.58 µg/ml (rabbit glue paint models) can be labelled with C392STP. The fluorescent proteins produced can be easily detected using spectroscopic methods as well as electrophoresis.

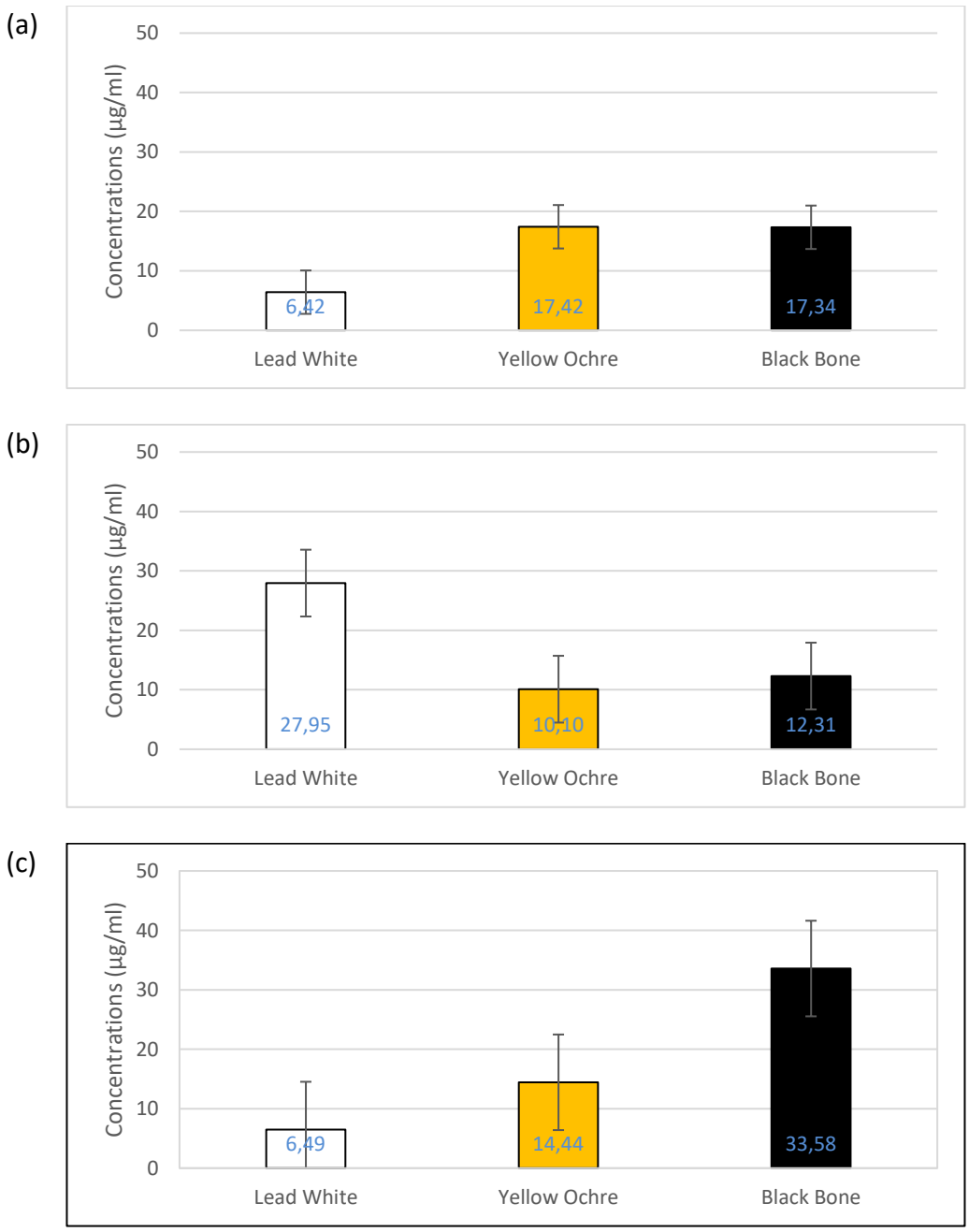

Figure 4.4 Protein content of paint models prepared from (a) hen's egg, (b) bovine milk, and (c) rabbit skin glue. The labels are the median ± SD of the 3 replicates.

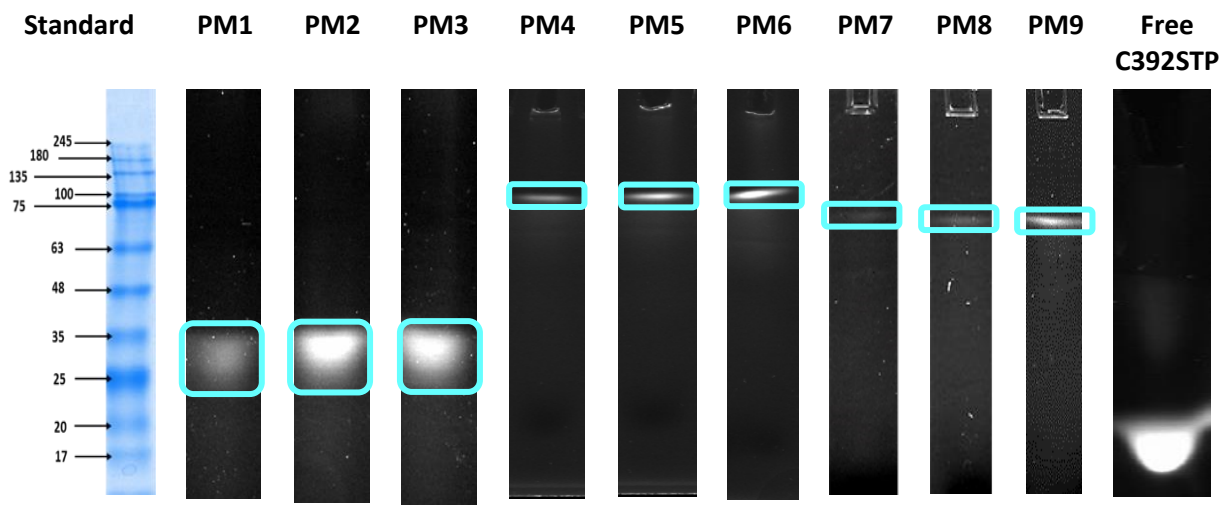

Figure 4.5 Electrophoretic profile of proteins extracted from the paint models labelled with fluorescent coumarin 392 TFP ester.

These results also indicated that the method shows high sensitivity, considering that it was able to detect proteic binders from paint model microsamples with protein content as low as 6.57 µg/ml (proteins extracted from paint models range from 6.49 µg/ml to 33.58 µg/ml) while the lowest concentration detected from unlabelled commercial protein samples was 0.0625 mg/ml. Thus, it is concluded that the origins of the proteins obtained from the aged paint models, corresponding to different matrices and pigments, can be identified with this methodology.

4.3.3 Electrophoretic profiles of paint models with three pigments

In the next step, we have taken into account the application of fluorescent methodology on the more complex matrices. Here, the protein was recovered from the paint containing proteinaceous binders with mixed pigments. Protein contents in the paint models, determined by the Bradford method as explained before, were 3.30 µg/ml, 2.09 µg/ml and 4.14 µg/ml for PMO, PMC and PMRG respectively (Figure 4.6). Promising results were found

under the same conditions of fluorescent labelling that it was employed for the labelling of commercial ovalbumin, commercial casein and rabbit glue.

The results also showed that this method can be applied on the labelling of paint microsamples with a minimal amount of C392STP. Looking at the electrophoretic profiles (Figure 4.7) we were able to observe fluorescent bands for all the paint models. Clear bands can be observed for all the labelled proteins extracted from the paint microsamples although the amount of chromophore was reduced from 0.585mg/ml to 0.025 mg/ml in the labelling process. It was possible to detect the proteins in all the paint models which also supported the fact that pigments did not influence the sample preparation. This fact as also been suggested by Fremout and colleagues (2010) who also used historical pigments such as lead white in paint models' preparation [12]. The present study with complex aged paint models has determined the applicability of fluorescent labelling on aged samples.

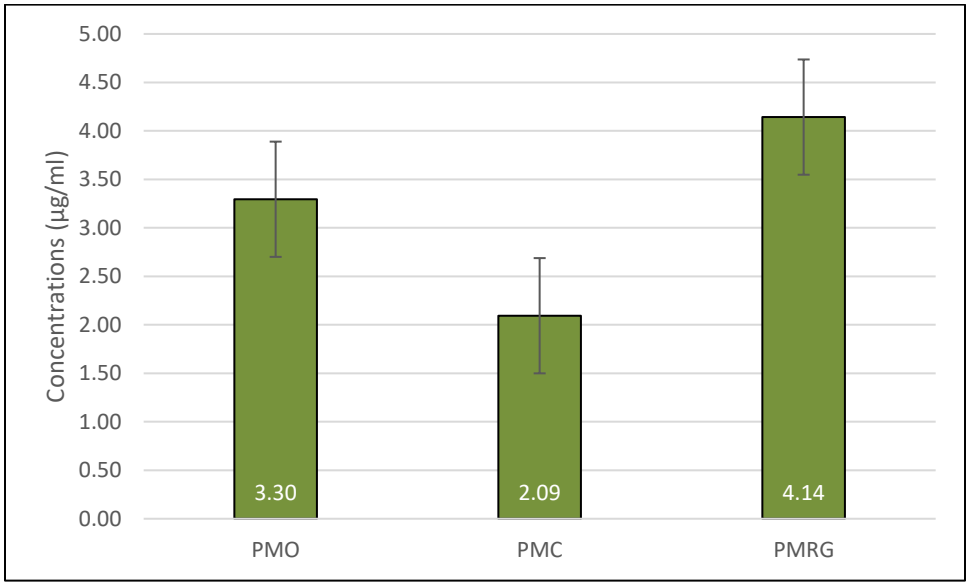

Figure 4.6 Protein content of the paint models prepared from hen's egg (PMO), bovine milk (PMC) and rabbit skin glue (PMRG). The labels are the median ± SD of 3 replicates.

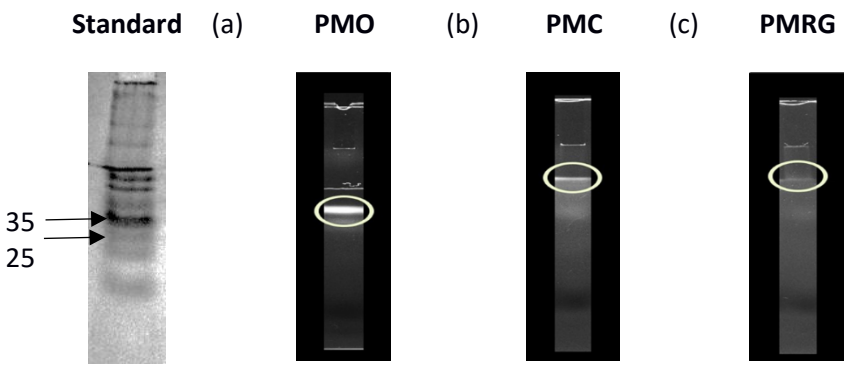

Figure 4.7 Electrophoretic profiles of (a) PMO, (b) PMC and (c) PMRG.

4.4 Conclusion

The methodology was tested on samples taken from paint models with single pigment and paint models with three pigments, submitted to an artificial aging process. The results of the previous tests on commercial proteins showed that temperature influence the binding process between protein and C392STP, so, the bonding process with microsamples of paint models were set at 40°C. By using this optimized fluorescent labelling methodology, it was possible to label the proteinaceous binders with C392STP. Following electrophoresis analysis, fluorescent bands were observed at >25 <35 kDa, for extracted ovalbumin (PM1-PM3), a clear fluorescent band was found at >100 <135 kDa for the extracted casein from the paint model (PM4-PM6) while a clear band was observed between 63 kDa and 75 kDa for the extracted rabbit glue (PM7-PM9). In the same way, fluorescent bands were also observed for PMO, PMC and PMRG which were made with a more complex matrix. Analysis on either single pigment or three pigments models have shown good results, with fluorescent bands being observed in all the paint models. It can be concluded that fluorescent labelling is effective on the detection of proteins from microsamples with complex compositions.

Bibliography

[1] A. Lluveras, I. Bonaduce, A. Andreotti, and M. P. Columbini, “GC/MS analytical procedure for the characterization of glycerolipids, natural waxes, terpenoid resins, proteinaceous and polysaccharide materials in the same paint microsample avoiding interferences from inorganic media,” *Anal. Chem.*, vol. 82, no. 1, pp. 376–386, 2010.

[2] C. D. Calvano, I. D. Van Der Werf, F. Palmisano, and L. Sabbatini, “Identification of lipid- and protein-based binders in paintings by direct on-plate wet chemistry and matrix-assisted laser desorption ionization mass spectrometry,” *Anal. Bioanal. Chem.*, vol. 407, no. 3, pp. 1015–1022, 2015.

[3] L. Cartechini, M. Vagnini, M. Palmieri, L.Pitzurra, T. Mello, J. Mazurek, and G. Chiari, “Immunodetection of proteins in ancient paint media,” *Acc. Chem. Res.*, vol. 43, no. 6, pp. 867–876, 2010.

[4] W. Fremout, S. Kuckova, M. Crhova, J. Sanyoya, S. Saverwyns, R. Hynek,…, and L. Moens, “Classification of protein binders in artist’s paints by matrix-assisted laser desorption/ionisation time-of-flight mass spectrometry: An evaluation of principal component analysis (PCA) and soft independent modelling of class analogy (SIMCA),” *Rapid Commun. Mass Spectrom.*, vol. 25, no. 11, pp. 1631–1640, 2011.

[5] A. Nevin, D. Comelli, G. Valentini, D. Anglos, A. Burnstock, S. Cather, and R. Cubeddu, “Time-resolved fluorescence spectroscopy and imaging of proteinaceous binders used in paintings,” *Anal. Bioanal. Chem.*, vol. 388, no. 8, pp. 1897–1905, 2007.

[6] C. Tokarski, E. Martin, C. Rolando, and C. Cren-Olivé, “Identification of Proteins in Renaissance Paintings by Proteomics,” *Anal. Chem.*, vol. 78, no. 5, pp. 1494–1502, 2006.

[7] G. Leo, L. Cartechini, P. Pucci, A. Sgamellotti, G. Marino, and L. Birolo, “Proteomic strategies for the identification of proteinaceous binders in paintings,” *Anal. Bioanal. Chem.*, vol. 395, no. 7, pp. 2269–2280, 2009.

[8] J. Arslanoglu, J. Schultz, J. Loike, and K. Peterson, “Immunology and art: Using antibody-based techniques to identify proteins and gums in artworks,” *J. Biosci.*, vol. 35, no. 1, pp. 3–10, 2010.

[9] C. Salvador, R. Bordalo, M. Silva, T. Rosado, A. Candeias, and A. T. Caldeira, “On the

conservation of easel paintings: evaluation of microbial contamination and artists materials," *Appl. Phys. A Mater. Sci. Process.*, vol. 123, no. 1, p. 80, 2017.

[10] A. Andreotti, M. Bonaduce, M. P. Colombini, G. Gautier, F. Modugno, and E. Ribechini, "Combined GC/MS analytical procedure for the characterization of glycerolipid, waxy, resinous, and proteinaceous materials in a unique paint microsample," *Anal. Chem.*, vol. 78, no. 13, pp. 4490–4500, 2006.

[11] M. T. Doménech-Carbó, "Novel analytical methods for characterising binding media and protective coatings in artworks," *Anal. Chim. Acta*, vol. 621, no. 2, pp. 109–139, 2008.

[12] W. Fremout, M. Dhaenens, S. Saverwyns, J. Sanyova, P. Vandenabeele, D. Deforce, and L. Moens, "Tryptic peptide analysis of protein binders in works of art by liquid chromatography-tandem mass spectrometry," *Anal. Chim. Acta*, vol. 658, no. 2, pp. 156–162, 2010.

[13] S. Dallongeville, M. Richter, S. Schäfer, M. Kühlenthal, N. Garnier, C. Rolanda, and, C. Tokarski, "Proteomics applied to the authentication of fish glue: application to a 17th century artwork sample," *Analyst*, vol. 138, no. 18, p. 5357, 2013.

[14] M. Palmieri, M. Vagnini, L. Pitzurra, P. Rocchi, B.G. Brunetti, A. Sgamellotti, and L. Cartechini, "Development of an analytical protocol for a fast, sensitive and specific protein recognition in paintings by enzyme-linked immunosorbent assay (ELISA)," *Anal. Bioanal. Chem.*, vol. 399, no. 9, pp. 3011–3023, 2011.

[15] C. D. Calvano, I. D. Van Der Werf, and F. Palmisano, "Fingerprinting of egg and oil binders in painted artworks by matrix-assisted laser desorption ionization time-of-flight mass spectrometry analysis of lipid oxidation by-products," *Anal Bioanal Chem*, vol. 400, no. 7, pp. 2229–2240, 2011.

[16] G. Sciutto, L.S. Dolci, A. Buragina, S. Prati, M. Guardigli, R. Mazzeo, and A. Roda, "Development of a multiplexed chemiluminescent immunochemical imaging technique for the simultaneous localization of different proteins in painting micro cross-sections," *Anal. Bioanal. Chem.*, vol. 399, no. 9, pp. 2889–2897, 2011.

[17] M. Potenza, G. Sabatino, F. Giambi, L. Rosi, A. M. Papini, and L. Dei, "Analysis of egg-based model wall paintings by use of an innovative combined dot-ELISA and UPLC-based

approach," *Anal. Bioanal. Chem.*, vol. 405, no. 2–3, pp. 691–701, 2013.

[18] M. Zangheri, G. Sciutto, M. Mirasoli, S. Prati, R. Mazzeo, A. Roda, and M. Guardigli, "A portable device for on site detection of chicken ovalbumin in artworks by chemiluminescent immunochemical contact imaging," *Microchem. J.*, vol. 124, pp. 247–255, 2016.

[19] R. Bordalo, C. Bottaini, C. Moricca, and A. Candeias, "Material Characterisation of a Florentine painter in Portugal in the Late 19th century: paintings by Giorgio Marini," *Int. J. Conserv. Sci.*, vol. 7, no. 4, pp. 967–980, 2016.

[20] N. Eastaugh, V. Walsh, T. Chaplin, and R. Siddall, *Pigment Compendium*: a dictionary of historical pigments, Routledge, 2013.

[21] J. Romero-Pastor, N. Navas, S. Kuckova, A. Rodríguez-Navarro, and C. Cardell, "Collagen-based proteinaceous binder-pigment interaction study under UV ageing conditions by MALDI-TOF-MS and principal component analysis," *J. Mass Spectrom.*, vol. 47, no. 3, pp. 322–330, 2012.

[22] M. M. Bradford, "A rapid and sensitive method for the quantitation of microgram quantities of protein utilizing the principle of protein-dye binding," *Anal. Biochem.*, vol. 72, no. 1–2, pp. 248–254, 1976.

[23] J.M.S. Arroyo, M.R. Martins, C. Salvador, M.F. Candeias, A. Karmali, and A.T. Caldeira, "Protein-polysaccharides of Trametes versicolor: production and biological activities," *Med. Chem. Res.*, vol. 21, no. 6, pp. 937–943, 2012.

[24] C. Salvador, M.R. Martins, M.F. Candeias, A. Karmali, J. Arteiro, and A.T. Caldeira, "Characterization and biological activities of protein-bound polysaccharides produced by cultures of Pleurotus ostreatus," *J. Agric. Sci. Technol.*, vol. 2, no. 11A, p. 1296, 2012.

Chapter 5 APPLICATION OF FLUORESCENT LABELLING METHODOLOGY ON REAL SAMPLES

Part of the results have been published in:

- **S. Y. Ooi**, C. Salvador, S. Martins, A. Pereira, A. T. Caldeira, and J. P. P. Ramalho, Abstract of "Approaches for the protein binders' determination on Easel paintings," INART 2018 3rd International Conference on Innovation in Art Research and Technology, pp. 91, 2018.

5.0 Overview

In this chapter the application of the fluorescent labelling method with C392STP coumarin on microsamples obtained from easel paintings will be demonstrated. Proteins were recovered from samples of easel paintings by Giorgio Marini (1836–1905), from the museum of Évora and private collections. The extracted proteins were submitted to the fluorescent labelling method. The fluorescent labelling was done using a coumarin derivative C392STP (sodium (*E/Z*)-4-(4-(2-(6,7-dimethoxy-coumarin-3-yl) vinyl) benzoyl)-2,3,5,6-tetrafluorobenzenesulfonate) as chromophore, which was mixed with the proteins extract for a period of 24 hours. The extracted proteins could be clearly observed in the electrophoretic profiles, after fluorescent labelling, which was not possible in the conventional electrophoresis performed. Fluorescent labelling with C392STP revealed that ovalbumin is present in all three paintings. The results indicate that fluorescent labelling with C392STP coumarin, followed by electrophoretic detection, is a simple and fast method with high sensitivity, that can act with high specificity in the identification of proteinaceous binders used in easel paintings.

5.1 Introduction

According to the previous chapter, protein binders' detection in paint models mimicking easel paintings by fluorescent labelling using the C392STP coumarin have worked well. After confirmation about the applicability of fluorescent labelling with protein recovered from artificial, laboratory made, complex matrices, we tried it on the microsamples from real easel paintings. For the last part of this research, the fluorescent labelling was tested on microsamples obtained from easel paintings exhibited in the Museum of Évora. Museum of Évora, established in 1915, has some collections of paintings which the earliest were painted in mid-14th century. One of the collections are the paintings by an Italian painter, Giorgio Marini (Florence 1836 — Castelo Branco, 1905), whose works were produced during the 19th

century. Being one of the innovative Italian painters who lived in Portugal, he produced high quality portraits, landscapes, religious and historic paintings. Despite the interest of his work, reflecting a mixture of cultures, his work is not well studied. Fortunately, most of the paintings available are in a good conservation state.

The present research intends to explore the proteinaceous binders used by Giorgio Marini. The paintings are dated from 1887 to 1897 including portraits and landscapes. The earliest painting by Giorgio Marini is a copy of the 18th century portrait of the archbishop of Évora, Frei Manuel do Cenáculo. The paintings were not studied until recently. *Bordalo et al.* (2016) [1] studied the paintings focusing on the pigments used by the artist in his paintings. Giorgio Marini preferred to use canvas as the support for the paintings. He painted the portraits with the emphasis on the face details with simple background and clothes. He preferred to sign using dark brown or black color on the paintings with light background while yellow and orange color were used on dark backgrounds. XRF combined with optical microscopy, Raman spectroscopy and SEM-EDX were used in identifying the palette used by Giorgio Marini. Additionally, Salvador and colleagues (2017) [2] investigated the origins of the microbial contamination on his paintings by characterizing the materials used. Energy-dispersive X-ray spectroscopy, μ-X-ray diffraction, μ-Raman, μ-FTIR and optical microscopy techniques were used in the materials characterization. It was found that Giorgio Marini prepared the ground layers with barium white and the painting media used are based on siccative oil and protein. From ELISA analysis studies, the presence of protein has been suggested to be the source of nutrition for microbial growth such as fungi of the genera *Aspergillus*, *Cladosporium*, *Mucor*, *Penicillium*, *Ulocladium* and *Scopulariopsis* that caused structural degradation on the paintings.

In order to study painting materials, many analytical techniques require the use of micro-samples taken from the art work. Microsamples should however be taken according to the conservation ethics, trying to reduce the level of destruction on the paintings. The researcher should only take the minimal amount of sample from the painting necessary for the analytical work. Some research [2–6] tried to scrap the samples from bottom corners or edges with the consideration to avoid aesthetical change on the artworks. In this chapter, the

applicability of the fluorescent labelling using C392STP coumarin on real artworks has been tested. After testing on laboratory models of easel paintings, the developed fluorescent labelling has been used for detection of proteins in painting microsamples. The results obtained from fluorescent labelling for proteinaceous binders' identification are presented in section 5.3. The knowledge on the material used, in particular the proteinaceous material can be very useful in providing information for conservation and restoration. The following of this chapter addressed the fifth research question as below:

5. Is the fluorescent labelling methodology applicable on microsample obtained from easel painting?

5.2 Methodology

5.2.1 Microsamples collections

Figure 5.1 shows the three easel paintings by Giorgio Marini (1836–1905) which were tested in this study. The portrait of Frei Manuel do Cenáculo (ME1281), dated 1887, is from the collection of the museum of Évora. Another two portraits: portrait of a bearded gentleman, dated 1897, and portrait of a lady, dated 1886, are from private collections. When the sampling process was carrying out, the factor that the sampling will not cause structural and aesthetic damage was carefully considered. The samples were collected using micro invasive methods, collecting only fragments that were not possible to be conserved and that would be eliminated during restoration work. Microsamples were scrapped off from the painting layers using a microscalpel.

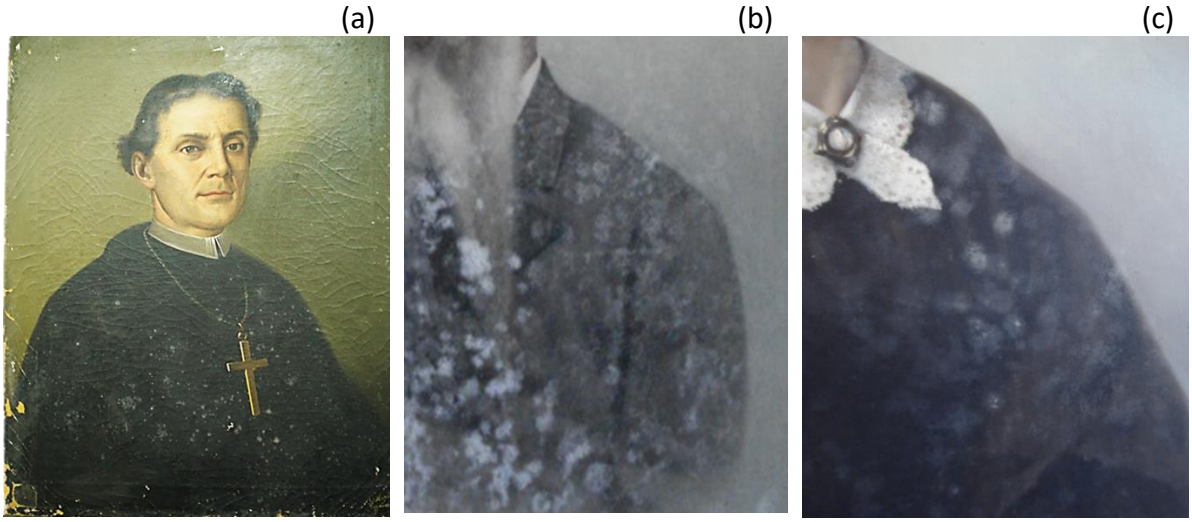

Figure 5.1 Portraits by Giorgio Marini (a) A portrait of Frei Manuel do Cenáculo, 1887, (ME1281), Museum of Évora (Évora, Portugal); (b) portrait of a bearded gentleman, 1897, and (c) portrait of a lady, 1886, private collection (Évora, Portugal).

The protein content was extracted from the microsamples using a previously optimized procedure [7]. Each sample was suspended in 1 ml of sodium bicarbonate buffer. The proteins

were extracted in three cycles consisting of a sonification step for an hour, and an incubation step at 37°C with orbital agitation for an hour, followed by an overnight incubation at 37°C as described by Salvador and colleagues [2, 7]. After those procedures, the protein extracts obtained were then submitted to the fluorescent labelling method.

5.2.2 Protein binders' identification

The protein extracted was bonded with C392STP using the developed fluorescent labelling method. The reactions were prepared by mixing the C392STP, at the concentration of 0.025 mg/ml, and the proteins recovered from easel paintings, in sodium bicarbonate buffer with a total volume of (1.0 ml) and stirred for a period of 24 h. Table 5.1 shows the conditions of the fluorescent labelling reactions performed. Identification of the fluorescent proteins produced was done by electrophoretic separation by PAGE.

Table 5.1 Conditions for the fluorescent labelling of the microsamples of easel paintings.

Reactions	Volume
M2 Portrait of Frei Manuel do Cenáculo, 1887, (ME1281)	100 µl of protein extract from microsamples 0.25 ml of 0.25 mg/ml C392STP 0.75 ml of phosphate buffer
Mb Portrait of a bearded gentleman, 1897	100 µl of protein extract from microsamples 0.25 ml of 0.25 mg/ml C392STP 0.75 ml of phosphate buffer
Md Portrait of a lady, 1886	100 µl of protein extract from microsamples 0.25 ml of 0.25 mg/ml C392STP 0.75 ml of phosphate buffer

5.3 Results and discussions

Figure 5.2 shows the FTIR spectra with the high absorption peaks observed ranging from 1510 and 1730 cm^{-1}. These results suggest that the absorption bands at 1510 to 1570 cm^{-1} may be attributed to the combination bands of N-H deformation and C-N stretching vibrations in amides while the peaks between 1630 to 1700 cm^{-1} may be attributed to the –C=O stretching vibrations of secondary amides (Amide-I band). The FTIR spectra thus confirm the presence of proteins in the portrait of Frei Manuel do Cenáculo. The absorption pattern is similar to the one obtained in a previous study which also suggested the presence of proteins in the top layer and ground layer of the painting [2]. Figure 5.3 and figure 5.4 show similar characteristic absorptions at the range from 1500 to 1710 cm^{-1}, for the portrait of a bearded gentleman, and from 1500 to 1700 cm^{-1} for the portrait of a lady. As evidenced in the literatures, the peak at 1545 cm^{-1} from IR reflectance spectroscopy [9] and the peak at 1542 cm^{-1} from IR spectrum [10], were suggested as amide II bands.

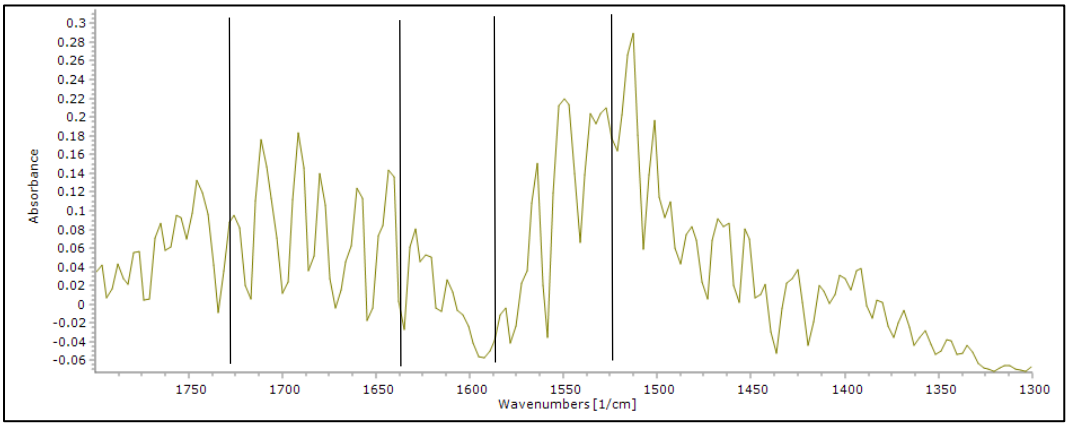

Figure 5.2 FTIR spectra of the microsamples from the portrait of Frei Manuel do Cenáculo.

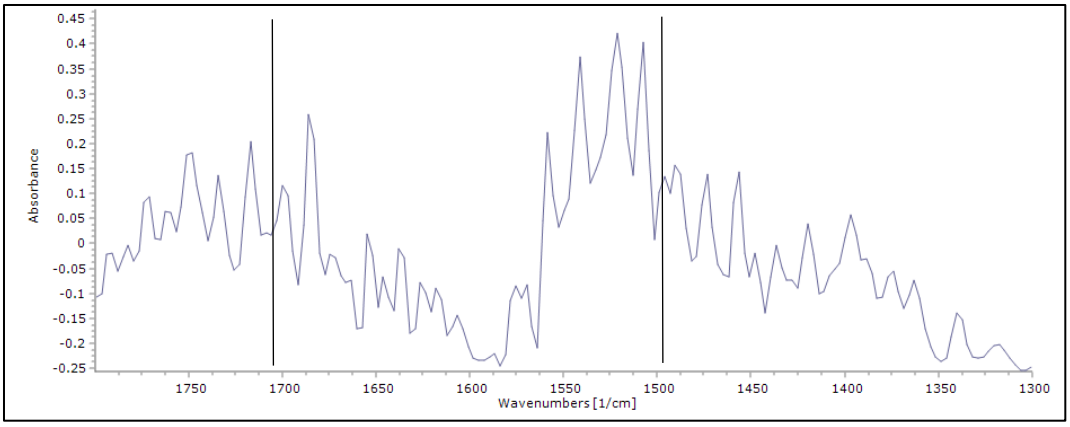

Figure 5.3 FTIR spectra of the microsamples from the portrait of a bearded gentleman.

Figure 5.4 FTIR spectra of the microsamples from the portrait of a lady.

After confirming the presence of the proteins, the proteins were recovered from the microsamples, according to Salvador el al, 2017 [2], giving 56.67 µg/ml, 89.05 µg/ml and 353.16 µg/ml, for Portrait of Frei Manuel do Cenáculo, 1887, (M2), Portrait of a bearded gentleman, 1897 (Mb) and Portrait of a lady, 1886 (Md) respectively. The recovered proteins were labelled as described in table 5.1 and were successfully bonded with the fluorescent labelling methodology (Figure 5.5). The electrophoresis profiles for the 3 easel paintings showed strong fluorescent bands (Figure 5.6) for all the portraits samples, similar to the band of ovalbumin.

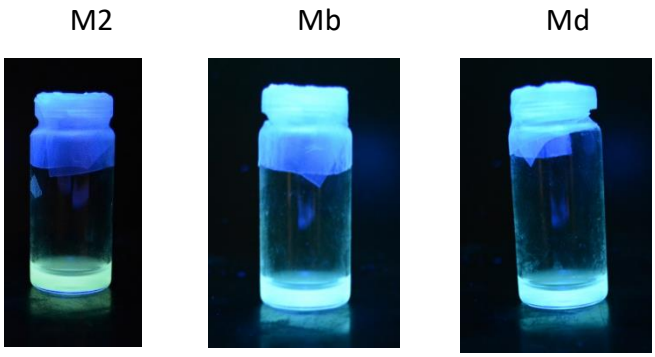

Figure 5.5 Fluorescent microsamples.

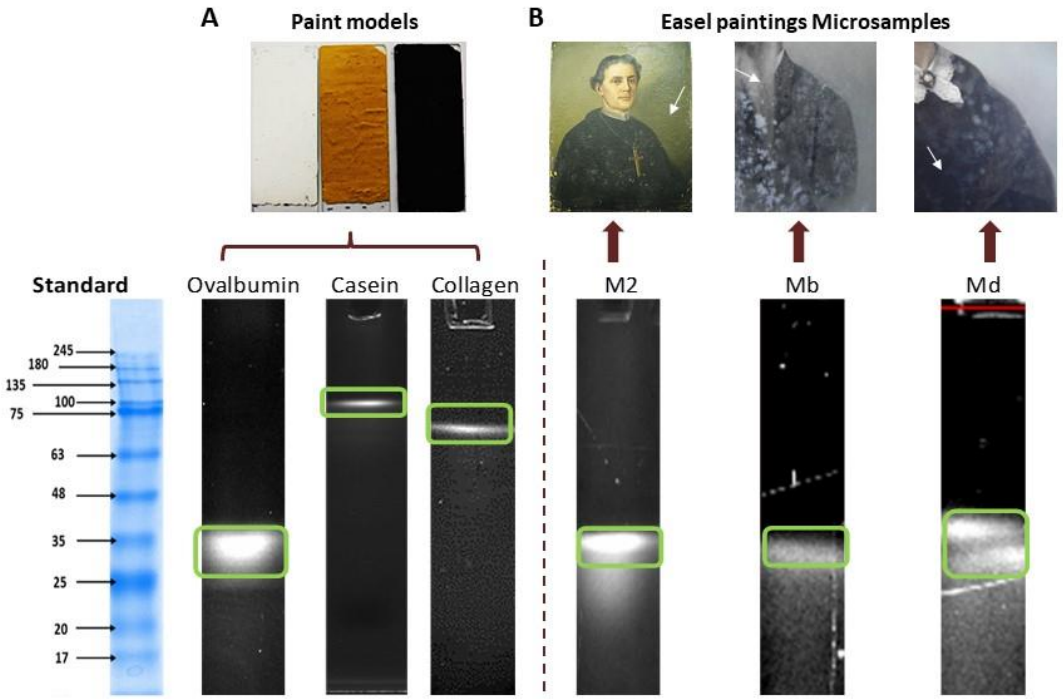

Figure 5.6 Electrophoresis profiles of microsamples extracted from paint models (A) and extracted from easel paintings (B). M2- portrait of Frei Manuel do Cenáculo, 1887, (ME1281), Museum of Évora (Évora, Portugal); Mb- portrait of a bearded gentleman, 1897, and Md- portrait of a lady, 1886, private collection (Évora, Portugal).

Painting from Marini may have the influence of Italian painting in which the use of egg-based varnish was common. As an example, ovalbumin was found at the top layer of paintings of an Italian painter, Nicolò Rondinelli, through chemiluminescent technique and IR reflectance spectroscopy [8]. Zangheri et al. (2016) [4], suggested that egg white has been used as varnish on the canvas painting, The Saint John (1600) (unknown artist, private collection in Italy), because the absorption bands of amide I and amide II were observed. Calvano and colleagues (2015) [9] also suggested that egg-based paint binder was used in the Italian panel paintings, Christ in Pity, St. Louis of Toulouse, St. Francis of Assisi, St. John Baptist, St. Anthony of Padua (1467) (Antonio Vivarini, Italy). The easel painting in the Santa Maria Santissima Church in Carrara, Italy also suggested the presence of egg and animal glue according to the PCA analysis [10]. Besides that, studies have also shown that egg was a popular binder used in the period of 19th century. MALDI-TOF mass spectroscopy [11] studies on Edward Munch's paintings produced in 1893 also found egg in the paintings. The proteomic approach used in analyzing the 19th century icons from Ortodox churches in Serbia has also found egg yolk in the painting layers [12].

Previous FTIR analysis on Marini paintings made in our research group [2] also reported the characteristic absorption bands of amide I in the top and ground layers, while the characteristic absorption band for the amide II was found in the ground layer of the paintings. These absorption bands are a clear indication of the presence of proteins. In the same study, ELISA analysis also confirmed the presence of proteins, in particular ovalbumin, in the Marini's paintings [2].

5.4 Conclusion

The opportunity to study these 19th century Easel paintings of the collection of Évora museum and private collections has demonstrated the efficacy of fluorescent labelling using C392STP in proteinaceous binders' identification. Ovalbumin has been proved to be presented in the all the examined paintings. Fluorescent labelling is a potential complementary test in determining the origins of proteinaceous materials used in the paintings. Fluorescent labelled proteins can be easily detected at a low cost as no expensive instrument is needed. Similarly,

indirect ELISA was also proved to be an effective technique in identifying the source of proteins [13–15]. However, one of the limitations of indirect ELISA is that is time-consuming [10] since the time of incubation for the reaction between antibody and protein is relatively longer [14]. Furthermore, it requires materials like commercially manufactured antibodies specifically tailored for cultural heritage study [16] that makes the cost of analysis much higher for indirect ELISA as compared to fluorescent labelling. In the light of the obtained results, both fluorescent labelling and indirect ELISA are recommended as complementary tools for proteins detection from complex matrices, along with the consideration of the cost and the level of specificity required.

Bibliography

[1] R. Bordalo, C. Bottaini, C. Moricca, and A. Candeias, “Material Characterisation of a Florentine painter in Portugal in the Late 19th century: paintings by Giorgio Marini,” *Int. J. Conserv. Sci.*, vol. 7, no. 4, pp. 967–980, 2016.

[2] C. Salvador, R. Bordalo, M. Silva, T. Rosado, A. Candeias, and A. T. Caldeira, “On the conservation of easel paintings: evaluation of microbial contamination and artists materials,” *Appl. Phys. A Mater. Sci. Process.*, vol. 123, no. 1, p. 80, 2017.

[3] M. Palmieri, M. Vagnini, L. Pitzurra, B. G. Brunetti, and L. Cartechini, “Identification of animal glue and hen-egg yolk in paintings by use of enzyme-linked immunosorbent assay (ELISA),” *Anal Bioanal Chem*, vol. 405, pp. 6365–6371, 2013.

[4] M. Zangheri, G. Sciutto, M. Mirasoli, S. Prati, R. Mazzeo, A. Roda, and M. Guardigli, “A portable device for on site detection of chicken ovalbumin in artworks by chemiluminescent immunochemical contact imaging,” *Microchem. J.*, vol. 124, pp. 247–255, 2016.

[5] P. Přikryl, L. Havlíčkova, V. Pacáková, J. Hradilová, K. Štulík, and P. Hofta, “An evaluation of GC-MS and HPLC-FD methods for analysis of protein binders in paintings,” *J. Sep. Sci.*, vol. 29, no. 17, pp. 2653–2663, 2006.

[6] G. Chiavari, G. Lanterna, C. Luca, M. Matteini, S. Prati, and I. C. A. Sandu, “Analysis of proteinaceous binders by in-situ pyrolysis and silylation,” *Chromatographia*, vol. 57, no. 9–10, pp. 645–648, 2003.

[7] C. Salvador, A. Branco, A. Candeias, and A. T. Caldeira, “Innovative approaches for immunodetection of proteic binders in art,” *E-Conservation J.*, no. 5, pp. 1–10, 2017.

[8] L. S. Dolci, G. Sciutto, M. Guardigli, M. Rizzoli, S. Prati, R. Mazzeo, and A. Roda, “Ultrasensitive chemiluminescent immunochemical identification and localization of protein components in painting cross-sections by microscope low-light imaging,” *Anal. Bioanal. Chem.*, vol. 392, no. 1–2, pp. 29–35, 2008.

[9] C. D. Calvano, I. D. Van Der Werf, F. Palmisano, and L. Sabbatini, “Identification of lipid- and protein-based binders in paintings by direct on-plate wet chemistry and matrix-assisted laser desorption ionization mass spectrometry,” *Anal. Bioanal. Chem.*, vol. 407,

no. 3, pp. 1015–1022, 2015.

[10] A. Andreotti, M. Bonaduce, M. P. Colombini, G. Gautier, F. Modugno, and E. Ribechini, “Combined GC/MS analytical procedure for the characterization of glycerolipid, waxy, resinous, and proteinaceous materials in a unique paint microsample,” *Anal. Chem.*, vol. 78, no. 13, pp. 4490–4500, 2006.

[11] S. Kuckova, R. Hynek, and M. Kodicek, “Identification of proteinaceous binders used in artworks by MALDI-TOF mass spectrometry,” *Anal. Bioanal. Chem.*, vol. 388, pp. 201–206, 2007.

[12] T. Tripković, C. Charvy, S. Alves, A.D. Lolić, R.M. Baošić, S.D. Nikolić-Mandić, and J.C. Tabet, “Electrospray ionization linear trap quadrupole Orbitrap in analysis of old tempera paintings: application to nineteenth-century Orthodox icons,” *Eur. J. Mass Spectrom.*, vol. 21, no. 4, pp. 679–692, 2015.

[13] M. P. Colombini and F. Modugno, “Characterisation of proteinaceous binders in artistic paintings by chromatographic techniques,” *J. Sep. Sci.*, vol. 27, no. 3, pp. 147–160, 2004.

[14] J. Arslanoglu, J. Schultz, J. Loike, and K. Peterson, “Immunology and art: Using antibody-based techniques to identify proteins and gums in artworks,” *J. Biosci.*, vol. 35, no. 1, pp. 3–10, 2010.

[15] J. R. Allred, “Characterization of Hidden Paint Layer Topography Using a Stereographic XRF Approach,” Delft University of Technology, 2017.

[16] C. M. Soares, R. M. Rodrigues, A. J. Cruz, and C. Rêgo, “Historical and material approach to the paintings at the Portugal National Library: contributions to the history of conservation and restoration of easel painting in the 19th century,” *Int. J. Herit. Digit. era*, vol. 1, no. supplement 1, pp. 283–288, 2012.

Chapter 6 FINAL REMARKS

6.1 General conclusion

In short, this PhD research has successfully explored a novel simple and inexpensive fluorescent labelling method (Figure 6.1) to detect and identify protein binders present in easel paintings by using C392STP coumarin as a fluorophore probe. It explores the photophysical properties of this coumarin, a novel low-cost coumarin dye with capability to react with primary amine groups, as a fluorescent dye with a potential for applications in biolabelling.

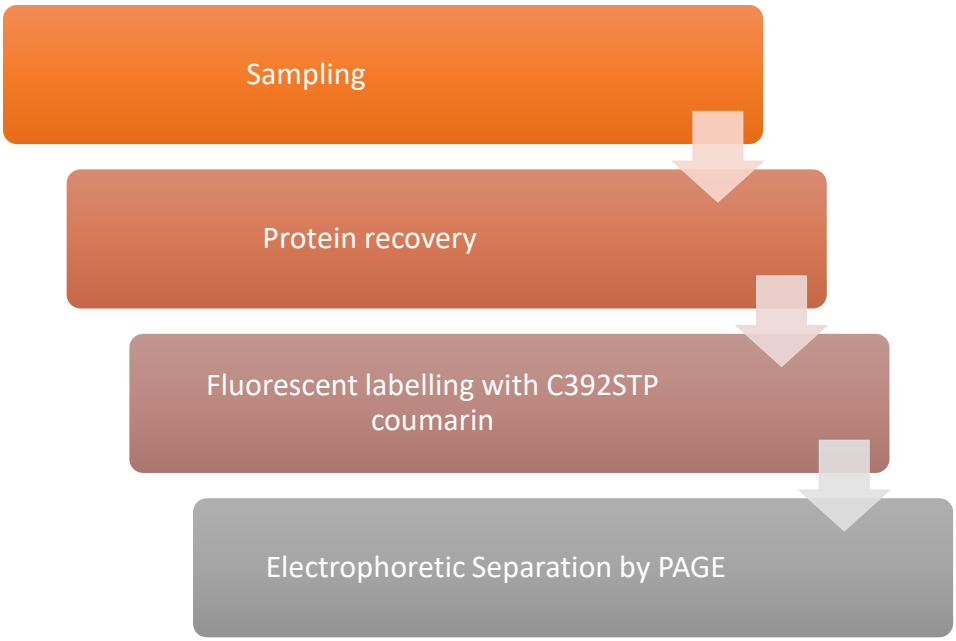

Figure 6.1 Scheme of fluorescent labelling procedure.

Through DFT and TD-DFT calculations, we were able to understand the electronic structure and spectral features of the C392STP coumarin. To gain a better understanding of the electronic structure and spectral features of the chromophore-protein complex, we have also performed DFT and TD-DFT calculations on both the *E* and *Z* conformers of a coumarin derivative that was intended to mimic the coumarin bonded to a protein amino acid side chain. Results of TD-DFT calculations presented good agreement with the experimental

absorption spectra and a comprehensive assignment of the main spectral features of the studied compounds was accomplished.

Subsequently, we have optimized the labelling method by using commercial proteins and proteins extracted from hen's egg yolk and white, bovine milk and rabbit skin. Fluorescent proteins thus produced can be detected by gel electrophoresis, without the need for the electrophoresis gel staining (Figure 6.2). UV-Vis and infrared spectra of the fluorescent proteins were measured. Fluorescent BSA, fluorescent ovalbumin, fluorescent casein, fluorescent collagen and fluorescent fish gelatin show a different profile in the infrared region of primary and secondary amides confirming the effectiveness of the labelling reaction of the related proteins.

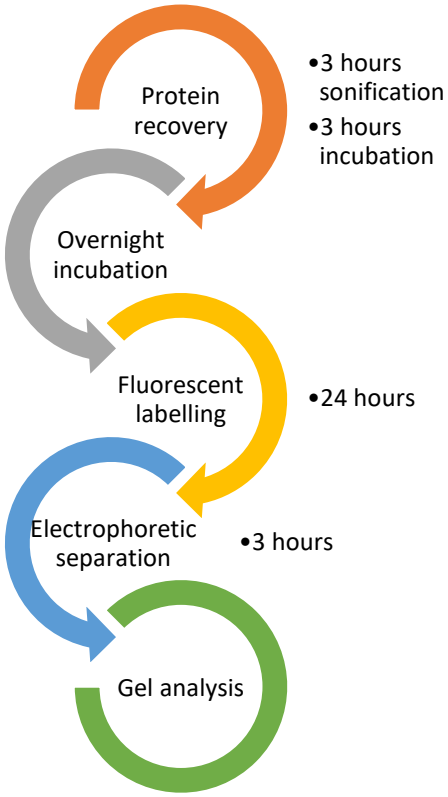

Figure 6.2 Time used for protein detection.

In order to mimic real conditions, paint models of easel paintings have been prepared by mixing proteins such as ovalbumin, casein and rabbit glue with different pigments (lead white,

chrome yellow and black bone). Paint layers with thickness around 50-150 µm were then applied on glass supports and submitted to an artificial aging process. The fluorescent labelling method was tested and the results revealed that proteins in a concentration as low as 6.0 µg/ml could be detected.

At the last stage, real samples obtained from easel painting were tested using the optimized method. Micro samples of three 19th century easel paintings by Giorgio Marini (1836–1905) from the museum of Évora and from private collections were analyzed. The extracted proteins were submitted to the fluorescent labelling method and could be clearly identified in the electrophoretic profiles. The electrophoretic profile showed that binder used in these three paintings was ovalbumin.

The reported results show evidence of the potential of the method as an effective and useful analytical tool in the identification of protein binders in samples obtained from easel paintings. In short, the advantages of this method are as follows:

- Inexpensive.
- Requires little analysis time
- High sensitivity
- Only common chemistry/biochemistry laboratory equipment is needed. No expensive equipment like mass spectrometers, gas chromatographers or modern advanced proteomics apparatus is necessary
- Can easily be implemented in a museum laboratory

Although the method requires the collection of microsamples from the easel paintings, only a small amount of material is necessary for the analyses. Given these points, the strategy reported in our work aims to serve as complementary analysis which can be used together with other existing methods, when the recognition of the origins of the proteinaceous binders is important. The simplicity, the good results of the methods and the economic aspect constitute important attractive features of this approach.

6.2 Recommendations for future research

Future improvements will include the optimization of the method in order to decrease the amount of material necessary for analysis, in view of its application to real works of art, with the aggravated problems typical of such objects, due to aging and the complex nature of the samples. Fluorescent labelling in cultural heritage studies is a relatively new field. Hence, efforts on the exploration of the fluorophore probe molecule properties are very important for better exploiting their characteristics and to develop new applications. The study of fluorescent label molecule properties like solubility, quantum yields and other photophysical and spectroscopic properties are a promising field of research.

Finally, although the method was designed and applied for the detection and identification of protein binders present in easel paintings, the potential of fluorescent labelling using C392STP coumarin in other art samples like:

a) Polychrome statues
b) Wood paintings
c) Mural paintings
d) Manuscripts

can be explored, as a method to complement the analysis of artworks.

APPENDIX

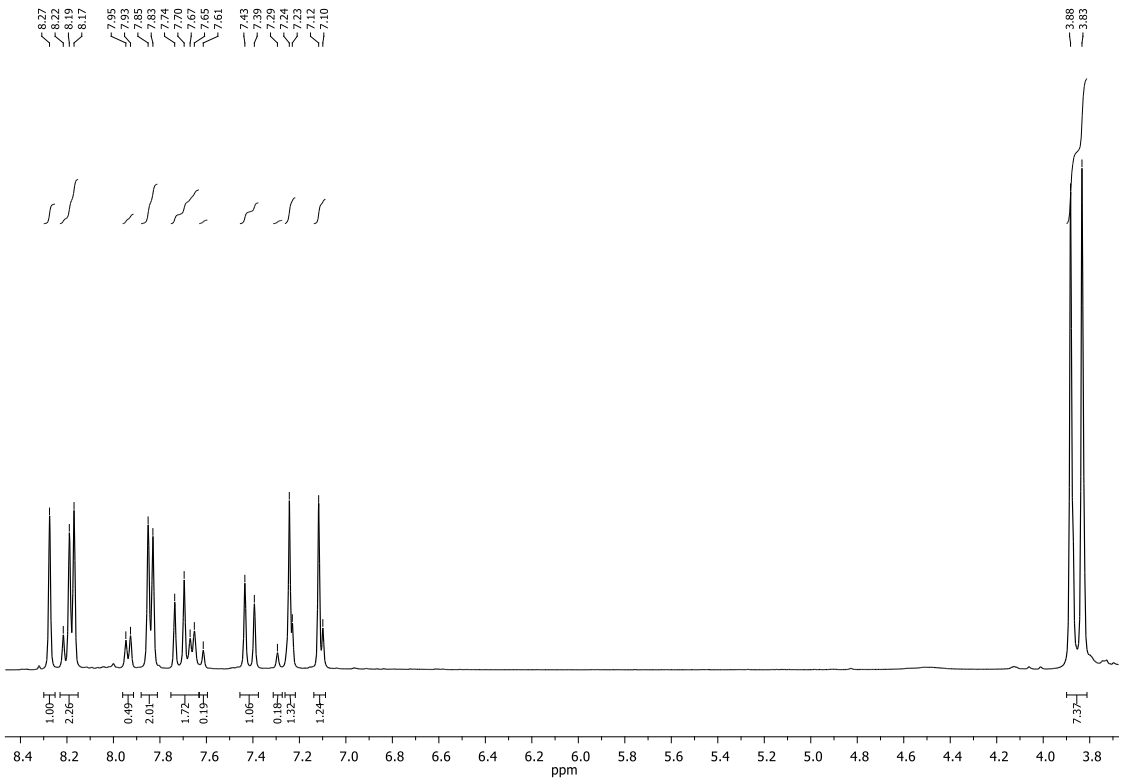

Figure 1 ^{1}H NMR spectrum (400 MHz, $(CD_3)_2SO$) of sodium (*E/Z*)-4-(4-(2-(6,7-dimethoxy-coumarin-3-yl) vinyl) benzoyl)-2,3,5,6-tetrafluorobenzenesulfonate (***E*-isomer,** 3.83 (3H, s, OCH3), 3.88 (3H, s, OCH3), 7.12 (1H, s, H-8), 7.24 (1H, s, H-5), 7.41 (1H, d, J=16.3, H-1'), 7.72 (1H, d, J=16.3, H-2'), 7.84 (2H, d, J= 8.2, H-4', H-8'), 8.18 (2H, d, J= 8.2, H-5', H-7'), 8.27 (1H, s, H-4); ***Z*-isomer**, 3.83 (3H, s, OCH3), 3.88 (3H, s, OCH3), 7.10 (1H, s, H-8), 7.23 (1H, s, H-5), 7.30 (1H, s, H-1'), 7.61 (1H, s, H-2'), 7.66 (2H, d, J= 8.0, H-4', H-8'), 7.94 (2H, d, J= 8.0, H-5', H-7'), 8.22 (1H, s, H-4)).

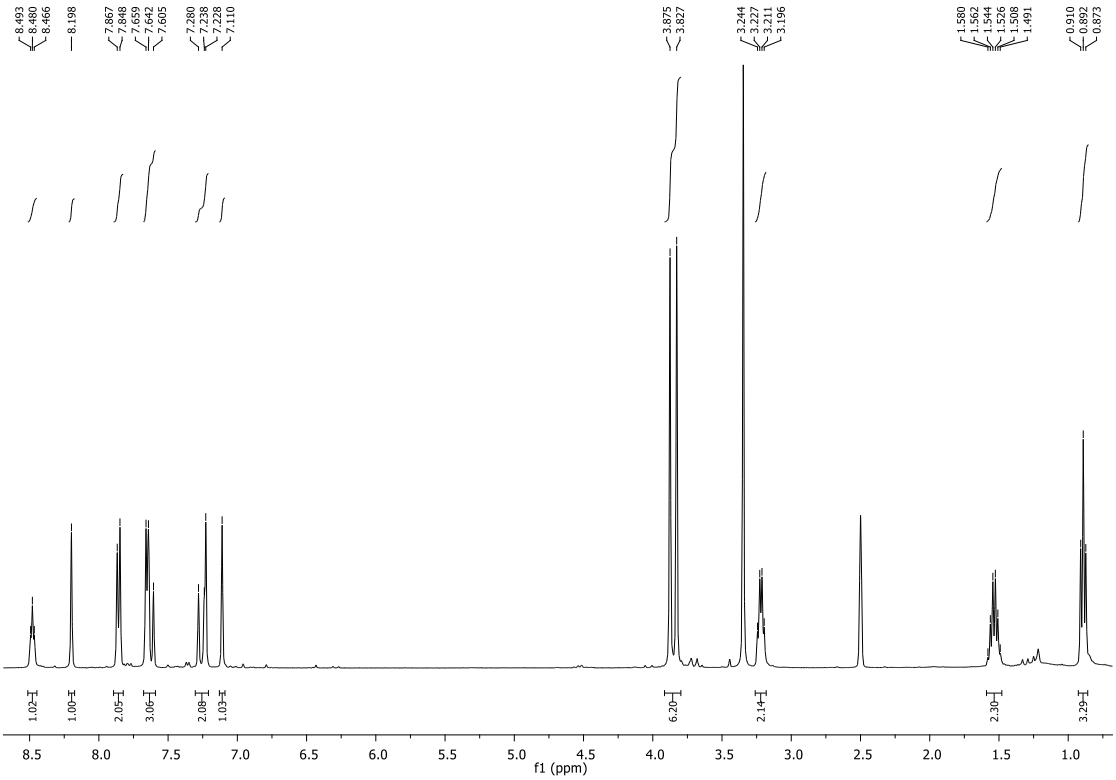

Figure 2 ^{1}H NMR spectrum (400 MHz, $(CD_3)_2SO$) of (*E*)-4-(2-(6,7-dimethoxy-coumarin-3-yl) vinyl)-*N*-propylbenzamide (0.89 (3H, t, J=7.6, $NHCH_2CH_2\underline{CH_3}$), 1.53 (2H,m, $NHCH_2\underline{CH_2}CH_3$), 3.22 (2H, m, $NH\underline{CH_2}CH_2CH_3$), 3.83 (3H, s, OCH3), 3.88 (3H, s, OCH3), 7.11 (1H, s, H-8), 7.23 (1H, s, H-5), 7.26 (1H, d, J=16.8, H-1'), 7.63 (1H, d, J=16.8, H-2'), 7.65 (2H, d, J= 6.8, H-4', H-8'), 7.86 (2H, d, J= 6.8, H-5', H-7'), 8.20 (1H, s, H-4), 8.48 (1H, t, J=5.6, $\underline{NH}CH_2CH_2CH_3$)).

Abstract in the book of abstract of XIX National Congress of Biochemistry

Labelling of proteinaceous binders: Density functional theory and time dependent density functional theory calculation on some coumarin derivatives [P5/02]

Ooi Su Yin [1], Ana Teresa Caldeira [1,2], António Pereira [1,2], João Paulo Prates Ramalho [2,3]
[1] HERCULES Laboratory, Universidade of Évora, Portugal
[2] Chemistry Department, Sciences and Technology School, Universidade of Évora, Portugal [3] CQE, Universidade of Évora, Portugal

Labelling is one of the most common methodologies used for bioanalytical purposes and has received special attention and showed remarkable progress in recent years. Presently we are exploring the use of different coumarin chromophores in order to develop new fluorescent labelling methodologies to identify different proteinaceus materials usually used in art. Results presented here explore the spectroscopic characteristics of a coumarin derivative chromophore (4-sulfotetrafluorophenyl coumarin ester), that can be used to label proteins, and two other coumarin derivatives that mimics the bonding of the coumarin chromophore with two protein amino acids, namely the lysine and tyrosine. Theoretical quantum chemical calculations based on the Time Dependent Density Functional Theory (TD-DFT) have been made on the coumarin derivatives in which optimizations were performed using the functional B3LYP and the low-lying excited states were calculated using several functionals, namely: CAM-B3LYP, M06 and Pbe0. Generally, calculations with the three functionals show that the lower energy transitions have mainly HOMO-1→LUMO character when the free coumarin chromophore is in water or acetonitrile solvent. However, for coumarin bonded with ethylamine or phenol, the transitions were mainly of HOMO→LUMO character. The TD-DFT calculations confirm the experimental trends in absorption wavelengths and are in good agreement with experimental absorption spectra. In all cases there is an important shift to higher energies of the most important band in the bonded coumarin compounds cases.

Keywords: Coumarin, quantum chemical calculation, TD-DFT, DFT, CAM-B3LYP, M06, Pbe0

Poster presented in the XIX National Congress of Biochemistry

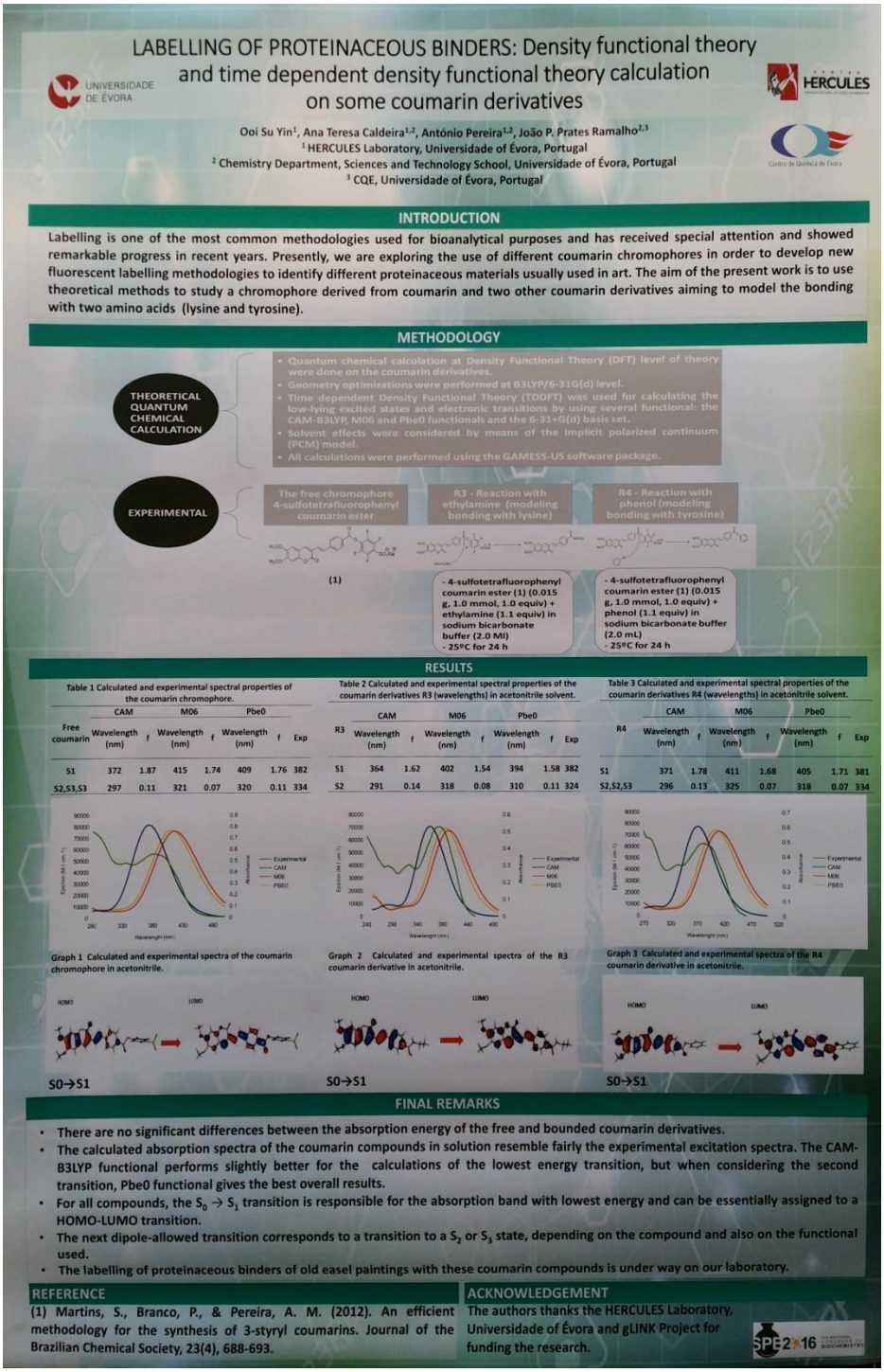

LABELLING OF PROTEINACEOUS BINDERS: Density functional theory and time dependent density functional theory calculation on some coumarin derivatives

Ooi Su Yin[1], Ana Teresa Caldeira[1,2], António Pereira[1,2], João P. Prates Ramalho[2,3]

[1] HERCULES Laboratory, Universidade of Évora, Portugal

[2] Chemistry Department, Sciences and Technology School, Universidade of Évora, Portugal

[3] CQE, Universidade of Évora, Portugal

INTRODUCTION

Labelling is one of the most common methodologies used for bioanalytical purposes and has received special attention and showed remarkable progress in recent years. Presently, we are exploring the use of different coumarin chromophores in order to develop new fluorescent labelling methodologies to identify different proteinaceous materials usually used in art. The aim of the present work is to use theoretical methods to study a chromophore derived from coumarin and two other coumarin derivatives aiming to model the bonding with two amino acids (lysine and tyrosine).

METHODOLOGY

THEORETICAL QUANTUM CHEMICAL CALCULATION

- Quantum chemical calculation at Density Functional Theory (DFT) level of theory were done on the coumarin derivatives.
- Geometry optimizations were performed at B3LYP/6-31G(d) level.
- Time dependent Density Functional Theory (TDDFT) was used for calculating the low-lying excited states and electronic transitions by using several functional: the CAM-B3LYP, M06 and Pbe0 functionals and the 6-31+G(d) basis set.
- Solvent effects were considered by means of the implicit polarized continuum (PCM) model.
- All calculations were performed using the GAMESS-US software package.

EXPERIMENTAL

The free chromophore 4-sulfotetrafluorophenyl coumarin ester

R3 - Reaction with ethylamine (modeling bonding with lysine)

R4 - Reaction with phenol (modeling bonding with tyrosine)

(1)

- 4-sulfotetrafluorophenyl coumarin ester (1) (0.015 g, 1.0 mmol, 1.0 equiv) + ethylamine (1.1 equiv) in sodium bicarbonate buffer (2.0 Ml)
- 25ºC for 24 h

- 4-sulfotetrafluorophenyl coumarin ester (1) (0.015 g, 1.0 mmol, 1.0 equiv) + phenol (1.1 equiv) in sodium bicarbonate buffer (2.0 mL)
- 25ºC for 24 h

RESULTS

Table 1 Calculated and experimental spectral properties of the coumarin chromophore.

Free coumarin	CAM Wavelength (nm)	CAM f	M06 Wavelength (nm)	M06 f	Pbe0 Wavelength (nm)	Pbe0 f	Exp
S1	372	1.87	415	1.74	409	1.76	382
S2,S3,S3	297	0.11	321	0.07	320	0.11	334

Table 2 Calculated and experimental spectral properties of the coumarin derivatives R3 (wavelengths) in acetonitrile solvent.

R3	CAM Wavelength (nm)	CAM f	M06 Wavelength (nm)	M06 f	Pbe0 Wavelength (nm)	Pbe0 f	Exp
S1	364	1.62	402	1.54	394	1.58	382
S2	291	0.14	318	0.08	310	0.11	324

Table 3 Calculated and experimental spectral properties of the coumarin derivatives R4 (wavelengths) in acetonitrile solvent.

R4	CAM Wavelength (nm)	CAM f	M06 Wavelength (nm)	M06 f	Pbe0 Wavelength (nm)	Pbe0 f	Exp
S1	371	1.78	411	1.68	405	1.71	381
S2,S2,S3	296	0.13	325	0.07	318	0.07	334

Graph 1 Calculated and experimental spectra of the coumarin chromophore in acetonitrile.

Graph 2 Calculated and experimental spectra of the R3 coumarin derivative in acetonitrile.

Graph 3 Calculated and experimental spectra of the R4 coumarin derivative in acetonitrile.

S0→S1

S0→S1

S0→S1

FINAL REMARKS

- There are no significant differences between the absorption energy of the free and bounded coumarin derivatives.
- The calculated absorption spectra of the coumarin compounds in solution resemble fairly the experimental excitation spectra. The CAM-B3LYP functional performs slightly better for the calculations of the lowest energy transition, but when considering the second transition, Pbe0 functional gives the best overall results.
- For all compounds, the $S_0 \rightarrow S_1$ transition is responsible for the absorption band with lowest energy and can be essentially assigned to a HOMO-LUMO transition.
- The next dipole-allowed transition corresponds to a transition to a S_2 or S_3 state, depending on the compound and also on the functional used.
- The labelling of proteinaceous binders of old easel paintings with these coumarin compounds is under way on our laboratory.

REFERENCE

(1) Martins, S., Branco, P., & Pereira, A. M. (2012). An efficient methodology for the synthesis of 3-styryl coumarins. Journal of the Brazilian Chemical Society, 23(4), 688-693.

ACKNOWLEDGEMENT

The authors thanks the HERCULES Laboratory, Universidade of Évora and gLINK Project for funding the research.

Abstract in the book of abstract TECHNART 2017 Non-destructive and microanalytical techniques in art and cultural heritage

Development of a simple method for the identification proteinaceous binders in easel painting

Ooi Su Yin[(1)], Cátia Salvador [(1)], António Candeias[(1,2)], António Pereira[(1,2)], Paulo Prates Ramalho[(2,3)], Ana Teresa Caldeira[(1,2)]

Easel paintings emerged in the Middle Ages and since then have been one of the most important art expressions, constituting today relevant Cultural Heritage assets with important historic and cultural value. Due to the high importance in the preservation of these artworks, the correct identification of proteinaceous binders is a crucial step for a better understanding of the techniques used by the artist, and to provide relevant information for conservation and restoration processes [1]. Easel paintings contain proteinaceous binders which are commonly produced from egg, milk or animal skin and bones but unfortunately the detection of the different protein materials in these complexes matrices is a difficult task. In this work a new fluorescent labelling methodology is developed using coumarin derivative chromophore (4-sulfotetrafluorophenyl coumarin ester) in order to increase the detection signals of proteins. Firstly, we have developed and optimized a simple method with high sensibility using commercial proteins such as BSA (A2153), ovalbumin (A5378), casein (C3400) and collagen (C9879) (all from Sigma-Aldrich). This method is efficient in showing the characteristic profiles of each commercial proteins tested with the advantages of higher sensitivity and less time required for the electrophoretic detection. The optimized method was also used to test proteins showed similar characteristic band profiles between the extracted and the commercial proteins.

To fulfill the aim in minimizing the amount of samples required and to try to mimic the real conditions, we performed paint mockups of easel paintings. For that, we mixed the proteins , animal skin with pigments like lead white, yellow ocre and bone black. The proteinaceous content was extracted from paint microsamples, using a previously optimized protocol [2] and the extracted proteins were used to bind with coumarin derivative chromophore which allowed to identify and distinguish the different protein binders used in each paint model. These results evidence the enormous potential to apply this optimized methodology as an effective and useful analytical tool in the identification of protein binders in samples obtained from easel paintings.

[1] C. Salvador, R. Bordalo, M. Silva, T. Rosado, A. Candeias, A.T. Caldeira, On the conservation of easel paintings: evaluation of microbial contamination and artists materials, Applied Physics A 123(80), 2017, 1.

[2] C. Salvador, A. Branco, A. Candeias, A.T. Caldeira, Innovative approaches for immunodetection of proteic binders in art, E-Conservation Journal (in press), 2016.

Poster presented in the TECHNART 2017 Non-destructive and microanalytical techniques in art and cultural heritage

Development of a simple method for the identification of proteinaceous binders in easel paintings

Ooi Su Yin[1], Cátia Salvador[1], António Candeias[1,2], António Pereira[1,2], João Paulo Prates Ramalho[2,3] and Ana Teresa Caldeira[1,2]

[1] HERCULES Laboratory, University of Évora, Portugal

[2] Chemistry Department, Sciences and Technology School, University of Évora, Portugal

[3] CQE, University of Évora, Portugal

Introduction

Easel paintings emerged in the Middle Ages have been one of the most important art expressions, constituting today relevant Cultural Heritage assets with important historic and cultural value. Due to the high importance in the preservation of these artworks, the correct identification of proteinaceous binders is a crucial step for a better understanding of the techniques used by the artist, and providing relevant information to conservation and restoration processes [1]. These easel paintings contain proteinaceous binders which are commonly extracted from egg, milk or animal skin and bones. The identification of the different protein binders can be done with a new fluorescent labelling methodology by using a coumarin derivative chromophore (4-sulfotetrafluorophenyl coumarin ester [2]).

New fluorescent labelling methodology development

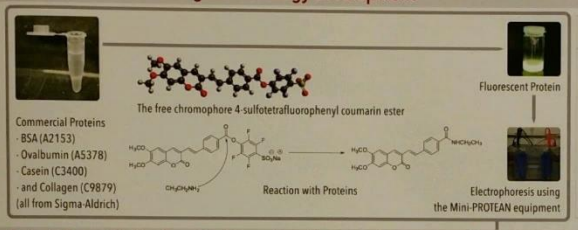

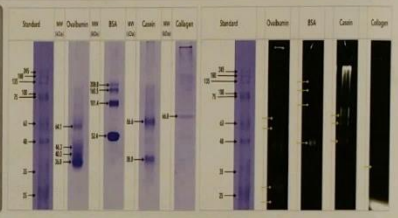

Test of the optimized method by using the proteins extracted from hen's egg yolk and white, bovine milk and animal skin

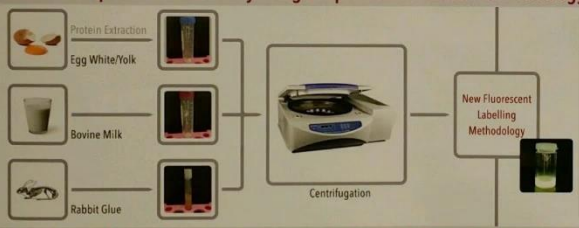

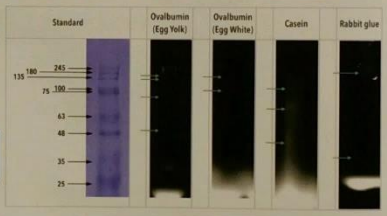

Simulation of the real conditions using paint models of easel paintings

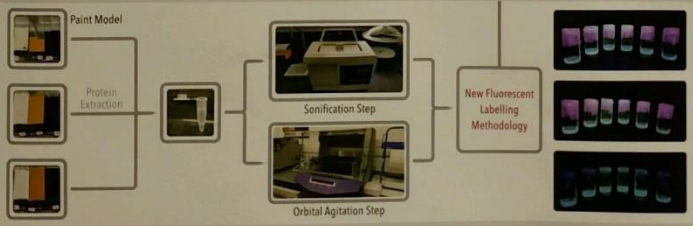

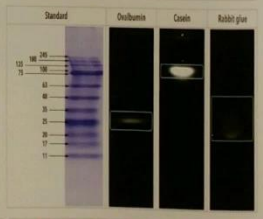

Final Remarks

- These results evidence the enormous potential of the possibility to apply this optimized methodology as an effective and useful analytical tool in the identification of protein binders in the samples obtained from easel paintings.
- The labelling of proteinaceous binders of old easel paintings with these coumarin compounds is under way in our laboratory.

Acknowledgement

The authors thanks the HERCULES Laboratory, University of Évora and gLINK Project for funding the research.

References

[1] C. Salvador, R. Bordalo, M. Silva, T. Rosado, A. Candeias, & A.T. Caldeira, On the conservation of easel paintings: evaluation of microbial contamination and artists materials, Applied Physics A 123(80), 2017, 1-13 DOI 10.1007/s00339-016-0704-5.

[2] S. Martins, P. Branco, & A. M. Pereira, An efficient methodology for the synthesis of 3-styryl coumarins, Journal of the Brazilian Chemical Society 23(4), 2012, 688-693.

Abstract in the book of abstract INART 2018 Innovation in Art Research and Technology

APPROACHES FOR THE PROTEIN BINDERS' DETERMINATION ON EASEL PAINTINGS

Ooi S.Y.*[1], Salvador C.[1], Martins S.[1], Pereira A.[2], Caldeira A.T.[2], Ramalho J.P.P.[3]

Keywords: fluorescent labelling method, protein binders, electrophoretic profiling, easel paintings, immunoenzymatic assay

[1]HERCULES Laboratory, Universidade of Évora, Évora, Portugal, [2]Chemistry Department, School of Sciences and Technology, Universidade of Évora, Évora, Portugal, [3]CQE, School of Sciences and Technology, Universidade of Évora, Évora, Portugal

Proteins have been commonly used as paintings medium, adhesives and coating layers in easel paintings. Hence, the proteins recognition is one important factor for the construction of an easel painting's conservation strategy. This work explores different approaches for proteinaceous binders' identification namely; conventional electrophoretic profile, fluorescent labelling method and immunological assay. The fluorescent labelling method was firstly tested on proteins extracted from an easel painting paint model. The paint models were made by mixing proteins such as ovalbumin, casein and rabbit glue with different pigments (lead white, chrome yellow and black bone). From the conventional electrophoresis, protein bands extracted were hardly observed on the electrophoresis gel. However, fluorescent band between 25 kDa to 35 kDa were clearly observed on the electrophoresis gel with fluorescent labelling. Results revealed that with fluorescent labelling, proteins extracted from the paint models, in a concentration of 6.0 μg/ml could be detected. Subsequently, proteins were extracted from samples of easel paintings by Giorgio Marini (1836–1905), from the museum of Évora and private collections. The extracted proteins were then submitted to the fluorescent labelling method and immunoenzymatic assay. The fluorescent labelling was done using Coumarin 392 TFP ester (C392) (4-sulfotetrafluorophenyl coumarin ester) as fluorophore, which was mixed with the proteins extract for a period of 24 hours. Simultaneously, immunoenzymatic assay (ELISA) was carried out on each sample, according to a previously optimized procedure by Salvador et al., 2016. These extracted proteins could be clearly observed in the electrophoretic profiles after fluorescent labelling, which was not possible in the conventional electrophoresis performed. Proteins such as ovalbumin, collagen and casein also proved to be present in the paintings, through the immunological assay. The results indicate that fluorescent labelling, followed by electrophoretic detection is a simple and fast method with high sensitivity; this method is like the immunoenzymatic assay which can act with high specificity in the identification of proteinaceous binders used in easel paintings.

C. Salvador, A. Branco, A. Candeias, A.T. Caldeira, Innovative approaches for immunodetection of proteic binders in art. E-Conserv. J. (in press) (2017)

Poster presented in the INART 2018 Innovation in Art Research and Technology

UNIVERSIDADE DE ÉVORA
INSTITUTO DE INVESTIGAÇÃO
E FORMAÇÃO AVANÇADA

Contactos:

Universidade de Évora

Instituto de Investigação e Formação Avançada - IIFA

Palácio do Vimioso | Largo Marquês de Marialva, Apart. 94

7002-554 Évora | Portugal

Tel: (+351) 266 706 581